Space Sci Rev (2017) 212:743–810
DOI 10.1007/s11214-017-0387-z

Water in the Earth's Interior: Distribution and Origin

Anne H. Peslier[1] · Maria Schönbächler[2] · Henner Busemann[2] · Shun-Ichiro Karato[3]

Received: 21 November 2016 / Accepted: 3 June 2017 / Published online: 9 August 2017

Abstract The concentration and distribution of water in the Earth has influenced its evolution throughout its history. Even at the trace levels contained in the planet's deep interior (mantle and core), water affects Earth's thermal, deformational, melting, electrical and seismic properties, that control differentiation, plate tectonics and volcanism. These in turn influenced the development of Earth's atmosphere, oceans, and life. In addition to the ubiquitous presence of water in the hydrosphere, most of Earth's "water" actually occurs as trace amounts of hydrogen incorporated in the rock-forming silicate minerals that constitute the planet's crust and mantle, and may also be stored in the metallic core. The heterogeneous distribution of water in the Earth is the result of early planetary differentiation into crust, mantle and core, followed by remixing of lithosphere into the mantle after plate-tectonics

This article has been corrected. Figure 3 was initially published with erroneous data because in Fig. 3B and 3D the x axis should be Cpx H_2O, instead of Grt H_2O.

The Delivery of Water to Protoplanets, Planets and Satellites
Edited by Michel Blanc, Allessandro Morbidelli, Yann Alibert, Lindy Elkins-Tanton, Paul Estrada, Keiko Hamano, Helmut Lammer, Sean Raymond and Maria Schönbächler

Electronic supplementary material The online version of this article (doi:10.1007/s11214-017-0387-z) contains supplementary material, which is available to authorized users.

✉ A.H. Peslier
anne.h.peslier@nasa.gov

M. Schönbächler
mariasc@ethz.ch

H. Busemann
henner.busemann@erdw.ethz.ch

S.-I. Karato
shun-ichiro.karato@yale.edu

[1] Jacobs, NASA-Johnson Space Center, Mail Code XI3, Houston, TX 77058, USA

[2] Institute of Geochemistry and Petrology, Department of Earth Sciences, ETH Zurich, Clausiusstrasse 25, 8092 Zurich, Switzerland

[3] Department of Geology and Geophysics, Yale University, New Haven, CT 06520, USA

started. The Earth's total water content is estimated at 18^{+81}_{-15} times the equivalent mass of the oceans (or a concentration of 3900^{+32700}_{-3300} ppm weight H_2O). Uncertainties in this estimate arise primarily from the less-well-known concentrations for the lower mantle and core, since samples for water analyses are only available from the crust, the upper mantle and very rarely from the mantle transition zone (410–670 km depth). For the lower mantle (670–2900 km) and core (2900–4500 km), the estimates rely on laboratory experiments and indirect geophysical techniques (electrical conductivity and seismology).

The Earth's accretion likely started relatively dry because it mainly acquired material from the inner part of the proto-planetary disk, where temperatures were too high for the formation and accretion of water ice. Combined evidence from several radionuclide systems (Pd-Ag, Mn-Cr, Rb-Sr, U-Pb) suggests that water was not incorporated in the Earth in significant quantities until the planet had grown to $\sim$ 60–90% of its current size, while core formation was still on-going. Dynamic models of planet formation provide additional evidence for water delivery to the Earth during the same period by water-rich planetesimals originating from the asteroid belt and possibly beyond. This early delivered water may have been partly lost during giant impacts, including the Moon forming event: magma oceans can form in their aftermath, degas and be followed by atmospheric loss. More water may have been delivered and/or lost after core formation during late accretion of extraterrestrial material ("late-veneer"). Stable isotopes of hydrogen, carbon, nitrogen and some noble gases in Earth's materials show similar compositions to those in carbonaceous chondrites, implying a common origin for their water, and only allowing for minor water inputs from comets.

Keywords Water · Hydrogen · Earth · Crust · Mantle · Core · Delivery · Origin · Solar system

1 Introduction

The importance of water for the development of life on Earth renders this compound one of the most intriguing for investigations aimed at understanding our origins. Water in the Earth is rarely present as H_2O molecules but is most abundant in the form of hydrogen (H) dissolved in various minerals of the planet's interior. Because of the ample abundance of H in the universe and its small size, it is likely present in nearly all phases, from the Earth's atmosphere to its core. Although water typically exists in trace quantities in the deep Earth, it influences tremendously how the Earth evolved from its formation, to its so far unique plate tectonic regime and with liquid water oceans on its surface.

This chapter summarizes the current knowledge of the water content of the Earth, the water distribution between our planet's different layers, and the water fluxes between these reservoirs. To this end, a vast range of data is utilized, encompassing actual measurements of water concentrations in crustal and mantle rock samples, experiments simulating the Earth's interior conditions for chemistry and rheology, geophysical data such as seismic wave propagation, electrical and thermal conductivities, ab initio calculations of molecular dynamics, and geodynamical and planetary accretion models.

This chapter also examines when water was incorporated into the Earth throughout its history, i.e. during and/or after the planet's accretion from the protoplanetary disk, using the latest findings from the isotopes of moderately volatile elements. Finally, we address from where in the solar system the Earth's water possibly originated, based on constraints from H isotopes and the behavior of other volatile elements and isotopes.

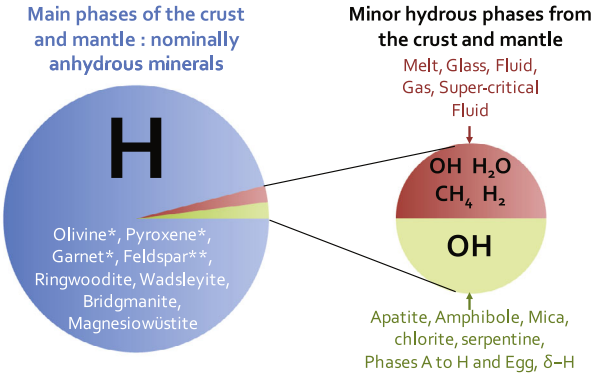

Fig. 1 Sketch illustrating the "water" species present in the various phases of the Earth's mantle and crust. The size of the pie slices represents the approximate volume percentage of the phases. The main reservoir of water in the mantle is nominally anhydrous minerals where hydrogen (H) enters their lattice in defects, and bonds to structural oxygen (*blue field*) (Bell and Rossman 1992b). *Olivine, pyroxene and garnet can incorporate water as H_2 under reduced conditions (Yang et al. 2016). **K-feldspar can sometimes include water as H_2O and NH_4 (Johnson and Rossman 2004)

2 Background

2.1 Definition of "Water"

Although water is primarily in the form of H_2O molecules in the hydrosphere (atmosphere and oceans), deeper in the Earth, what is generally referred to as "water" is actually H incorporated as various species in minerals, melts and fluids (Fig. 1). In the latter, i.e. *silicate/carbonate melts or volatile-rich fluids*, H can occur as water H_2O, hydroxyl OH, hydrogen gas H_2, methane CH_4, hydrogen sulfide H_2S, and possibly more complex H-bearing molecules at high pressures (e.g., Stolper 1982; Dixon et al. 1988; Carroll and Webster 1994; Kohn 2000; Luth 2003; Mookherjee et al. 2008; Song et al. 2009; Zhang and Duan 2009; Hirschmann et al. 2012; Bali et al. 2013; Armstrong et al. 2015). Melts and aqueous fluids are generally thought to become miscible at high pressure (> 6 GPa) in the upper mantle and the resulting super-critical fluids may contain water as both H_2O and OH (e.g., Kennedy et al. 1962; Bureau and Keppler 1999; Mibe et al. 2007). The relative proportions of these H-bearing species in fluids depend on melt composition and structure, the concentrations of other volatiles (C, F, Cl, S), pressure, temperature, water and oxygen fugacities (Holloway and Blank 1994). For example, methane and H_2 are present in fluids in reduced environments while OH and H_2O are prominent in oxidized conditions (e.g., Matveev et al. 1997; Frost and McCammon 2008; Mysen et al. 2009). When a melt is quenched at the surface in a volcanic eruption or in an experiment at high temperature (> 700 °C), the relative proportions of water species may change and the glass incorporates H principally as H_2O with minor OH (Shen and Keppler 1995; Zhang 1999; Kohn 2000).

Hydrous minerals incorporate "water" as hydroxyl OH. These hydrous phases such as mica, amphibole, apatite, serpentine and chlorite are only stable at relatively low mantle temperatures (e.g., Luth 2003). Consequently, these minerals play an important role in carrying water into the deep mantle in subducting slabs, which are cold relative to the surrounding mantle. Once in the deeper mantle, these hydrous minerals transform into high-pressure minerals such as phases B, D, H, Egg and AlOOH (e.g., Frost 2006;

Smyth 2006). Hydrous minerals contain H as a major stoichiometric element, but occupy only a small fraction of the total mantle.

The main phases of the mantle and crust are *nominally anhydrous minerals* (NAM) in which water is only present as a trace element (< 0.1 weight %). The main mineral phases are olivine ($(Mg, Fe)_2SiO_4$), pyroxene ($(Mg, Fe, Ca)SiO_3$), feldspar ($(K, Na, Ca_{0.5})AlSi_3O_8$) and garnet ($(Mg, Fe, Ca)_3Al_2Si_3O_{12}$) at depth < 410 km and high pressure forms of olivine called ringwoodite and wadsleyite as well as perovskite (of compositions (Mg, Fe, Al)(Si, Al)O_3 and $CaSiO_3$) at deeper mantle levels. In these phases, "water" is in reality H located in defects of the crystal lattice and bonded to structural oxygen (e.g., Beran 1976; Bell 1992; Rossman 1996; Johnson and Rossman 2004; Smyth 2006; Wright 2006). Interestingly, a recent study has evidenced that water could also be present as H_2 molecules in olivine, pyroxene and garnet under the reduced conditions prevailing in parts of the upper mantle (Yang et al. 2016). A significant amount of Earth's water is located in nominally anhydrous minerals, probably amounting to more than one mass of the Earth's oceans stored in this manner in the Earth's mantle (see Sect. 3.2). Several additional oceans' mass equivalents could also be stored in the metallic core (see Sect. 3.3). As a result, this chapter uses a very wide definition for the word "water", in most cases referring to H incorporated in silicate minerals. Water concentrations are reported here in part per million weight H_2O (ppm wt H_2O) in silicate phases and in ppm wt H in metals.

2.2 Chemical Behavior of Water in the Earth's Interior

To understand the water distribution in the Earth's interior, four key behaviors of water are relevant: (1) *incompatible partitioning behavior between melt and solid*, (2) *fast diffusion*, (3) *degassing from magmas and* (4) *sub-solidus re-equilibration*. These four topics are discussed in more detail below as well as how these features can affect the final water content measured in geological samples.

First, during melting of rocks or crystallization of melts, *water behaves as an incompatible element*, i.e. preferentially partitions into a silicate melt relative to a silicate solid (Moore 1970; Dixon et al. 1988; Michael 1988; Koga et al. 2003; Aubaud et al. 2004, 2008; Hauri et al. 2006; Grant et al. 2007b; Tenner et al. 2009; O'Leary et al. 2010; Hamada et al. 2013; Novella et al. 2014; Rosenthal et al. 2015). In contrast to previous assumptions, growing evidence shows that H is less incompatible than K or the light rare earth elements (LREE, e.g., Ce) (discussion in Sect. 3.2.2). Regarding conditions relevant to the Earth's core, H is incompatible in a solid-melt iron system, and may even still partition into Fe melt in the presence of silicate melt at these high pressures (Okuchi 1997; Okuchi and Takahashi 1998).

Second, *H is one of the fastest diffusing elements* in silicate melts and nominally anhydrous minerals at typical pressures and temperatures in the Earth's interior (e.g., Kohlstedt and Mackwell 1998; Demouchy and Mackwell 2006; Ingrin and Blanchard 2006; Farver 2010; Zhang and Ni 2010; Johnson and Rossman 2013; Padrón-Navarta et al. 2014; Sun et al. 2015; Ferriss et al. 2016). Careful consideration is therefore necessary to ascertain the significance of measured concentrations in natural minerals of mantle rocks and lavas because water may be lost or gained by diffusion during transit from the mantle to the surface. Mantle samples can be brought up to the surface as chunks, called xenoliths, ripped from the mantle as magma ascends through it. In these, olivine can sometimes experience H loss by diffusion even if a typical host-magma (alkali basalt or kimberlite) takes less than a day to travel from the mantle to the surface (Demouchy et al. 2006; Peslier and Luhr 2006; Peslier et al. 2008, 2015; Denis et al. 2013; Thoraval and Demouchy 2014). Recently, H loss has also been evidenced in orthopyroxene from mantle

xenoliths (Tian et al. 2017). In contrast, transfer of water from a host magma to the minerals of a xenolith has not yet been observed and experimental data indicates no water addition from a kimberlite melt to olivine in less than a day (Baptiste et al. 2015). On the other hand, H loss by diffusion is likely pervasive in minerals from erupted basaltic magmas, whose sources are located in the mantle (Jamtveit et al. 2001; Wade et al. 2008; Hamada et al. 2011; Nazzareni et al. 2011; Xia et al. 2013b; Liu et al. 2015; Weis et al. 2015; Edmonds et al. 2016). Finally, on the Earth's surface, alteration of minerals or glasses can occur through interaction with meteoritic and oceanic water or hydrothermal fluids, and this needs to be carefully assessed. Modification of water concentration and/or speciation by such alteration has been evidenced in silicate glass, feldspar and apatite (e.g., Friedman et al. 1966; Johnson and Rossman 2004; Webster and Piccoli 2015; Seligman et al. 2016).

The third behavior of water that can affect the water content of natural samples is *magma degassing*. As the magmas reach upper crustal levels and pressure decreases, volatiles become less soluble in silicate melts and exsolve as a gas phase (e.g., Sparks et al. 1994). Degassing is a strong concern for most analyses of silicate glasses, because their water concentration may not reflect that of their parent melt (e.g., Dixon et al. 1991; Dixon 1997; Clay et al. 2015). Some silicate glasses, which were quenched fast enough or erupted under significant pressure, for example at the bottom of the ocean (> 500 m of water column) or under a significant volume of ice, experience only minimal degassing (Moore and Schilling 1973; Jambon and Zimmermann 1987; Dixon and Stolper 1995; Saal et al. 2002). The water content of silicate melts can also be inferred from that of melt inclusions, drops of melt trapped early in the crystallization sequence of a magma in a growing mineral such as olivine, spinel, garnet, or diamond. Encapsulation by these host minerals may prevent the inclusion from losing its water during magma ascent (Danyushevsky 2002; Wallace 2005; Kent 2008). However, disturbances of the water content in melt inclusions in olivine are documented and need careful evaluation prior to data interpretation (Chen et al. 2013; Lloyd et al. 2013, 2014; Le Voyer et al. 2014; Hartley et al. 2015).

Finally, the fourth important process affecting water in mantle rocks is *sub-solidus re-equilibration*. In the case of the slow (several Ma) tectonic rise of mantle units (i.e., orogenic massifs or abyssal peridotites), re-distribution of water (H) among co-existing minerals likely occurs because the hydrogen partition coefficient between minerals is a function of the thermodynamic conditions and mineral composition (Katayama et al. 2006; Warren and Hauri 2014). Even peridotites found as xenoliths experienced sub-solidus re-equilibration. Subsequent re-distribution of their H among minerals occurs after peridotites, the residues of melting events at relatively high-temperatures, equilibrate at the lower temperatures of the ambient upper mantle after melting ceases (Schaffer et al. 2016).

In this chapter, all data are filtered to exclude any measurements of a phase affected by water loss or gain, and we only take into account initial (mantle or pre-degassing magmatic) water concentrations. All water concentrations and ancillary data for lower crustal and upper mantle samples used in this chapter are available in the online electronic supplementary Table 1.

2.3 Methods of Water Determination in the Earth's Interior

A brief summary of the techniques used to estimate the amount of water in the Earth's interior is given here. A comprehensive review of analytical techniques available to measure water in minerals and glasses of natural samples or experiments is given by Rossman (2006). Briefly, the two main techniques are Fourier transform infrared spectrometry (FTIR)

and secondary ion mass spectrometry (SIMS). Both now achieve similar detection limits (< 0.5 ppm wt H_2O) and have their own advantages and disadvantages. FTIR is a non-destructive technique that allows detection of the speciation of water and H-defect location (e.g., Libowitzky and Beran 2004), but requires cumbersomely made doubly-polished samples for transmission quantitative analysis. SIMS, on the other hand, can be performed on samples polished on a single side but is destructive. Its advantage is the simultaneous measurement of water concentration and H isotopes or other volatiles (Cl, F, C, S). Nano-SIMS can also achieve a smaller spatial resolution ($< 1 \times 1$ μm) compared to FTIR ($> 20 \times 20$ μm) (Hauri 2002; Hauri et al. 2011). SIMS, however, requires suitable standards (Hauri et al. 2002; Aubaud et al. 2007; Mosenfelder et al. 2011), while FTIR necessitates composition-specific absorption coefficients (Bell et al. 1995, 2003a; Johnson and Rossman 2003; King et al. 2004; Koch-Müller and Rhede 2010; Withers et al. 2012; Thomas et al. 2014; Mosenfelder et al. 2015). Geophysical methods such as seismology and electrical conductivity can be employed to infer the amount of water in the deep Earth (Jacobsen 2006; Karato 2006b, 2011). Among various geophysical observations, electrical conductivity is particularly useful because it is highly sensitive to the water content but relatively insensitive to other parameters such as major element chemistry, temperature and oxygen fugacity (Karato 2006a, 2011; Gardés et al. 2014).

3 Concentration and Distribution of Water in the Earth's Interior

3.1 Water in Crustal Minerals

A detailed account of the distribution of water in the crust is beyond the scope of this chapter. The crust contains many water-bearing minerals such as mica, amphibole and clay minerals in its igneous and metamorphic units and water-rich sediments (Taylor and McLennan 1985; Rudnick and Fountain 1995; Bodnar et al. 2013). Water is also present in pores and fractures. In the upper crustal lithologies, originating from basaltic to evolved igneous or metamorphic processes, trace amounts of water are incorporated in pyroxene, feldspar, quartz and olivine (Aines and Rossman 1984; Rossman and Smyth 1990; Nakashima et al. 1995; Kronenberg et al. 1996; Herd et al. 2000; Ito and Nakashima 2002; Johnson and Rossman 2003, 2004; Filip et al. 2006; Andrut et al. 2007; Müller and Koch-Müller 2009; Stalder and Konzett 2012; Seaman et al. 2013). The lower continental crust, primarily consists of granulite, and also contains water in nominally anhydrous minerals (Xia et al. 2006; Koch-Müller et al. 2007; Yang et al. 2008a; Seaman et al. 2013; Schmädicke et al. 2015). Finally, water can be found in accessory phases from crustal units of igneous or metamorphic origin like rutile, zircon, quartz and kyanite (Vlassopoulos et al. 1993; Bell et al. 2004a; Beran and Libowitzky 2006; Lucassen et al. 2013; De Hoog et al. 2014). The average water content of the continental crust (amphibolite + granulite) is estimated to be ~ 1.3 wt% H_2O (0.1–5 wt% H_2O), while that of the oceanic crust (basalt + gabbro) is ~ 1.5 wt% H_2O (Bodnar et al. 2013).

3.2 Water in the Mantle

3.2.1 Water in the Continental Mantle Lithosphere

The Earth's lithosphere is on average thickest under continents, particularly beneath the oldest crustal units, that can date back to the Archean (Jordan 1978; Boyd et al. 1985;

Artemieva and Mooney 2001; Sleep 2005; Priestley and McKenzie 2006; Eaton et al. 2008; Rychert and Shearer 2009; Fisher et al. 2010; Yuan and Romanowicz 2010). These old parts of the continental lithosphere are called cratons and can be 200–300 km thick. In that respect, these cratonic roots resemble the submerged part of icebergs in the ocean (analog of the asthenosphere). They are isolated from asthenospheric convection and are thus colder than the surrounding asthenosphere with heat transmitted through conduction (e.g., Jaupart and Mareschal 1999; Michaut et al. 2009). The amount and distribution of water in the mantle lithosphere below the continental crust is especially well documented because of the abundance of mantle xenoliths and other mantle samples (megacrysts, diamonds) found in these settings.

Water in Olivine and Lithospheric Strength The amount of water stored in the continental lithosphere has implications on how strong and rigid tectonic plates are. The old ages of cratonic roots are a particularly puzzling case (e.g., Walker et al. 1989; Pearson et al. 1995a; Griffin et al. 2004). They are surrounded by hotter convecting asthenosphere and therefore would be expected to be eroded and destroyed from below, i.e. "delaminated", over > 3 billion year (Ga). Water plays a fundamental role in how the mantle lithosphere resists delamination over time by influencing its deformation properties (e.g., Mackwell et al. 1985; Pollack 1986; Karato 1993, 2010; Hirth et al. 2000; Sleep 2003; Lee et al. 2010; Wang 2010).

The key to evaluating the strength of the mantle lithosphere relative to that of the asthenosphere is the mineral olivine, the main mineral of the upper mantle (> 50% in volume) in its dominant lithology, peridotite (Boyd 1989; Griffin et al. 2009). The presence of trace amounts of water (tens of ppm wt H_2O) in its structure weakens olivine (e.g., Mackwell et al. 1985; Demouchy et al. 2012; Girard et al. 2013; Faul et al. 2016; Tielke et al. 2017). The distribution of olivine with different water contents in the lithospheric mantle (lateral and with depth) is thus of particular importance for assessing lithospheric strength. In contrast, water does not weaken clinopyroxene, and the weakening effect on orthopyroxene depends on mineral orientation (Gavrilenko et al. 2010; Ohuchi et al. 2010). The fact that olivine is the most interconnected phase of the upper mantle causes its hydrolytic weakening properties to control the weakening of peridotite, even though olivine typically contains about 10 times less water than pyroxenes (e.g., Peslier 2010; Demouchy and Bolfan-Casanova 2016). Figure 2A shows water concentrations in olivine as a function of depth for peridotite xenoliths from the Kaapvaal (Southern Africa), Siberian (Russia) and Tanzanian (Eastern Africa) cratons (Kurosawa et al. 1997; Grant et al. 2007a; Peslier et al. 2008, 2010; Baptiste et al. 2012; Doucet et al. 2014; Hui et al. 2015). The depth, i.e. the pressure at which equilibration occurred, and the equilibration temperature are obtained by comparing the major element composition of peridotite minerals (for example Al exchange between orthopyroxene and garnet) to those of laboratory experiments calibrated at known pressures (e.g., Brey and Köhler 1990). Each craton has a different water concentration distribution with depth (Fig. 2A). The Tanzanian craton displays the lowest concentrations (1–39 ppm wt H_2O), that of the Kaapvaal craton is characterized by water-poor olivines (< 10 ppm wt H_2O) at > 190 km and the Siberian craton exhibits the largest range of water contents (7–223 ppm wt H_2O).

These water contents, along with equilibration temperatures and pressures, can be inserted into a flow law for the deformation of olivine aggregates (Li et al. 2008). Viscosity variation with depth in each craton (i.e., along the cratonic geotherm) can then be calculated for a constant water content (curves in Fig. 2B) or for individual peridotite samples (symbols in Fig. 2B). The majority of the calculated viscosities for individual peridotites are

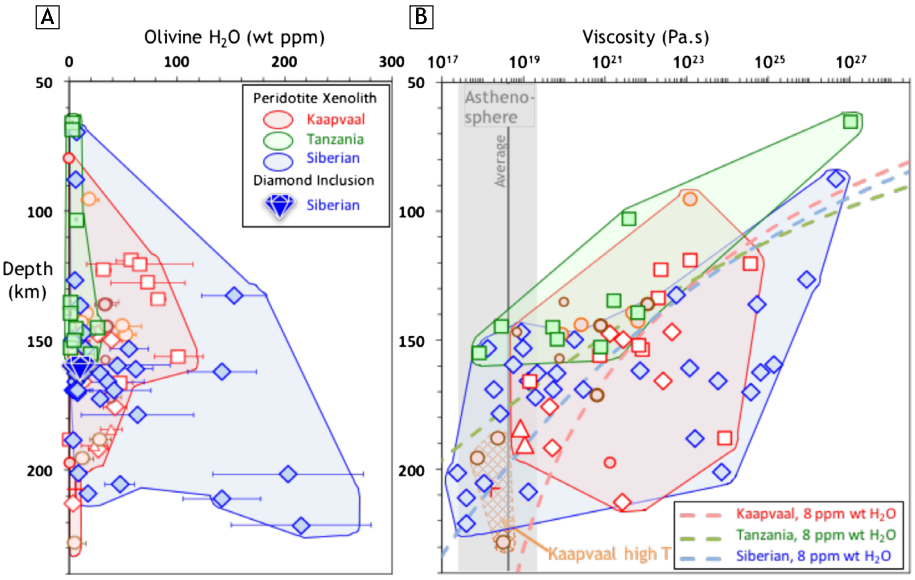

Fig. 2 **A**: Water contents of olivine versus depth of equilibration for peridotites from the mantle lithosphere of the Kaapvaal, Siberian and Tanzanian cratons. Each symbol represents one peridotite xenolith (Kurosawa et al. 1997; Grant et al. 2007a; Peslier et al. 2008, 2010; Baptiste et al. 2012; Doucet et al. 2014; Hui et al. 2015; Kolesnichenko et al. 2016), except the diamond which represents the average of the water contents of 29 olivine inclusions found in diamonds from the Siberian craton (Novella et al. 2015; Jean et al. 2016; Taylor et al. 2016). Although the pressure of equilibration of the olivine inclusions in diamonds is not precisely known, they are shown here at 5 GPa (~ 160 km depth), a formation pressure determined for a Siberian craton diamond from the same location, the Udachnaya kimberlite field (Nestola et al. 2011). The *red symbols* correspond to different kimberlite locations where the xenoliths were found in the Kaapvaal (*circle*: various Lesotho locations, *square*: Kimberley, *triangle*: Finsh, *cross*: Premier). The Siberian and Tanzanian craton xenoliths come from only one location in each craton (Udachnaya and Labait, respectively). Water contents obtained from FTIR data are calculated with the absorption coefficient of Withers et al. (2012). **B**: Viscosity versus depth of equilibration calculated for each xenolith using the water content measured in olivine and its equilibration depth entered in a flow law for olivine aggregates. Viscosity calculated for 8 ppm wt H_2O in olivine along the pressure-temperature variation of the geotherm of each craton is also shown (*dashed lines*). The Tanzanian craton has a hotter geotherm than the two others. The range and average viscosity of the asthenosphere is shown in grey. At depths < 200 km, peridotites from the Kaapvaal and Siberian craton record viscosities higher than that of the asthenosphere, consistent with a strong mantle lithosphere. At depths > 200 km, the peridotites from the Kaapvaal that have anomalous high temperatures (Kaapvaal high T field, their high temperatures being linked to a Mesozoic heating event (Thaba Putsoa) or plume event (Premier); Pearson et al. 1995a; Bell et al. 2003b) and the peridotites from the Siberian craton have similar viscosities to that of the asthenosphere

consistent with the mantle lithosphere at depths < 180 km having a higher viscosity than the asthenosphere (Fig. 2B). This indicates that the water contents and equilibration temperatures are consistent with a rigid lithosphere, as expected (Pollack 1986; Karato 1993; Hirth et al. 2000; Sleep 2003).

The viscosities at the bottom of the lithosphere (> 200 km depth), however, are the ones that warrant closer inspection to understand why cratonic roots do not get delaminated by the surrounding asthenosphere. A high viscosity contrast between the lithosphere and the asthenosphere (> 3 to > 50 times depending on estimated conditions) is necessary for the survival of a cratonic root for several billion years (Shapiro et al. 1999; Sleep 2003; O'Neill et al. 2008; Karato 2010; Wang et al. 2014). Viscosity estimates for the astheno-

sphere can be inferred from post-glacial rebound and earthquake data (Pollitz et al. 1998; Sjöberg et al. 2000; Larsen et al. 2005; Fleming et al. 2007; Masuti et al. 2016). The viscosity calculated for the deepest xenoliths from the Kaapvaal craton is high enough compared to the asthenosphere average viscosity to suggest that the low water content of olivines at the base of that craton could play a role to maintain its strength and help prevent its delamination (Fig. 2B, Peslier et al. 2010).

On the other hand, the viscosities calculated for the deepest Siberian craton xenoliths or for the anomalous high-temperature Kaapvaal peridotites are similar to those of the asthenosphere (Fig. 2B, Doucet et al. 2014). If these xenoliths were representative of the cratonic root, that of the Siberian craton should have been delaminated. However, we know that the Siberian craton still has a deep cratonic root as evidenced by the presence of xenoliths equilibrated down to $>$ 200 km (7 GPa) and by seismic data (Priestley and Debayle 2003). In contrast, olivine inclusions in diamonds from the Siberian craton, all display low water contents (average 8 ± 8 ppm wt H_2O; Novella et al. 2015; Jean et al. 2016; Taylor et al. 2016). Consequently, the xenoliths with high water contents in olivine cannot be representative for the overall Siberian craton. They instead represent a biased sampling of local water-rich zones in the mantle (see next paragraph).

The kimberlites, the host magma of xenoliths in cratonic settings, may use some of these water-rich zones, perhaps shear zones, in the mantle lithosphere as conduits to pass through (Doucet et al. 2014). Interestingly, there may be a link between metasomatic conduits in the mantle and the formation of kimberlite melts. Modification of the cratonic mantle by melts and fluids (metasomatism) is often characterized by the formation of orthopyroxene (Kelemen et al. 1998). It has also been proposed that melts of kimberlitic composition may be generated by carbonatite melts dissolving orthopyroxene (Russell et al. 2012). In this scenario, melts ultimately forming kimberlites would preferentially follow metasomatic zones with their abundance of orthopyroxenes and their relative high water concentrations. These melts also pick up mantle samples on their way to the surface (xenoliths, diamonds), but a large proportion of the xenoliths are thereby unrepresentative of the whole cratonic mantle, with compositions dominated by water-rich metasomatized peridotite. The water-poor olivine from diamond inclusions are likely more representative because encapsulation in diamond protected the olivines from being re-enriched in water by localized circulation of water-rich melts or fluids (Novella et al. 2015; Jean et al. 2016; Taylor et al. 2016). In particular, the viscosity-pressure curve calculated for 8 ppm wt H_2O and the Siberian craton geotherm intersects with the viscosity range of the asthenosphere at $\sim$ 200 km depth, i.e. close to the lithosphere-asthenosphere boundary. This suggests that the water content of olivine in the Siberian craton, as represented by that of olivine inclusions in diamond, have low enough water contents to provide the high viscosities that are necessary for preserving a thick (200 km) cratonic root from delamination.

Additional evidence for the "dry" nature of cratonic mantle lithosphere comes from the interpretation of geophysical data: electrical conductivity and seismic anisotropy. The presence of hydrogen in minerals enhances their *electrical conductivity* (Karato 1990; Karato and Wang 2013; Pommier 2014). Electrical conductivity profiles across the Kaapvaal craton are best explained with olivine having $<$ 20 ppm wt H_2O at a depth of 100 km (Jones et al. 2013b). For the Slave craton in Canada, another thick Archean craton, electrical conductivity data is best modeled with olivine water contents decreasing from 150 to mostly $<$ 20 ppm wt H_2O from 100 to 200 km depth (Jones et al. 2013a). In the center of the Tanzanian craton, $<$ 100 ppm wt H_2O has been inferred for the mantle lithosphere between 90 km and the lithosphere-asthenosphere boundary. At the eastern edge of the craton, decreasing water contents from 10 ppm wt H_2O at 60 km depth to $<$ 1 ppm wt H_2O at 150 km

depth match best electrical conductivity data (Selway et al. 2014), i.e. the water contents are mostly lower than those measured in mantle xenoliths from this region (20 ± 12 ppm wt H_2O, Fig. 2A; Hui et al. 2015). Overall, electrical conductivity measurements reveal regional and depth variations of water concentrations, likely linked to local metasomatic enrichments (see next section on Water and Metasomatism). Interestingly, electrical conductivity also predicts low water contents at the base of the lithosphere of the Slave and Tanzanian cratons. These observations provide additional evidence that the deepest xenoliths with water-rich olivines are not representative of the overall cratonic lithosphere.

Observations of the dominant *micro-structure of cratonic mantle xenoliths* can also provide constraints on the amount of water present when the fabric was formed (Karato 2006a; Karato et al. 2008). Laboratory experiments on olivine-aggregate deformation constrain which type of fabric (lattice-preferred orientation, "LPO") forms as a function of water content, temperature and pressure (Jung and Karato 2001a, 2001b; Karato et al. 2008; Ohuchi et al. 2011; Ohuchi and Irifune 2013). However, results from these experiments are contradictory. For example, experiments at high pressures (7 GPa, i.e., $\sim$ 223 km depth) obtain the so-called "Type-A" fabric, i.e. a coarse ($>$ 1 mm grains) granular fabric, with high water contents ($>$ 127 ppm H_2O) in olivine. But at low pressures ($<$ 2 GPa or $<$ 64 km depth), it is experiments with low olivine water contents ($<$ 10 ppm H_2O) that generate the Type A fabric (Karato 2006a; Ohuchi and Irifune 2013). Moreover, the link between water content and fabric is not always obvious in natural samples. Observations in a tectonically-uplifted mantle section (Josephine peridotite) and in a xenolith suite from Udachnaya (Siberian craton) are nevertheless consistent with the more deformed fabrics associated with the highest water concentrations (Skemer et al. 2013; Kolesnichenko et al. 2016). However, no correlation was observed in Kaapvaal mantle xenoliths between the dominant fabric of peridotite (Type-A; Ben-Ismail et al. 2001) and their water content, suggesting that water could have been added locally after the main fabric was set, after melting and early deformation and annealing events (Baptiste et al. 2012). Water could also be lost from fabrics characteristic of formation in wet conditions (so called "E-type" fabric) if the final equilibration temperature of such a peridotite is low ($<$ 800 °C). This is because the solubility of water in olivine decreases with decreasing temperature (Chin et al. 2016). Deformation fabrics (LPO) are directly connected to the observed *seismic anisotropy*. Seismological observations of the cratonic lithosphere are most consistent with the dominance of the Type-A fabric (Mainprice and Silver 1993; Vinnik et al. 1996; Gung et al. 2003; Karato 2006b; Baptiste and Tommasi 2014). If further studies of natural mantle samples confirm that this fabric is generally associated with dry olivine it would imply that the cratonic mantle lithosphere has primarily olivines with $<$ 10 ppm wt H_2O at depths $<$ 190 km.

Water and Metasomatism Cratonic peridotites formed by partial melting in the Archean and Proterozoic, and are the solid residues of these melting processes (e.g., Walker et al. 1989; Pearson et al. 1995a, 1995b; Carlson et al. 1999; Doucet et al. 2015). Since then, however, their compositions have been modified by melts or fluids percolating through the cratonic lithosphere, i.e. they have been metasomatized. We now further investigate further the hypothesis of the previous section that the range of their water content is primarily the result of various degrees of metasomatism. To this end, we compare the variations of water content with those of other trace elements and with modal composition in olivine, pyroxene and garnet. Evidence for metasomatism in peridotites vary with the type of metasomatic agent involved (for example fluids, silicate melts of alkalitic, kimberlitic and ultramafic compositions, carbonatitic melts). It includes (i) addition of "secondary" clinopyrox-

ene or orthopyroxene, (ii) increase of the Ti content of garnet, (iii) increase of incompatible trace element concentrations like rare-earth elements (REE) and Na in clinopyroxene and (iv) oxidation (increase of $Fe^{3+}/\Sigma Fe$ in clinopyroxene, spinal and garnet) (e.g., Harte 1983; Menzies and Hawkesworth 1987; Kesson and Ringwood 1989; Boyd et al. 1997; Kelemen et al. 1998; Griffin et al. 1999; Lee and Rudnick 1999; Grégoire et al. 2003; Burgess and Harte 2004; Bell et al. 2005; Creighton et al. 2009; Ionov et al. 2010; Doucet et al. 2013).

Water contents of the peridotite minerals for individual cratonic xenolith suites exhibit positive trends with these metasomatism indicators as illustrated in Fig. 3. For example, the water content of garnet correlates with its Ti contents in two Kaapvaal xenoliths suites and also roughly in that of Udachnaya from the Siberian craton (Fig. 3A). The water content of clinopyroxene correlates with REE, Na and $Fe^{3+}/\Sigma Fe$ in clinopyroxene from Liqhobong xenoliths in the Kaapvaal craton (Fig. 3B). Importantly, the highest water contents in olivine of the Siberian xenoliths are associated with the highest clinopyroxene modal proportions (Fig. 3C) and the highest REE concentrations in clinopyroxene (not shown), highlighting the role of water-bearing metasomatic melts in the most water-rich Udachnaya xenoliths. Overall, these trends signify that the range of water contents in cratonic mantle xenoliths is linked to water addition by melts or fluids (Bell and Rossman 1992a; Peslier et al. 2012; Doucet et al. 2014). As discussed in the previous section, circulation of metasomatic agents through the lithosphere is probably facilitated in zones of preexisting weaknesses such as faults, ancient sutures or magma conduits. In addition, these zones are also likely the preferred path of kimberlite melt ascent, the host-magma that brings up xenoliths in cratonic settings. It is thus no surprise that the kimberlites would provide us with a biased sample of the cratonic lithosphere, with an overabundance of metasomatized and water-rich peridotite xenoliths.

On the other hand, olivine inclusions in diamonds from the Siberian craton are relatively unaffected by metasomatism. This is indicated by the relatively high forsterite contents (Mg/(Mg+Fe)) of these olivines combined with their low Ni, Co and Ti concentrations compared to those of most olivines from Udachnaya xenoliths (Fig. 3E and F) (Kelemen et al. 1998; Jean et al. 2016). The diamonds may thus have acted as a protective shell around their inclusions, preventing late interactions with water-bearing metasomatic agents. The inclusions, therefore, preserve a more representative cratonic water content of peridotite minerals (Novella et al. 2015; Taylor et al. 2016).

Similar conclusions can be derived from garnet and pyroxene inclusions in diamonds. Water contents of two peridotitic clinopyroxene from diamond inclusions are at the low end of the range (< 100 ppm H_2O) of their counterparts found in xenolith peridotites (Fig. 4B). In contrast, peridotitic garnet inclusions from diamonds display water contents that span the whole range of water contents of garnets from peridotite xenoliths (Fig. 4D). Garnet, however, is the phase with the least amount of water in peridotite (< 30 ppm H_2O, Fig. 4). Eclogitic garnet inclusions in diamond, on the other hand, have lower water contents than garnet in eclogite xenoliths (Fig. 4C). These observations are based on limited data, but are overall consistent with the conclusion that diamonds protect their pyroxene and garnet inclusions from interaction with water-bearing metasomatizing agents, as we discussed above for olivine inclusions in diamond.

Two small cratons stand out compared to the larger Kaapvaal and Siberian cratons in terms of pyroxene water contents: the Tanzanian craton peridotites have low water contents, and those from the Colorado Plateau (USA) have high water contents compared to those of the Kaapvaal craton (Fig. 4B and 4C; Li et al. 2008; Hui et al. 2015). The high water contents of the Colorado peridotites were explained by metasomatism induced by subduction-related

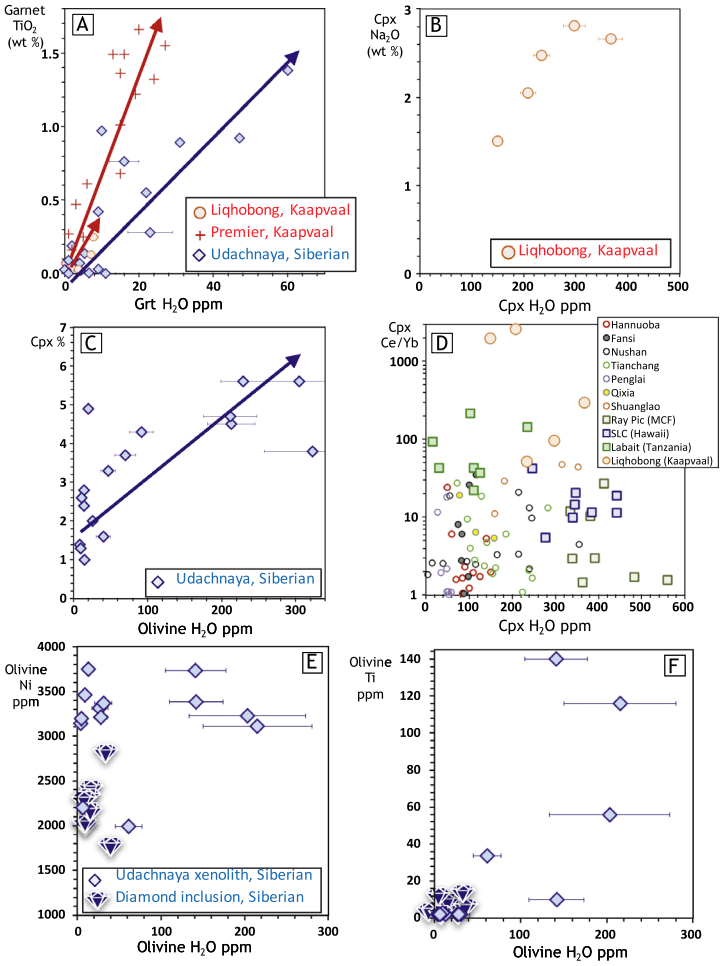

Fig. 3 Examples of water content variation with indices of metasomatism in mantle minerals. **A**: Garnet Ti concentrations increase with increasing water contents in three cratonic xenoliths suites (Premier, Kaapvaal craton, Bell and Rossman 1992a, Liqhobong, Kaapvaal craton, Peslier et al. 2012 and Udachnaya, Siberian craton, Doucet et al. 2014). *Arrows* indicate the trends. **B**: The Na_2O and water contents of clinopyroxene are positively correlated in Liqhobong clinopyroxenes (Kaapvaal craton; Peslier et al. 2012). **C**: Water contents of Udachnaya olivine increase with the modal proportion of clinopyroxene in peridotites from the Siberian craton (Doucet et al. 2014). These trends illustrate that the highest water contents measured in peridotite minerals from cratonic xenoliths can be explained by the addition of water by metasomatic fluid or melts. **D**: Water content versus Ce/Yb ratio of clinopyroxene from various xenolith suites in plume-lithosphere tectonic settings (*square symbols*), cratonic setting (*large round symbols*, Liqhobong, Kaapvaal), and Phanerozoic continental lithosphere beneath China (*small round symbols*) (Yang et al. 2008b; Xia et al. 2010, 2013a; Peslier et al. 2012; Denis et al. 2015; Hui et al. 2015; Hao et al. 2016). Cerium is more incompatible than Yb resulting in Yb primarily reflecting melting processes, while Ce is sensitive to metasomatism by REE-bearing melts. The lack of correlation between water content and Ce/Yb ratio indicates that water and LREE like Ce are decoupled during metasomatism of nominally anhydrous minerals. Error bars on the clinopyroxene water contents are omitted in **D** for clarity. Cpx = clinopyroxene, MCF = Massif Central in France, SLC = Salt Lake Crater. **E** and **F**: Water versus Ni and Ti concentrations in Siberian craton mantle olivines. The low water, Ni and Ti concentrations of the olivines from diamond inclusions relative to those found in xenoliths may indicate that diamonds protected the inclusions from being metasomatized and enriched in water. In contrast, most olivines found in peridotites have high Ni, Ti and water contents derived from metasomatism (Jean et al. 2016)

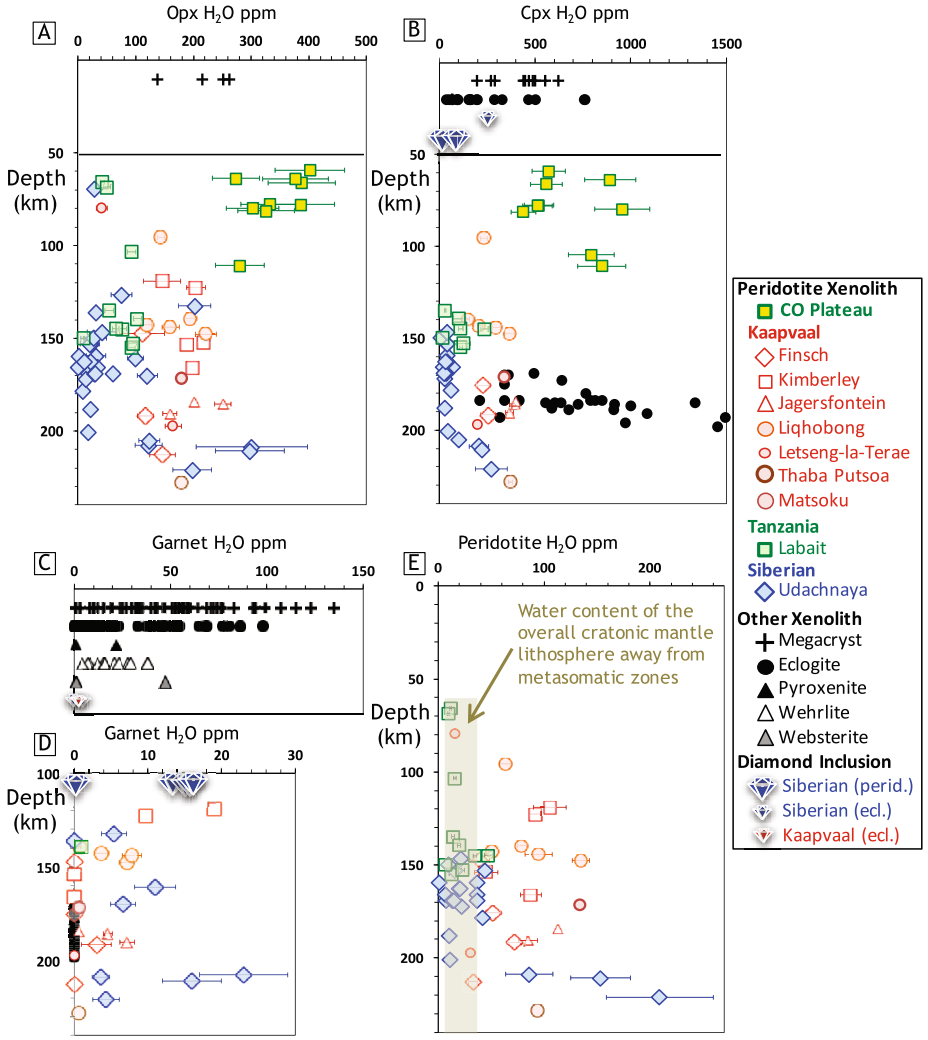

Fig. 4 Water contents of orthopyroxene (Opx), clinopyroxene (Cpx), garnet and those calculated for bulk-rock peridotites versus depth in the cratonic mantle lithosphere for mantle xenoliths from the Kaapvaal, Siberian, Tanzanian, and Colorado (CO) plateau cratons (Bell and Rossman 1992b; Grant et al. 2007a; Li et al. 2008; Sundvall and Stalder 2011; Peslier et al. 2012; Doucet et al. 2014; Hui et al. 2015; Kolesnichenko et al. 2016). Water contents in minerals from non-peridotitic lithologies from the Kaapvaal and Siberian cratons are shown at the top of the diagrams when their depth of equilibration is not known (Smyth et al. 1991; Bell and Rossman 1992a; Matsyuk et al. 1998; Bell et al. 2004b; Koch-Müller et al. 2004, 2007; Matsyuk and Langer 2004; Sundvall and Stalder 2011; Huang et al. 2014). The water contents of clinopyroxene and garnet inclusions in diamonds from the Siberian and Kaapvaal cratons are also shown in **B**, **C** and **D** (Bell and Rossman 1992a; Novella et al. 2015; Jean et al. 2016; Taylor et al. 2016)

water-rich melts, which were initiated by the Farallon plate subducting beneath the southwestern US (Usui et al. 2003; Dixon et al. 2004; Li et al. 2008; Behr and Smith 2016). The relative "dryness" of the peridotite minerals from the Tanzanian craton, however, is

puzzling because this craton is placed on top of one of the largest deep mantle upwelling (plume) of the Earth and has been extensively metasomatized by it (Lee and Rudnick 1999; Aulbach et al. 2008). Although no water measurements in melts erupted from that plume exist, plume melts are generally considered water-rich (see section on oceanic mantle below). The interpretation for the low water content of the Tanzanian xenoliths is that either the plume melts that metasomatized that craton were water-poor, or water and other incompatible elements were decoupled during the metasomatizing process (Hui et al. 2015).

Decoupling of incompatible elements and H during metasomatism has also been observed in peridotites from off cratonic settings and is illustrated by the lack of correlations between water content and the Ce/Yb ratio of clinopyroxene in individual xenolith suites (Fig. 3D) (Yang et al. 2008b; Xia et al. 2010, 2013a; Peslier et al. 2012; Denis et al. 2015; Hui et al. 2015; Hao et al. 2016). Finally, melt inclusions in olivine that are particularly water-rich (2–4 wt% H_2O for undegassed ones) from Columbia River basalts (USA, a plume setting impinging on continental lithosphere) were interpreted as their source being a mantle enriched in water by prior subduction events and re-melted during plume upwelling (Cabato et al. 2015).

Other cratonic mantle lithologies besides peridotites have been analyzed for water (Smyth et al. 1991; Bell and Rossman 1992a; Matsyuk et al. 1998; Bell et al. 2004b; Koch-Müller et al. 2004, 2007; Matsyuk and Langer 2004; Huang et al. 2014). Megacrysts represent crystallized minerals from melts in the mantle lithosphere, pyroxenites represent crystallized cumulate melts or metasomatic veins at depth, while eclogites may represent either crystallized melts or remnants of subducted slabs (e.g., MacGregor and Manton 1986; Smyth et al. 1989; Bodinier and Godard 2003; Foley et al. 2003; Bell and Moore 2004; Jacob 2004). The water content of pyroxene and garnet from these lithologies extend to more water-rich values than those of peridotites (Fig. 4). This can be explained by the incompatible behavior of water; these crystallized melts become enriched in water relative to the peridotites which are the melting residues. For the same reason, the water content of megacrysts correlates with major and trace elements concentrations which reflect crystallization processes of melts in the mantle (Bell and Rossman 1992a; Bell et al. 2004b). More exotic and rare lithologies with a high proportion of hydrous minerals such as the PIC and MARID xenolith suites (for mica (phlogopite)–ilmenite–clinopyroxene and mica–amphibole–rutile–ilmenite–clinopyroxene (diopside), respectively) may represent locally crystallized water-rich metasomatic melts (Dawson and Smith 1977; Grégoire et al. 2002; Konzett et al. 2014). Interestingly, the type of volcanism characteristic of cratonic settings, kimberlites, is characterized by volatile-rich (mainly CO_2 and H_2O) compositions as evidenced from a high proportion of hydrous minerals and the explosive character of their eruption (Mitchell 1986; Russell et al. 2012; Sparks 2013). There is a controversy, however, on when the kimberlite magmas acquired their water. One possibility is that kimberlite parent melts are water-rich, and they could be the surface expression of the PIC and MARID mantle melts (Dawson and Smith 1977; Sweeney et al. 1993; Konzett et al. 1998; Grégoire et al. 2002). However, there is growing evidence that most of the water contained in kimberlites was acquired during hydrothermal processes at the surface while their source was carbonate-rich rather than water-rich (Russell et al. 2012; Giuliani et al. 2014; Kamenetsky et al. 2014).

Summary of Water Content Distribution in the Continental Lithosphere The bulk-rock water contents of cratonic peridotite xenoliths, calculated from the water content measured in individual minerals combined with the modal mineralogy, range from 7 to 209 ppm wt H_2O (average 65 ± 47 ppm wt H_2O, Fig. 4E). However, the cratonic lithosphere is mostly

dry, as indicated by mineral inclusions in diamonds. There are localized water-rich zones linked to melt/fluid infiltration which are over-represented in the xenolith population. Eight ppm wt H_2O is a reasonable estimation for the water content of cratonic olivine, and this amounts to $\sim 24 \pm 21$ ppm wt H_2O in the overall cratonic lithosphere when pyroxene is taken into account (Table 1). The low water content of olivine in the overall cratonic lithosphere contributes to the strength and longevity of cratonic root for billions of years.

Water contents vary regionally in the off-craton continental mantle lithosphere. For example, peridotite xenolith suites with low or no water content in their minerals (Letseng-la-Terae in Lesotho in the Kaapvaal craton or Nuomin in northeast China) are found < 100 km away from peridotite xenoliths containing several hundreds ppm H_2O (Peslier et al. 2012; Hao et al. 2016). Similarly, water-rich pyroxenes from the Colorado plateau (USA) or Jiande (southwest China) lithospheric mantle are localized occurrences (Li et al. 2008; Hao et al. 2014).

The water content of the lithospheric mantle is therefore highly heterogeneous laterally on a regional scale but also vertically with depth. These water content variations originated from the local melting and metasomatic history of the mantle, that was sampled as xenoliths or diamond inclusions by each alkali basalt or kimberlite host-magma. Overall they depend on the pressure, the temperature and oxygen fugacity conditions at any given depth, and thereby water fugacity.

Water Solubility in Minerals Laboratory experiments equilibrating a water-bearing fluid with a silicate mineral provide estimates of solubility for a variety of temperature, pressure, oxygen and water fugacity conditions and fluid composition. Such experiments are particularly useful to constrain the maximum amount of water (i.e. "storage capacity", Hirschmann et al. 2005) that could be present at depths in the Earth from which samples are not available (see Sect. 3.2.3 on the transition zone and Sect. 3.2.4 on the lower mantle).

The first important observation is that mantle minerals from xenoliths have lower water contents compared to their maximum storage capacity estimated from experiments (Bali et al. 2008; Ardia et al. 2012; Férot and Bolfan-Casanova 2012; Tenner et al. 2012; Yang et al. 2014; Yang 2015). This implies that the lithospheric mantle is under-saturated in water (Fig. 5).

The second observation is that the solubility of water in olivine increases with increasing pressure, and these predictions from experiments are in agreement with the maximum amounts of water reported for olivine from mantle xenoliths at a given depth (Demouchy and Bolfan-Casanova 2016). Water solubility strongly depends on the volatile species present in the fluid: pure H_2O fluid results in a higher solubility of water in olivine compared to that of a fluid with less water, but containing other volatile species like CO_2, H_2 or CH_4 in addition to H_2O (Fig. 5A). The amount of water that will enter mantle phases consequently depends strongly on the water fugacity of the melt or fluid it equilibrates with (Gaetani et al. 2014; Baptiste et al. 2015; Yang 2016). In cratonic lithospheres, where conditions are increasingly reducing with depth (Woodland and Koch 2003; McCammon and Kopylova 2004), the proportion of CH_4 in the metasomatic agent could play a role in the amount of water present. For example, the Kaapvaal is slightly more reduced at 160–223 km depths than the Siberian craton, which could explain the lower maximum water contents recorded in the Kaapvaal craton olivines compared to those of the Siberian ones (Fig. 2A; Doucet et al. 2014).

Water solubility in pyroxene, in contrast, is expected to decrease with increasing pressure at depths < 300 km. This is because the more Al, the more water can enter the crystal structure of pyroxene, and the amount of Al in pyroxene decreases with depth due to the enhanced stability of garnet, an Al-rich mineral (Brey et al. 1990; Stalder and Skogby 2002;

Table 1 Estimates of water concentration, mass of water, relative mass to that of the Earth's oceans and H isotopes of the main reservoirs of the Earth. See text for references

			Volume[a] 10^9 km^3	Mass[a] 10^{24} g	Concentration[b] H_2O ppm wt	Concentration[b] H ppm wt	Mass water[b] 10^{23} g H_2O	X Mass oceans[b]	δD_{SMOW} ‰
Hydrosphere	Rivers, Ice, Atmosphere						0.4	0.03	
	Oceans						13.7	1	0
	Total Hydrosphere			1.41			14.1		
Crust	Continental Crust		8.16	21.78	20000	2238	2.8–3.6	0.2–0.3	
	Oceanic Crust		2.14	6.34	15000	1679	1.2–1.4	0.1	−34 to 46
Mantle	Upper Mantle	Continental Mantle Lithosphere Craton[c]			24–100	3–11			
		Continental Mantle Lithosphere off-Craton			50–100	6–11			−92 to −113
		Oceanic Mantle Lithosphere			50–100	6–11			−60 to −130
		Asthenosphere[d]			55–400 (200)	6–45 (22)	1.2	0.1	−20 to −100
		Total Upper Mantle	16.10	584.00	200	22	1.2	0.1	
	Transition Zone[e]		10.70	400.00	3140–5100 (3350)	351–571 (375)	12.6–20 (13.5)	0.9–1.4 (0.96)	
	Lower Mantle[f]		60.60	3030.00	100–2000? (1340)	11–224? (168)	3.0–61.0? (40.6)	0.2–4.5? (2.9)	
	Subduction Zone	Mantle Wedge (Arc Basalt Source)			600–8000	67–895			−55 to −12
		Slab in Upper Mantle[g]			300–3000	37–336			−33 to −126
	Primitive Mantle				330–1200	37–134			< −218
	Total mantle		**87.40**	**4014.00**	**382–2564 (1374)**	**43–287 (167)**	**15.4–103.0 (55.3)**	**1.1–7.4 (4)**	

Table 1 (*Continued*)

		Volume[a] 10^9 km^3	Mass[a] 10^{24} g	Concentration[b] H_2O ppm wt	Concentration[b] H ppm wt	Mass water[b] 10^{23} g H_2O	X Mass oceans[b]	δD_{SMOW} ‰
Core[f]		17.70	1928.70		20–7300? (1000)	2.4–960? (17.4)	0.2–90.0? (12)	
Total	Without Hydrosphere			404–36442 (3898)	45–4078 (436)	24.1–1370 (234)	1.7–97.7 (16.7)	−43
	Including Hydrosphere			638–36668 (**3921**)	71–4103 (**439**)	38.6–1380 (**248**)	2.8–98.8 (**17.6**)	

[a]Reservoir volume and mass estimates from McDonough (2005) and Bodnar et al. (2013)

[b]When possible, a likely reasonable average is given in parentheses. See text for details. X mass oceans = times the mass of the oceans

[c]The overall water content of the cratonic mantle lithosphere is probably low (~ 24 ppm H_2O) while localized metasomatized zones have more water

[d]The source of depleted MORB has ~ 20–250 ppm H_2O but the deepest part of the upper mantle may have higher water content due to the increasing solubility of water in olivine and less depletion with depth

[e]The amount of water in the transition zone is heterogeneous. The ranges are calculated with 2–30% water-rich zones (at 10,000 ppm H_2O) and the rest being drier (3000–6000 ppm H_2O). The 3350 ppm H_2O is calculated with 5% at 10,000 ppm H_2O and 95% at 3000 ppm H_2O

[f]The amounts of water in the lower mantle and core are controversial, thereby the question mark next to the range provided

[g]Amount of water measured in pyroxenite and eclogite samples

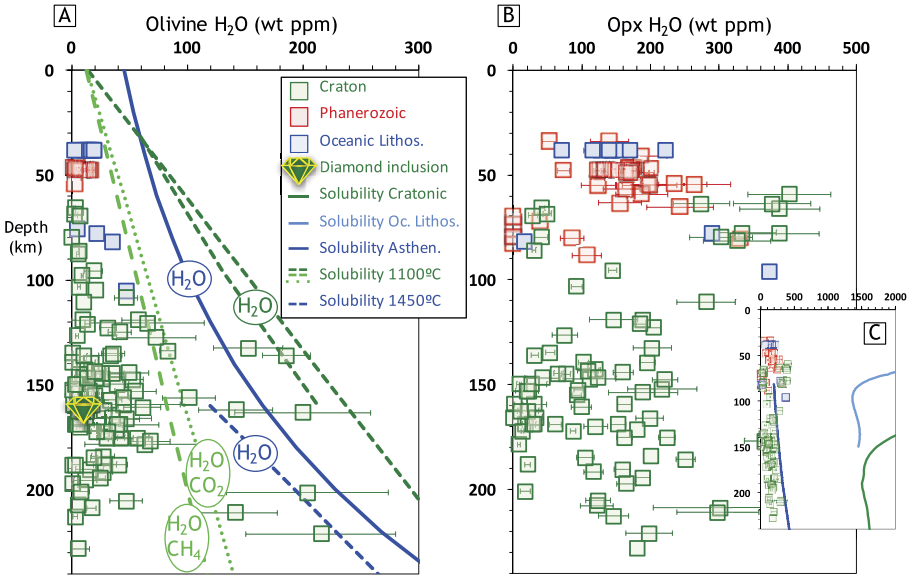

Fig. 5 Water contents of olivine (**A**) and orthopyroxene (**B**) in mantle peridotites compared to solubility curves obtained experimentally. H_2O, H_2O-CH_4 or H_2O-CO_2 indicate the volatiles present in the fluid the minerals equilibrated with in the experiments. The *dotted* and *dashed solubility curves* for olivine are calculated from experiments at a set temperature: H_2O, H_2O-CH_4 or H_2O-CO_2 at 1100 °C (*in green*, Yang et al. 2014; Yang 2015), H_2O at 1450 °C (*in blue*, Ardia et al. 2012; Tenner et al. 2012). The H_2O *blue solid curve* is calculated with a geotherm for the convective mantle (Asthen., Férot and Bolfan-Casanova 2012). All concentrations for olivine, natural or experimental, obtained from FTIR data are calculated with the absorption coefficient of Withers et al. (2012). *Inset* figure C shows the contrasting estimates for the solubility of water in orthopyroxene (Opx): for Al-saturated and Fe-free Opx (Mierdel et al. 2007), the water storage capacity of the lithosphere is high (> 1000 ppm wt H_2O, *light blue* and *green curve*), while the solubility curve of water in Opx for the convective mantle (Férot and Bolfan-Casanova 2012) provides lower water contents (< 250 ppm wt H_2O, *dark blue curve*). The oceanic lithosphere (Oc. Lithos.) geotherm used in the opx solubility calculation (*light blue*) is for a 40 Ma old lithosphere moving at a rate of 10 mm per year (i.e. Pacific plate conditions). Peridotite data from the literature (Kurosawa et al. 1997; Peslier et al. 2002, 2008, 2010, 2012; Grant et al. 2007a; Baptiste et al. 2012; Doucet et al. 2014; Demouchy et al. 2015; Hui et al. 2015; Peslier and Bizimis 2015; Kolesnichenko et al. 2016; Schaffer et al. 2016). Peridotites are grouped by tectonic setting: cratonic, continental Phanerozoic and oceanic. Oceanic peridotites include peridotites from Hawaii and the Ontong-Java plateau (Demouchy et al. 2015; Peslier and Bizimis 2015). The peridotite xenoliths from Hawaii do not contain any garnet and a pressure of equilibration could thus not be calculated. They are shown here, however, at 38 km depth, a reasonable assumption for these spinel peridotite lithospheric samples (Bizimis et al. 2004). The main conclusion from these figures is that natural olivine and pyroxene from the mantle lithosphere are under-saturated in water

Stalder 2004; Hirschmann et al. 2009; Stalder et al. 2015). The amount of Al in pyroxene at depths > 300 km is relatively constant and low, limiting the maximum water intake of pyroxene. This effect may cause the orthopyroxenes at depths < 100 km to record the highest water contents in natural peridotites (> 300 ppm wt H_2O; Fig. 5B). Experiment-based estimations for the water storage capability of orthopyroxene, however, vary by almost an order of magnitude (Fig. 5C), with Al- and water-saturated experiments predicting > 1000 ppm wt H_2O and experiments in undersaturated conditions predicting < 300 ppm wt H_2O. The latter is close to the maximum water content recorded in orthopyroxenes from natural peridotites (Mierdel et al. 2007; Férot and Bolfan-Casanova 2012).

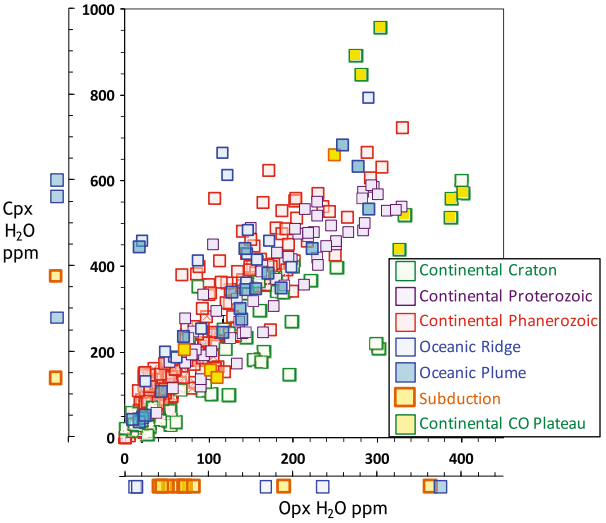

Fig. 6 Water content in clinopyroxene (Cpx) and orthopyroxene (Opx) of peridotites from mantle xenoliths, abyssal peridotites, and tectonically exhumed massifs grouped by tectonic setting (see online supplementary Table 1 for data and references). Uncertainties on water contents are omitted for clarity and are typically 10 to 35% depending on the dataset. When only one mineral was analyzed for water, these are shown to the *left* or *bottom* of the figure

3.2.2 Water in the Asthenosphere and Oceanic Mantle Lithosphere

Mantle xenoliths in oceanic settings are rare, but abyssal peridotites, mantle zones tectonically lifted to the ocean floor at mid-oceanic ridges, also offer samples of the shallow oceanic mantle. Water concentration data from these *direct samples of the oceanic mantle lithosphere*, however, are limited (Gose et al. 2009, 2011; Schmädicke et al. 2011; Warren and Hauri 2014; Bizimis and Peslier 2015; Demouchy et al. 2015; Peslier and Bizimis 2015; Peslier et al. 2015). The water content of these oceanic lithospheric peridotites (blue symbols in Fig. 6) is similar to that of continental peridotites (red and green symbols in Fig. 6). Oceanic pyroxenites contain three to four times more water than peridotites (Fig. 7, Bizimis and Peslier 2015). Two reasons may be proposed for this difference. First pyroxenites primarily consist of pyroxene in which water is more compatible than in olivine, the main mineral of peridotites. Second, they represent crystallized melts at depth, and melts should be water-rich due to the incompatible behavior of water during mantle melting.

On the other hand, abundant water data exists on *indirect samples of the mantle below the lithosphere*, i.e. basalts from mid-oceanic ridge (MORB) and oceanic island (OIB) settings from which the water content of the mantle can be inferred. The water content of their sources in the mantle can be calculated from the analyses of their un-degassed glasses and melt inclusions using reasonable assumptions for the degree and style of partial melting and partition coefficients (Dixon and Clague 2001; Dixon et al. 2002; Saal et al. 2002; Wallace 2002; Workman et al. 2006; Cabral et al. 2014; Kendrick et al. 2014, 2015; Jackson et al. 2015). Basalts from oceanic islands are generally more water-rich than MORB, which implies that their sources are more water-rich than those of MORB (Fig. 7). This is explained by MORB sampling the shallow asthenosphere, depleted in incompatible elements such as H (DM for depleted mantle in Fig. 7; e.g., Dixon et al. 1988; Michael 1988). The source of normal MORB typically has 50–230 ppm wt H_2O (Fig. 7, Dixon et al. 2002; Schaffer et al. 2016). These estimates are consistent with electrical conductivity results that were measured for the oceanic mantle away from any plume influence. These analyses reveal a dry lithosphere (< 50 ppm wt H_2O) underlain by a progressively wetter asthenosphere with depth (400 ppm wt H_2O at 300 km depth; Hirth and Kohlstedt 1996; Evans et al. 2005; Baba et al. 2006; Dai and Karato 2009; Naif et al. 2013; Gardés et al. 2014; Pommier 2014;

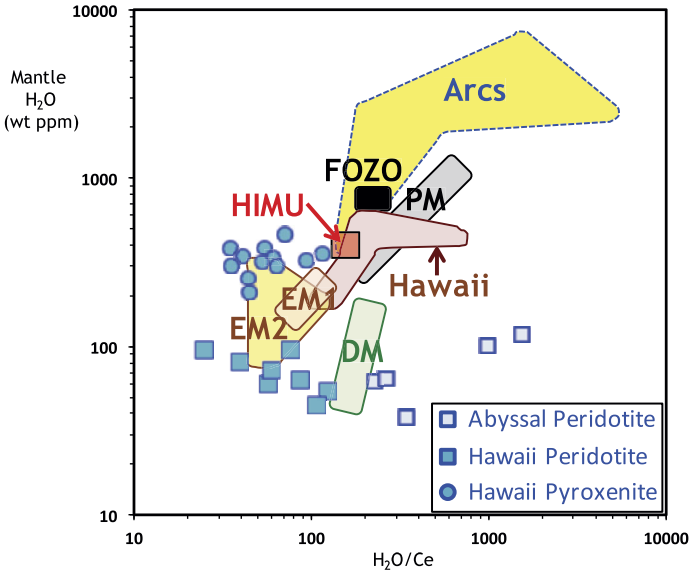

Fig. 7 Water and water/Ce ratio in the oceanic mantle and in subduction zones. Water in subduction zones is obtained from basalts from oceanic arc settings (Arcs; Plank et al. 2009, 2013). Water in the oceanic mantle can be obtained using actual mantle samples (peridotites and pyroxenites) or oceanic basalts which are melts from the mantle (DM, EM1 and 2, HIMU, Hawaii). For peridotites, the water contents are calculated from water analyses of their minerals and each symbol represents an individual sample (Warren and Hauri 2014; Bizimis and Peslier 2015; Peslier and Bizimis 2015). For basalts, the water content of their sources is shown and is calculated from numerous measurements in glasses and melt inclusions. Oceanic basalt end-members are: DM = depleted mantle, the source of mid-oceanic ridges (MOR in Fig. 9) (Michael 1988), and oceanic island (OI in Fig. 9) basalts: EM = enriched mantle (Wallace 2002; Workman and Hart 2005; Workman et al. 2006; Dixon et al. 2008; Kendrick et al. 2014, 2015); and HIMU = "high-mu," with mu being defined as $(^{238}U/^{204}Pb)_{t=0}$ (Cabral et al. 2014; Jackson et al. 2014, 2015). The H_2O/Ce ratio is that of the bulk peridotites, pyroxenites and basalts. Theoretical mantle reservoirs are also shown: PM = primitive mantle (Sun and McDonough 1989; O'Neill and Palme 1998; Dixon and Clague 2001) and FOZO = focal zone (Dixon et al. 2002). The large variations of the water/Ce ratio for a given mantle water content in peridotites and oceanic island basalts indicates that water and Ce are decoupled during mantle processes. See text in Sect. 3.2.2 for details

Sarafian et al. 2015; Khan 2016; Masuti et al. 2016). Such a dry oceanic lithosphere is rigid enough to be passively transported above the hotter convecting asthenosphere from its formation at ridges towards subduction zones or passive continental margins.

Oceanic island basalts sample a broader range of sources, which is indicated by their large range of Sr, Nd, Hf, Pb and noble gases isotopic compositions. Some of these sources are deeper than those of MORB, and OIB are the surface expression of deep mantle upwelling, generally called "plume". The sources of OIB are not well constrained but likely include deep fertile reservoirs, recycled subducted slabs and the depleted upper mantle. Several compositional isotopic end-members have been defined (e.g., Sun 1982; Zindler and Hart 1986; Hart et al. 1992; Brandon et al. 1998; Hofmann 2003; Stracke et al. 2005; Jackson et al. 2007; Delavault et al. 2016). The enriched mantle 1 (EM1) could involve recycled continental mantle or Archean sediments, while EM2 may incorporate recycled continental crust into its source. Another end-member is high-μ (HIMU, with μ being defined as the present-day $^{238}U/^{204}Pb$ ratio of a basalt) and may represent recycled subducted oceanic crust. Primitive mantle (PM) is a theoretical reservoir representing the mantle prior

the melt extraction that formed the crust; some remnants of this original mantle may still exist in the deep upper mantle or lower mantle. Finally, focal zone (FOZO) is defined by a convergence of isotopic trends to a relatively undegassed reservoir. Inclusion of deep mantle material in OIB plumes seem inevitable because they originate from the deep mantle, possibly from the core-mantle boundary at the edges of so called large low shear wave velocity provinces (LLSVP, Burke et al. 2008; Garnero et al. 2016; Mundl et al. 2017). The high water content of OIB thus is linked to the incompatible element enriched nature of their sources, either because they sample (i) undegassed reservoirs (lower mantle, core-mantle boundary), (ii) water-rich reservoirs (for example the transition zone, see Sect. 3.2.3) or (iii) water-rich lithologies (for example pyroxene-rich lithologies like pyroxenites and eclogites) that result from recycling via subduction zones (see Sect. 4; Dixon et al. 2002; Bizimis and Peslier 2015). The water-rich nature of plume sources is also confirmed by analyses of another type of rare primitive (Mg-rich) magma called komatiites, whose melt inclusions are as rich in water as those of OIB (Gurenko et al. 2016), and by electromagnetic imaging of plumes (Tada et al. 2016). Finally, the inventory of noble gas isotopic systems of K-Ar, Xe and Ne are best explained if a primordial volatile-rich reservoir is still present in the mantle and is being sampled by plumes (Marty 2012; Mukhopadhyay 2012; Caracausi et al. 2016; Mundl et al. 2017). The sources of OIB contain from 80 to 800 ppm wt H_2O (Dixon et al. 2002; Cabral et al. 2014).

Finally, we would like to caution the reader regarding the use of a popular alternative method for estimating the amount of water in oceanic basalt sources, which is to use concentration ratios of water over an element of presumed similar incompatibility during partitioning between silicate melt and solid (e.g., Ce, K, La). This idea derives from the observation that these ratios (e.g., water/Ce in Fig. 7) span a narrow range for MORB in each ocean and thus likely represent those of the basalt source (Michael 1995). However, several observations have questioned this approach, primarily the difficulty in explaining the lack of correlation between Ce enrichments and water enrichment in OIB and oceanic peridotites (Fig. 7) (Workman et al. 2006; Kendrick et al. 2014; Warren and Hauri 2014; Hartley et al. 2015; Peslier and Bizimis 2015). Moreover, mantle lithosphere that was pervasively metasomatized by plume-related melts, and thereby enriched in incompatible elements such as LREE, does not exhibit enriched water contents, as evidence from Hawaii, the Tanzanian craton, and many other locations demonstrates (Fig. 3D) (Hui et al. 2015; Peslier and Bizimis 2015). This is best interpreted by decoupling of water from incompatible elements like Ce during mantle processes, with several mechanisms proposed. One is that the fast diffusion of H relative to other slower incompatible elements (e.g., REE) either dilutes water contents in the upper mantle and in the oceanic mantle lithosphere or generates preferential loss of water in subduction zones (Workman et al. 2006; Kendrick et al. 2014; Jackson et al. 2015; Peslier and Bizimis 2015). Subducted material in the mantle could thus be drier than previously thought and its incorporation in a plume source would not generate water-rich OIB. Other mechanisms invoke more fundamental differences of behavior between water and other incompatible elements. One hypothesis is that the large sizes of REE atoms could hinder their incorporation into mantle minerals when pressure increases because of the shrinking radii of the lattice sites. This results in lower REE concentration in the mantle minerals from greater depths. The small H atom, on the other hand, is less prone to this effect. This could affect the water/Ce ratio of the various sources of basalts (Karato 2016). Moreover, melts from the deepest sources will have lower water/Ce ratios then those from shallower levels because Ce will preferentially partitions into the melt at the higher pressures (Adam et al. 2016). Another mechanism that could explain water and Ce decoupling relates on the dependency of H partitioning on water speciation in the melt resulting in H being less incompatible than Ce (Adam et al. 2016;

Schaffer et al. 2016). It is therefore suggested that water estimates that are based on constant ratios of water over other incompatible elements, such as LREE or K, are not reliable.

3.2.3 Water in the Transition Zone

At 410 km depth, pyroxene is no longer stable and transforms into garnet while olivine changes into the denser wadsleyite structure, which in turn is converted into ringwoodite at 520 km depth. The transition zone thus comprises 56% wadsleyite and 44% majorite, a high pressure garnet of formula $(Mg, Fe, Ca)_3(Mg, Si, Al)_2Si_3O_{12}$ from 410 to 520 km, and 56% ringwoodite and 44% majorite from 520 to 660 km depth (e.g., Frost 2008). Experiments show that the water storage capacity of wadsleyite, ringwoodite and majorite is high (0.5–2, 0.3–2, and 0.07–0.2 wt% H_2O respectively) (Smyth 1994; Inoue et al. 1995; Kohlstedt et al. 1996; Bolfan-Casanova et al. 2000; Katayama et al. 2003; Demouchy et al. 2005; Panero et al. 2013; Thomas et al. 2014; Ohtani 2015; Pigott et al. 2015; Thomas et al. 2015). We have discussed earlier that the storage capacity does not necessarily reflect the actual water content with the example of the upper mantle being undersaturated in water. However, additional evidence from natural samples suggests that some regions of the transition zone are indeed particularly rich in water. Two diamonds were found from these depths, each with a mineral inclusion containing water (Wirth et al. 2007; Pearson et al. 2014): a ringwoodite inclusion containing 1.5 wt% H_2O, and a hydrous mineral inclusion called Phase EGG ($AlSiO_3(OH)$), named after its discoverer Eggleton (Eggleton et al. 1978). Although these samples provide very important direct evidence for water in the transition zone, it is not clear whether these two samples represent the typical water content of this mantle layer.

Geophysical studies used to remotely map the mantle are indeed more consistent with regionally variable water contents in the transition zone (Karato et al. 2001; Huang et al. 2005; Karato 2011; Koyama et al. 2013; Khan 2016). Electrical conductivity and global seismic data are consistent with a heterogeneous transition zone that is on average undersaturated in water (i.e. ~3000–6000 ppm wt H_2O), but still about 10 times more water-rich than the asthenosphere (Karato et al. 2001; Huang et al. 2005; Smyth and Jacobsen 2006; Houser 2016; Khan 2016). Some areas of the transition zone, for example beneath China or southwestern USA, are strongly hydrated with > 10,000 ppm wt H_2O (Karato et al. 2001; Courtier and Revenaugh 2006; Khan et al. 2011; Khan and Shankland 2012; Houser 2016; Khan 2016). Water-rich inclusions in diamonds might have come from such regions. The total amount of water that the transition zone could hold can be expressed in masses of present Earth's oceans. Given that the mass of the Earth's oceans is $\sim 13.7 \times 10^{23}$ g, estimating the mass of the transition zone (4×10^{26} g) from its average density and its volume, and assuming the water-rich zones constitute 5–30% (Houser 2016) of the transition zone, the transition zone contains from 1 to 2 Earth's oceans in mass (Fig. 8, Table 1, Bodnar et al. 2013; Nestola and Smyth 2015).

3.2.4 Water in the Lower Mantle

The main phase (80% volume) of the lower mantle is a dense Mg-perovskite called bridgmanite ($(Mg, Fe, Ca)SiAlO_3$) and the minor phases are magnesiowüstite ((Mg, Fe)O) and calcium silicate perovskite ($CaSiO_3$) (e.g., Frost 2008). The results of experiments attempting to determine their water storage capacity are contradictory. However, except possibly Al-rich bridgmanite and calcium perovskite, the water solubility in major lower mantle minerals is generally low (< 1000 ppm wt H_2O; Bolfan-Casanova 2005; Ohtani 2015;

Panero et al. 2015; Walter et al. 2015; Townsend et al. 2016). Minor hydrous phases are stable under lower mantle conditions, and could be brought down by subducting material all the way to the core-mantle boundary (Sano et al. 2008; Ohira et al. 2014; Walter et al. 2015; Hu et al. 2016, 2017; Nishihara and Matsukage 2016).

There are some diamond inclusions that show evidence for a lower mantle origin (e.g., Stachel et al. 2000; Kaminsky et al. 2001; Tappert et al. 2008; Walter et al. 2011), but the water content in these samples has not been measured. The hydrous mineral assemblage (brucite and $Mg(OH)_2$) found in one of these diamond inclusions, however, is best explained by the presence of hydrous melt in the lower mantle (Palot et al. 2016). In addition, there are no geophysical constraints on the water content of the lower mantle because the existing laboratory data cannot be used to infer the water content from geophysical observations at these high pressure and temperature conditions.

However, there is some indirect evidence for the transport of water into the lower mantle. This is the observation of low velocity regions near the top of the lower mantle and at the core-mantle boundary (Revenaugh and Meyer 1997; Garnero and McNamara 2008; Schmandt et al. 2014; Garnero et al. 2016). One possible interpretation is that these low velocity regions correspond to regions of partial melting. Partial melting in the lower mantle is impossible without water (Walter et al. 2015). Therefore, if these low velocity regions are caused by partial melting, some water is likely present. Alternatively, water could be stored in these lower most parts of the mantle in Al-postperovskite (Townsend et al. 2016).

In summary, the water content of the lower mantle is not well constrained and could vary from 0.2 to 4.3 times the mass of the ocean (Bodnar et al. 2013; Nestola and Smyth 2015). We estimated that if the lower mantle consists of 80% bridgmanite with $\sim$ 800 ppm H_2O, 11% magnesiowüstite with $\sim$ 2000 ppm H_2O, 8% $CaSiO_2$ with 3500 ppm H_2O and 1% of hydrous minerals with $\sim$ 20000 ppm H_2O (numbers from the review of Ohtani 2015), then it contains on average 1340 ppm H_2O, i.e. 2.9 times the mass of the oceans (Fig. 8A, Table 1).

3.3 Hydrogen in the Core

The core mainly consists of an Fe-Ni alloy and is liquid from 2900 to 5150 km depth and solid to the center of the Earth (e.g., Birch 1952; Dziewonski and Anderson 1981; Fiquet et al. 2008). The presence of a few % of light elements in the inner core has been invoked to explain core densities inferred from seismology (e.g., Birch 1952; Poirier 1994). One candidate is H because it is ubiquitous in planetary interiors and highly compatible in Fe liquid metal (Okuchi 1997; Abe et al. 2000). The solubility of H in Fe far exceeds that in the transition zone minerals at high pressures, and the core is potentially the largest reservoir of hydrogen in the Earth (e.g., Fukai 1984; Kuramoto and Matsui 1996; Ohtani et al. 2005; Shibazaki et al. 2009; Terasaki et al. 2012; Karato 2015; Iizuka-Oku et al. 2017). A recent temperature estimate of the outer core is lower than previously suggested and would necessitate a large amount of a light element to maintain its liquid state (Nomura et al. 2014). In this case and assuming the only light element is H, then as much as 80 times the mass of oceans could be stored in the core (Genda 2016). Mass balance constraints and planetary accretion models, however, predict relatively low concentrations of H in the core, from 20 to $<$ 200 ppm H (McDonough 2005; Rubie et al. 2015). Moreover, first principles calculations of the effect of H on the properties of iron suggest that seismological observations cannot be explained by the presence of H in the solid core (Caracas 2015; Umemoto and Hirose 2015). In summary, and emphasizing the enormous uncertainties on these numbers, the core could contain 20 to 7300 ppm wt H, i.e. the equivalent of 0.2 to 90 times the present mass of the Earth's oceans (Table 1). The higher estimates ($>$ 2300 ppm wt% H in the core; e.g., Shibazaki et al. 2012;

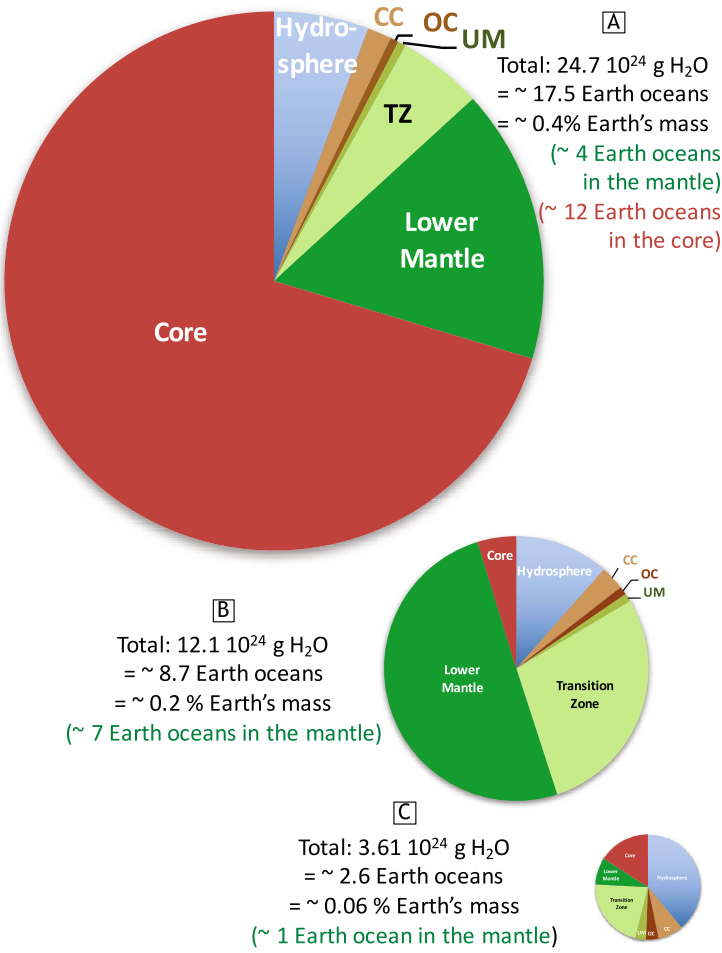

Fig. 8 Sketch of the relative amount of water (in mass %) in Earth's layers from our estimate (**A**) and two recent compilations, **B**: Nestola and Smyth (2015) and **C**: Bodnar et al. (2013). The size of the pie charts corresponds to the total mass of water calculated. The key difference between the three estimations is the amount of water in the lower mantle and core which are not well constrained. The estimate of water in the core in **B** and **C** is from the planetary accretion models of Rubie et al. (2015), while in **A**, it is based on the compatibility of H into iron derived from silicate-iron partitioning experiments. The mass of water in the core was calculated as H_2O for comparison with the silicate oxide layers of the Earth. However, "water" in the core is H in metal and this calculation does not necessary imply that oxygen is present in the metallic core. CC = continental crust, OC = oceanic crust, UM = upper mantle, TZ = transition zone

Genda 2016; Iizuka-Oku et al. 2017) are upper limits because they assume the unlikely scenario that H is the only volatile in the core. Other light elements (for example O, S, C or Si) are likely present in the core (e.g., Poirier 1994; Wood et al. 2013; Badro et al. 2014; Chabot et al. 2015). A more conservative estimate is to be within one order of magnitude of the planetary accretion models (10× ~ 100 ppm H) and about half the amount necessary to explain seismic wave velocity of the inner core and core density with H as the only volatile element (2300/2), i.e. ~ 1000 ppm H in the core, equivalent to 12 times the mass of the oceans (Fig. 8A, Table 1).

3.4 Amount of Water in the Earth

The largest uncertainties on the total amount of water of the Earth are the water contents of the lower mantle and core (Table 1). Based on experiments that show that H is strongly compatible in metal relative to silicate at high pressures (e.g., Ohtani et al. 2005), our model assumes that the core contains the equivalent of 12 masses of the Earth's present oceans. The mantle in our model contains the equivalent of 4 present masses of the Earth's oceans and this is based on a water rich but heterogeneous transition zone and a lower mantle with 1340 ppm H_2O. Including the hydrosphere, this results in a total amount of water for the Earth of 0.4 wt% H_2O (Fig. 8A). A conservative model suggests < 1 present mass of the oceans in the lower mantle (Bodnar et al. 2013) and, combined with an estimate of the water content in the core of 0.4 the oceans mass from planetary accretion modeling (Rubie et al. 2015), results in the total amount of water contained in the Earth, including the hydrosphere, at 0.06 wt% H_2O (Fig. 8C). An intermediary estimate calculates about 7 times the present ocean masses in the mantle (Nestola and Smyth 2015), and combined with the water content in the core of Rubie et al. (2015), results in 0.2 wt% water for the Earth, including the hydrosphere, or 8.7 times the present mass of the oceans (Fig. 8B). Our estimate for the concentration of water in the Earth ($\sim$ 3900 ppm H_2O, Table 1) is within uncertainties to that inferred from noble gas systematics (2700 $\pm$ 1350 ppm H_2O) (Marty 2012).

4 The Water Cycle in the Earth

4.1 Water in Subduction Zones

Subduction zones are the main location of water exchange between the deep Earth and the atmosphere, with the highest fluxes estimated between any terrestrial layers. The fate of water in subduction zones is not only unique to Earth, but also plays a crucial role in the origin of its volcanism, mantle geodynamics and plate tectonics. A detailed account is beyond the scope of this chapter and several reviews are available (Hacker 2008; Grove et al. 2012; Faccenda 2014; Ohtani 2015). A short summary of essential observations is given here.

As subducted slabs are entrained into the mantle, they carry with them water-logged lithologies such as sediments, with structural (i.e., incorporated in mineral lattices) and pore water, and basalt, gabbro and mantle lithologies altered by sea water (e.g., Peacock 1990; Plank and Langmuir 1998; Rüpke et al. 2004; Hacker 2008). They also carry down unaltered crustal and mantle lithologies which, as discussed in the previous sections, contain hundreds to tens of thousands ppm wt H_2O. The input of water is also facilitated by the presence of hydrated faults generated when the plate is stretched through bending downwards towards the subduction trench (Garth and Rietbrock 2014). About 60–90% of this water returns to the oceans via faults and diffusion along the bottom of accumulated material in subduction trenches, called the accretionary prism, because this material is being compacted and clays start to dehydrate (e.g., Jarrard 2003). As the remaining material is transported to higher pressures, metamorphic processes dehydrate the slab minerals and water is transferred to the mantle wedge. This is evidenced by dehydration experiments on hydrous phases like serpentine and amphibole at relevant pressure and temperature, and low seismic velocities and high electrical conductivities observed in the mantle wedge (e.g., Schmidt and Poli 1998; Jarrard 2003; Luth 2003; Kawamoto 2006; Soyer and Unsworth 2006; Kawakatsu and Watada 2007; Rondenay et al. 2008; Ichiki et al. 2009; Frezzotti and Ferrando 2015). These

fluids or melts are typically oxidized, which likely increases their water fugacity (Wood et al. 1990; Brandon and Draper 1996; Debret et al. 2015). Finally, water solubility in subduction zone fluids could also be enhanced by their relatively high Cl content derived from the contribution of sea water to subducted material (Bénard et al. 2017; Keppler 2017).

Given that the presence of water facilitates melting by triggering it at lower temperatures (e.g., Green 1973; Hirose and Kawamoto 1995; Médard and Grove 2008), this water-rich zone (dehydrating slab and mantle-wedge above) is the source of extensive volcanism (McGary et al. 2014). Subduction zone volcanoes therefore produce the most water-rich lavas on Earth (Danyushevsky et al. 1993; Sisson and Layne 1993; Stolper and Newman 1994; Sobolev and Chaussidon 1996; Ruscitto et al. 2012; Plank et al. 2013). Based on the measured water content in melt inclusions, the amount of water in the source of arc volcanoes is higher than that of any other basalt sources (Fig. 7). Note that for subduction zone lavas in Fig. 7 (Arcs), only data from oceanic arc volcanoes have been utilized. Oceanic arc volcanoes have the advantage that their interaction with crustal units is minimal because they only traverse relatively thin oceanic lithosphere (Wallace 2005). Therefore their water content may reflect more accurately the water content of their mantle sources than lavas from subduction zones along continents. Another evidence for the water-rich nature of the mantle wedge may be found in fluid inclusions, which are trapped droplets of fluids embedded in nominally anhydrous minerals. Typical fluid inclusions from upper mantle peridotites not related to subduction contain primarily CO_2 and little to no water (Roedder 1984). This has been interpreted as the result of (i) metasomatism by an ascending volatile-rich melt with CO_2 that exsolves more extensively than water, or (ii) diffusive loss of water from the inclusion during xenolith ascent, or (iii) as evidence that fluids in the shallow upper mantle are not hydrous (Pasteris 1987; Andersen and Neumann 2001; Frezzotti et al. 2012). Fluid inclusions in subduction zones, however, can contain significant amounts of water, which are best explained by particularly water-rich subduction mantle wedges (Roedder 1965; Schiano et al. 1995; McInnes et al. 2001).

It should be noted that some arc basalts are water poor (< 0.5 wt% H_2O; Sisson and Bronto 1998; Wade et al. 2008). In addition, the few subduction zone peridotites (xenoliths from Simcoe (WA, USA), Kamtchatka (Russia) and Papua-New Guinea; exhumed peridotites in China) analyzed so far for water do not have pyroxenes more water-rich than those from continental or oceanic peridotites (yellow symbols in Fig. 6; Peslier et al. 2002; Soustelle et al. 2010, 2013; Cao et al. 2015; Tollan et al. 2015; Wang et al. 2016). The only evidence for possible enrichment of mantle peridotite by water-rich subduction metasomatism is provided by xenoliths from the Colorado plateau in southwestern USA (Fig. 4A and B; Dixon et al. 2004; Li et al. 2008). Occasionally dry zones in the mantle wedge above subduction zones could result from (i) prior melting events that depleted the mantle wedge, (ii) upwelling of comparatively water-poor asthenospheric mantle, perhaps related to back-arc initiation or slab breaking occurrences, (iii) the low water fugacity of rare reduced slab fluids or melts, potentially generated via the melting of subducted organic matter, or by segregation of immiscible C-H-O fluids with low water fugacity (Karato 1986; Sisson and Bronto 1998; Wang et al. 2007; Song et al. 2009; Li 2017). Recent results from thermal modeling also suggest that the majority of mantle fore-arcs are not water-rich because most slabs are too cold to dehydrate rapidly enough over an arc life span (Abers et al. 2017).

Finally, despite the extensive melting that occurs in subduction zones, the mantle residue from this process is probably still relatively rich in water (i.e. it contains the same amount of water as the MORB source or upper asthenosphere; Hirth and Kohlstedt 2004). Therefore, water in the peridotitic mantle wedge likely contributes to the rehydration of the

asthenosphere via downward passive entrainment above a subducted slab ("corner flow", Fig. 9B), in addition to the water-rich slab lithologies described in the next paragraph. This mantle flow is facilitated by the low viscosity (similar to that of the asthenosphere) of this relatively water-rich mantle (Billen and Gurnis 2001; Hirth and Kohlstedt 2004; Behr and Smith 2016).

4.2 Water Transport to the Deep Earth

Not all subducted water is returned to the surface in subduction-related volcanoes. Some water is entrained deeper, locked in slab minerals that do not dehydrate completely despite the increasing pressures, in part due to the colder temperature of the sinking slab compared to the surrounding mantle (Dixon et al. 2002; Rüpke et al. 2006; Ohtani 2015; Chang et al. 2017). Eclogites, metamorphic rocks of subduction origin, contain significant amounts of water locked in their minerals amounting to 460–3000 ppm wt H_2O in the bulk-rock (Katayama and Nakashima 2003; Katayama et al. 2006). At higher pressures, phases like hydrous Mg or Al silicates, or Al or Si oxides, have been synthesized in laboratory experiments. Such minerals could carry water to the transition zone (hydrous ringwoodite, akimotoite, stishovite, Phases A, B, C, D, E, X, EGG, δ-H, $(FeOOH)TiO_2$), the lower mantle, and all the way down to the core-mantle boundary (δ-AlOOH, phase H) (e.g., Panero et al. 2003; Bolfan-Casanova 2005; Komabayashi 2006; Lawrence and Wysession 2006; Sano et al. 2008; Ohira et al. 2014; Ohtani 2015; Nishihara and Matsukage 2016).

In particular, the main reason why the transition zone (Sect. 3.2.3) comprises water-rich zones might be that cold subducted slabs seem to stagnate as these depths (Fig. 9). Imaging by seismic tomography (van der Hilst et al. 1991; Fukao et al. 2009) shows these slabs, which entails that subducted water could accumulate locally in the transition zone via this process (e.g., Braunmiller et al. 2006; Suetsugu et al. 2006; Richards and Bercovici 2009; van Mierlo et al. 2013). Although water-rich minerals (hydrous wadsleyite and ringwoodite) have been invoked to explain seismic velocities within the transition zone and the seismic contrast seen at 410 km (Smyth and Frost 2002; van der Meijde et al. 2003; Smyth et al. 2004; Hirschmann et al. 2009), widespread presence of water-rich solid material is not supported by geophysical observations (Houser 2016). Another hypothesis is that water-rich melts are generated at the top and at the bottom of the transition zone by material flowing through the transition zone (Fig. 9A). In the framework of this hypothesis, partial melting could occur at the top of the transition zone, linked to the transformation of olivine into wadsleyite at cold slab temperatures or the stagnation of upwelling transition zone dense melts (Bercovici and Karato 2003; Sakamaki et al. 2006; Frost and Dolejš 2007). A melt layer at 410 km depth is consistent with both seismic and electrical conductivity data (Revenaugh and Sipkin 1994; Song et al. 2004; Yoshino et al. 2006). Downward flow of transition zone material to the lower mantle involves the transformation of hydrous ringwoodite to bridgmanite, which could generate water-rich melts at the top of the lower mantle and could explain the sudden decrease in seismic velocities at 660 km (Ghosh and Schmidt 2014; Schmandt et al. 2014).

4.3 Fluxes of Water Between Earth's Geological Reservoirs

The water cycle in the Earth can be constrained by combining the estimated amount of water in each reservoir (hydrosphere, continental crust, oceanic crust, upper mantle, transition zone, lower mantle and core, Fig. 9A, Table 1) with the estimated net flux at the main locations of water transfer in and out of each reservoir for a given period of time (e.g.,

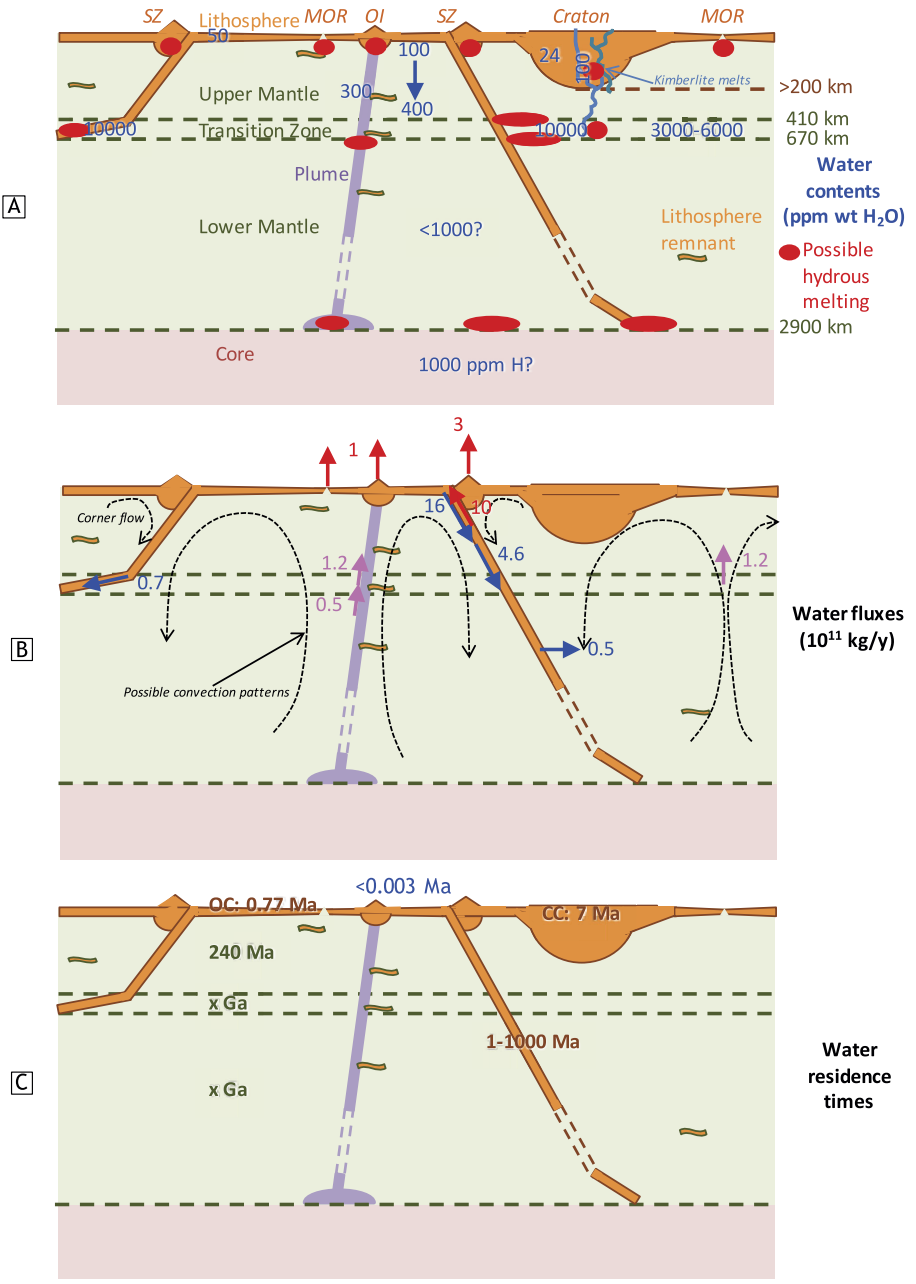

Fig. 9 Sketch of the key layers, tectonic settings and processes of a dynamic Earth interior in relation to water with **A**: average water concentrations (ppm weight H_2O) and zones where partial melting occurs (*red*), **B**: present water fluxes between reservoirs in 10^{11} kg/y (*solid colored arrows*) and schematic mantle convection patterns (*dotted black arrows*), and **C**: residence time of water for various reservoirs. MOR = mid oceanic ridge, OI = oceanic island, SZ = subduction zone, × Ga = several billion years, OC = oceanic crust, CC = continental crust. See text for references

Bodnar et al. 2013; Magni et al. 2014). Figure 9B shows averages of water fluxes in the Earth in 10^{11} kg/y from estimations of the last 25 years (Peacock 1990; Bebout 1996; Schmidt and Poli 1998; Wallmann 2001; Hilton et al. 2002; Bercovici and Karato 2003; Rüpke et al. 2004; Wallace 2005; Rüpke et al. 2006; Hacker 2008; van Keken et al. 2011; Faccenda et al. 2012; Parai and Mukhopadhyay 2012; Bodnar et al. 2013; Faccenda 2014; Magni et al. 2014). Details can be found in online supplementary Table 2.

The primary regions of water exchange between Earth's interior and hydrosphere are subduction zones (Fig. 9B). It is estimated that ∼25% of the water entering subduction zones reaches the transition zone and ∼3% reaches the lower mantle (Bodnar et al. 2013). Compared to subduction volcanism, mid-oceanic ridge and oceanic island volcanisms contribute a minor percentage of the total water loss from the Earth's interior to the hydrosphere. Yet, oceanic basaltic volcanism constitutes the main exhaust of water from the deep mantle to the surface via mantle convection and plume upwelling processes. The net balance of input versus output of water results in addition of water to the mantle over time. Assuming that plate tectonics has operated over the last 3 Ga (Farquhar et al. 2002; Shirey and Richardson 2011; Debaille et al. 2013), a first order calculation results in about half the mass of the Earth's present oceans being added to the mantle over that time period. It should be emphasized, however, that the uncertainty on the estimated fluxes presented here is high (∼50%).

4.4 Residence Time and Origin of Distribution of Water in the Earth

The highly heterogeneous distribution of water in the Earth is a remarkable conclusion. Particularly important is the inferred layered structure of water content in the mantle. Although diffusion of water (i.e., hydrogen) in silicates is fast compared to that of other elements in silicates, diffusion is ineffective to modify the water content at a large scale: for typical asthenospheric conditions, diffusion of H over a distance of ∼10 km takes ∼1 Ga (Karato 2007; Peslier and Bizimis 2015). However, because of mantle convection, water contents should be homogeneous among regions of more than ∼100 km size, not considering partial melting and resultant melt-solid segregation.

Heterogeneity in the water concentrations within the terrestrial reservoirs was first established during the early planetary differentiation processes, i.e. the formation of the metal core and the first silicate reservoirs. The processes include magma ocean degassing, as well as silicate differentiation in the magma ocean and water extraction from the mantle via crustal building over time (e.g., McKenzie 1985; Rudnick 1995; Hirth and Kohlstedt 1996; Hirschmann 2006; Labrosse et al. 2007; Elkins-Tanton 2008). Evidence for a water-rich reservoir in the Archean mantle comes from the water analyses of melt inclusions in 2.7 Ga old komatiites, which are primitive magmas that erupted primarily in the Archean (Sobolev et al. 2016). Heterogeneity is sustained by (i) recycling of water-bearing material via subduction processes, (ii) partial melting via solid material vertical transport, with resulting melt ascent or sinking depending on density, and (iii) inefficient re-homogenization by convection processes over Earth's history. Further evidence for this inefficient mixing stems from H isotopes. Melt inclusions of primitive basalts have low D/H isotopic ratios that were inherited from their source, possibly a primordial reservoir deep in the mantle that may still carry solar nebula H isotopic ratios (see Sect. 5.2.1; Hallis et al. 2015). Basalt glasses with OIB-like geochemical signatures also carry H isotopic signatures consistent with preservation of subduction-derived H, signifying that water in slabs was not diluted over time in the ambient mantle but stayed isolated during the recycling process over Ma to 1 Ga (Shaw et al. 2012).

Residence times for water shown in Fig. 9C are taken from Bodnar et al. (2013) and calculated using the amount of water in each reservoir and the estimated fluxes between

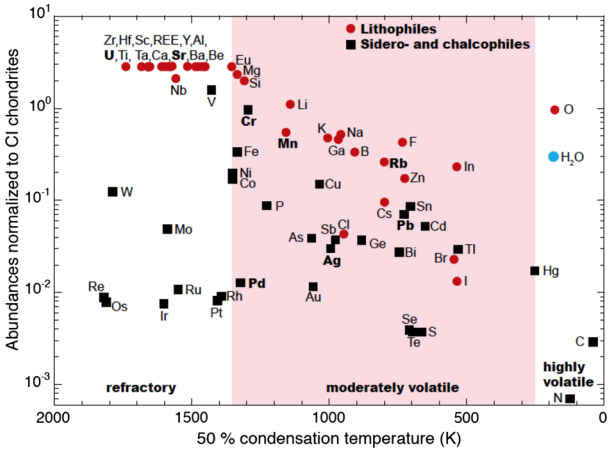

Fig. 10 The elemental abundances in the Earth's mantle normalized relative to CI chondrites as a function of the 50% condensation temperature (T_c) (from Lodders 2003; Palme and O'Neill 2014b). At this temperature, 50% of an element is in solid form, during condensation from a gas of solar system composition at low pressure conditions and under the assumption of complete chemical equilibrium. Lithophile elements define a distinct trend that correlates with condensation temperatures, while siderophile and chalcophile elements are depleted relative to this trend due to sequestration into the Fe-Ni core

them. Shortest residence times are in the hydrosphere (< 3000 years) and lithosphere (0.77–7 Ma), and water could stay locked in the transition zone and lower mantle for billions of years. If we assume that plate tectonics started at least 3 Ga ago (Farquhar et al. 2002; Shirey and Richardson 2011; Debaille et al. 2013), a H atom may have travelled from the oceans to the deeper mantle and back 3 times since then. You could be drinking water from the mantle right now!

5 Acquisition of the Earth's Water

5.1 Timing of Water Delivery to Earth

The total water budget of the Earth today (Table 1) reflects the integrated history of a long evolution starting with the formation of the Earth and the water present in the building blocks, followed by processes that modified its water content. An example for the latter is magma ocean degassing (Chap. 12) that resulted in an atmosphere, which in turn experienced losses through impacts, thermal processing and interaction with the radiation from the active young Sun (Chaps. 13 and 14). Moreover, water may also have been acquired by the Earth through a later delivery by water-rich asteroids and comets after the Earth had already reached > 99% of its current size.

To assess the potential presence of water in the building blocks of the Earth, we first evaluate the general volatile depletion trend of the Earth. In this context, the cosmochemical classification of elements becomes important (e.g., Lodders 2003; Palme and O'Neill 2014a). This classification is based on the condensation sequence of the chemical elements from a gas with solar composition at pressures of 10^{-4} bar (Fig. 10). The first elements to condensate when the solar gas cools are refractory elements (half mass condensation temperatures (T_c) = 1850–1355 K, Fig. 10). They are followed by the so-called main component

elements (e.g., Si, Fe and Mg; $T_c = 1355$–1250 K, not highlighted in Fig. 10), then the moderately volatile elements ($T_c = 1250$–250 K), and, at the end of the sequence, the highly volatile elements ($T_c < 250$ K, e.g., H), which condense after the nebular gas had cooled to below 250 K. Of particular interest for our purpose are the moderately volatile elements, which provide powerful constraints on the presence of volatiles. Subsequently, we establish the link to the highly volatile compounds and in the next section (Sect. 5.2), we summarize attempts to use isotopic constraints of the highly volatile elements to assess the origin of Earth's water.

5.1.1 The Formation of the Earth

The birth of our solar system started with the gravitational collapse of an interstellar molecular cloud that contained gas and dust from a variety of stellar sources. The cloud collapsed and most of the mass accumulated in the center to form the young Sun, surrounded by a protoplanetary disk. Within this disk, dusty materials collided and accreted into small planetary bodies (planetesimals, planetary embryos), most of which further accumulated to build the terrestrial planets including the Earth (Chaps. 2 and 10).

The combination of heat released from radioactive nuclides and impacts on the growing proto-Earth likely triggered the formation of a deep magma ocean or potentially even several generations of magma oceans (Chap. 12). In these, metal segregation and sinking occurred resulting in core formation (e.g., Wood et al. 2008; Rubie et al. 2011). Dynamic modeling indicates that the last giant impact at the end of terrestrial accretion created the Moon (e.g., Benz et al. 1986; Canup 2012). This last potentially Mars-sized impactor, and the subsequent magma ocean, most likely concluded the terrestrial core segregation, and it also could have brought volatile elements to the Earth (Halliday 2004; Schönbächler et al. 2010). After this event, only a small amount of material ($< 1\%$, Chou 1978; Walker 2009) has been accreted to the Earth until today. This late material was added to the mantle only and did not experience metal segregation to the core. This latest episode of extraterrestrial material addition is referred to as "late veneer" (e.g., Wang and Becker 2013), "late accretion" (e.g., Walker 2009), or terminal bombardment (Willbold et al. 2011). In this work, we use the term "late veneer". Its existence was originally proposed based on the elevated highly siderophile element (HSE) abundances in chondritic proportions in the Earth's mantle (Chou 1978), which could not be explained by core formation in a magma ocean that would have almost exclusively sequestered these elements into the core.

5.1.2 Volatile-Poor Early Accretion

The Sun, which comprises $> 99\%$ of the mass in the solar system, and CI chondrites display nearly identical elemental compositions, with a few exceptions (e.g., Li, Be, the highly volatile elements H, O, N, C and the noble gases). This implies that CI chondrites reflect the average solar system composition for most elements and are therefore usually taken as a reference (Chap. 3). The Earth and other terrestrial planets are depleted in moderately and highly volatile elements relative to CI chondrites and the Sun (Fig. 10). Some of the depleted elements (e.g., Ag, Mn, Rb and Pb) are part of a radioactive decay system such as the short-lived decay systems ^{53}Mn-^{53}Cr (half-life of 3.5 ± 0.4 Ma) and ^{107}Pd-^{107}Ag (half-life of 6.5 ± 0.3 Ma), the long-lived chronometer ^{87}Rb-^{87}Sr (half-life of 49 Ga), and the U-Pb double decay system, where ^{238}U decays to ^{206}Pb with a half-life of 4.47 Ga and ^{235}U to ^{207}Pb with a half-life of 710 Ma. Manganese, Ag, Rb and Pb possess lower condensation temperatures than Cr, Pd, Sr and U (Lodders 2003, Fig. 10), and for this

reason they are fractionated from each other by volatile depletion events. This fractionation can be dated by the chronometers. It is noteworthy that Pd-Ag, Mn-Cr and U-Pb also fractionate during core formation (Ballhaus et al. 2013; Kiseeva and Wood 2013; Rubie et al. 2015), because the involved elements (except U) partition to different degrees into the core. This needs to be taken into account for the interpretation.

The short-lived decay systems provide very powerful constraints because their signatures are established within the first 10–30 Ma of our solar system and are not modified by later radiogenic ingrowth. It can be shown that the Cr isotope composition of the bulk silicate Earth (= crust and mantle) is relatively unradiogenic, i.e. contains relatively small amounts of radiogenic ^{53}Cr from the decay of ^{53}Mn, compared to the volatile-rich CI chondrites (e.g., Trinquier et al. 2008; Qin et al. 2010). This implies that the volatile ^{53}Mn was lost early, presumably within the first 2 Ma after the start of the solar system dated by oldest known solar system materials—calcium-aluminum-rich inclusion (CAI) (Trinquier et al. 2008; Qin et al. 2010; Palme and O'Neill 2014a). A longer presence of the volatile ^{53}Mn would have generated a more radiogenic ^{53}Cr-rich composition. The Mn-Cr data was incorporated into different accretion models, i.e. simple two-stage models, but also models that take core formation into account and use exponential growth curves for the Earth (Trinquier et al. 2008; Schönbächler et al. 2010; Carlson et al. 2015). These models agree that a large amount of the Earth's building blocks were significantly depleted in the moderately volatile element Mn. Evidence from the long-lived Rb-Sr system also argues for early volatile depletion (Halliday and Porcelli 2001; Schönbächler et al. 2010; Nebel et al. 2011; Hans et al. 2013; Carlson et al. 2015), despite some uncertainties regarding the initial Sr isotope composition of the solar system (e.g., Hans et al. 2013).

Similarly, evidence from the U-Pb system is also in agreement with an early depletion (Wood and Halliday 2010; Nebel et al. 2011; Albarède et al. 2013; Ballhaus et al. 2013). However, the interpretation of the U-Pb system has long been a matter of debate. There are some uncertainties regarding the estimate of the Pb isotope composition of bulk silicate Earth, partly due to the high concentration of Pb in the crust (Hofmann 2001). Other works illustrated the potential sensitivity of volatile elements such as Pb to the late veneer and proposed that all Pb was delivered by the late veneer (Albarède et al. 2013; Ballhaus et al. 2013). Most studies agree, however, that the Earth started with a high U/Pb ratio (volatile depleted) and that this ratio was further enhanced around 100–150 Ma after the start of the solar system formation, either by Pb loss through volatilization (e.g., during the giant impact, Connelly and Bizzarro 2016) or partitioning into the core (Wood and Halliday 2010).

In summary, radioactive decay systems, which involve moderately volatile elements, provide strong evidence that the Earth accreted on average from volatile depleted materials. Since moderately volatile elements display higher condensation temperatures than the highly volatile elements and compounds (Fig. 10), it is likely that the highly volatiles (e.g., H) were even more depleted in the early building blocks of the Earth. Selective adsorption on the surface of olivine in the protoplanetary disk could be a potential mechanism to incorporate water into the terrestrial building blocks without significant amounts of moderately volatile elements (e.g., Vattuone et al. 2013). However, the amount of water (H_2O) that can be tolerated in the early building blocks of the Earth is limited. This is because models of metal-silicate partitioning in a deep magma ocean, which are based on high-pressure experiments, generally require reduced material in the early stages of terrestrial accretion to successfully match the metal-silicate partitioning behavior of the elements in the Earth (e.g., Wood et al. 2008; Rubie et al. 2011; Rubie et al. 2015; Chap. 11), although a more oxidized scenario has also been suggested (Siebert et al. 2013). Hydrogen instead of H_2O could have been present under early reducing conditions (Hirschmann et al. 2012;

Sharp et al. 2013). While the proto-Earth is small, and because H is easily lost from cooling magmas (Sharp et al. 2013), a significant proportion of H was presumably lost to space. Given that there is ample evidence for the addition of volatile-rich/bearing material later (see below), this early signal is likely swamped by the later addition.

Another limiting factor for water retention for the early proto-Earth is the small size of the proto-Earth and the impacting bodies, which does not allow gravitational retention of an atmosphere. To a first order, the proto-Earth must be massive enough such that its Bondi radius is larger than its physical radius to retain an atmosphere. The Bondi radius is the radius at which the escape velocity from the planets gravitational potential is equal to the thermal velocity of the gas molecules. If the average thermal velocity of the gas molecules is larger than the escape velocity of the planet, it cannot hold on to any primordial atmosphere. For the conditions relevant for the Earth (Hayashi 1981), the proto-Earth at 1 AU needs to be at least 0.002 of its current mass to retain some H- and He-bearing envelope from the protoplanetary disk (Inamdar and Schlichting 2015). At the same time, the accreted material is heated by radioactive isotopes and accretion, which will lead to degassing of the interior and volatile loss. The meteorite record shows that small differentiated bodies (e.g., Vesta or the Angrite parent body) are generally volatile-poor (e.g., Hans et al. 2013), but they are not completely devoid of water (Sarafian et al. 2013, 2017; Scully et al. 2015).

In addition, the concept of the snowline further supports water-poor building blocks for the Earth. The snowline marks the boundary between condensation and vaporization of water in the protoplanetary disk. In the framework of the snowline model, rocky planetesimals form inside and icy planetesimals outside the snowline, where ice particles can exist and accrete. The temperature in the protoplanetary disk at 1 AU distance from the Sun is estimated to 270 K by Hayashi (1981). In a protoplanetary disk of solar composition, water ice forms below ~180 K (Lodders 2003). Therefore, the calculated warm temperature at 1 AU would not allow condensation of water ice. Water remained in the gas phase and could not be accreted as ice. This resulted in the formation of water-poor planetesimals in the 1 AU region, which is the main "feeding zone" for the early accreted material of Earth (e.g., O'Brien et al. 2006, 2014; Raymond et al. 2006).

5.1.3 How Late Did the Volatiles Arrive?

While there is powerful isotopic evidence that the Earth's accretion started volatile poor as discussed in Sect. 5.1.2 above, the timing of volatile addition to the Earth is more uncertain. Small amounts of H may have been accreted early (before the Earth reached ~60–80% of its current size), but larger amounts of moderately volatile elements can be excluded. Hence, a later addition for these elements is required and they are likely coupled with significant amounts of highly volatile elements as, for example, provided by carbonaceous chondrites (Alexander 2017).

The combined modeling of several radionuclide systems (Pd-Ag, Mn-Cr, Rb-Sr and Hf-W) shows that the Earth most likely accreted heterogeneously; first, materials depleted in moderately volatile elements accreted, while the later accretion history was dominated by volatile-rich materials (Schönbächler et al. 2010). Their preferred model encompasses that the Earth first grew to 86% of its present mass from volatile-depleted material, with similar or slightly lower volatile content than the Earth today. Considering the uncertainties, the model allows for volatile-depleted accretion of the first 60–70% of the Earth's mass, before the volatile—rich material arrives (Fig. 11). This result is in good agreement with several other recent studies that employed very different approaches and techniques (O'Brien et al. 2006; Wood et al. 2008; Rubie et al. 2011, 2015; Marty 2012;

Hirschmann 2016; Fischer-Gödde and Kleine 2017). While Schönbächler et al. (2010) based their conclusions on the combined modeling of radioactive decay systems, other studies (Wood et al. 2008; Rubie et al. 2011, 2015) used high-pressure experiments to model metal-silicate partitioning in a deep magma ocean. Others (Marty 2012; Hirschmann 2016) modeled C/H, C/N and C/S ratios or their element concentrations (water, C, N and noble gases) in the bulk silicate Earth and concluded that some of the volatile budget (in particular some H; Hirschmann 2016) were acquired prior to the late veneer. The nucleosynthetic Ru isotope composition of the Earth compared to those of chondrites supports this conclusion and even indicates that the late veneer could have been water poor and similar to enstatite chondrites in composition (Fischer-Gödde and Kleine 2017). O'Brien et al. (2006) employed numerical simulations to determine the final stages of accretion of the terrestrial planets and concluded that volatile-rich material was added late during the Earth's accretion history, but that a part of it was incorporated when core formation was still proceeding. In this so-called "classical" model (O'Brien et al. 2006; Raymond et al. 2006; Chap. 10), the volatile-rich material is delivered by bodies from the primordial asteroid belt beyond ~2.5 AU. In the more recently proposed "Grand Tack" model, which takes gas giant planet migration into account, some volatile-rich material is also delivered during ongoing core formation—but in this model the water-rich bodies originate from between and beyond the present orbits of the gas giant planets (O'Brien et al. 2014; Chap. 10).

The model of substantial volatile delivery starting during core formation stands in contrast to other studies (Albarède 2009; Albarède et al. 2013; Ballhaus et al. 2013), which argue that the Earth's volatiles were exclusively delivered by the late veneer. Although it is possible that the late veneer delivered volatile-rich material (e.g., similar to CM chondrites; Wang and Becker 2013), delivering *all* the volatiles during the late veneer would lead to significantly higher HSE abundances than observed in the bulk silicate Earth. Moreover, this scenario would generate a strong radiogenic signal in the Ag isotope composition of the Earth's mantle due to the decay of the refractory isotope ^{107}Pd, which is very abundant relative to Ag in volatile depleted material. Such a radiogenic signature is not observed (Schönbächler et al. 2010; Schönbächler and Nimmo 2011). Mixing of previously accreted materials with volatile-rich material during the late veneer would modify and dilute such a strong radiogenic signal. In addition, admixture of more than 10% by mass of volatile-rich material during the late veneer event would be required (Schönbächler and Nimmo 2011). This is not realistic because of the relatively low HSE content in the Earth's mantle (e.g., Wood et al. 2010). Special scenarios invoked to explain the missing high HSE abundances (e.g., late sulphide or metal segregation; Albarède et al. 2013; Ballhaus et al. 2013) fail to relax the Ag isotope argument.

5.1.4 Summary

In summary, geo- and cosmochemical evidence indicates that the last third of the Earth's growth involved volatile-rich (water containing) material (Fig. 11). The amount of water added before the late veneer is, however, uncertain. The Earth's total water budget is estimated at 2–18 Earth ocean masses (Fig. 8), but large uncertainties on the core and lower-mantle water contents extend the range from 0.2 to 90 (Table 1). Because the inferred amount of water in Earth is small compared to that of carbonaceous chondrites or planetary bodies from the outer part of the solar system, it is conceivable that some fraction of the Earth's water might have been acquired very early, before water-rich materials were accreted later from regions beyond the snowline. Incorporation of

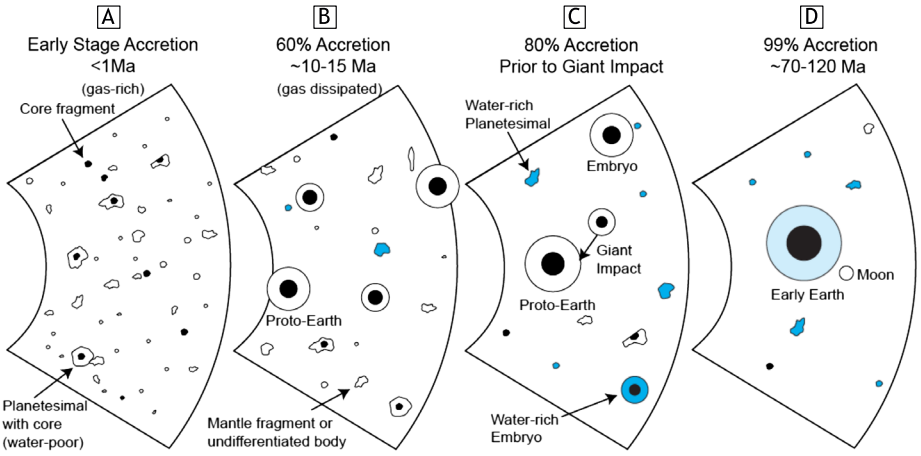

Fig. 11 Schematic evolution of water delivery to the Earth. The view looks down onto the accreting disk of the solar system and shows snapshots of the section of the disk where the Earth formed (around 1 AU) at different times. It illustrates the planetary materials that likely were near the Earth's orbit, i.e. the material available at each time period to be accreted to the Earth (not everything will be accreted). The amount of water-rich bodies in the "feeding zone" of the Earth increases from *left* to *right*. The Earth started relatively dry, i.e. water-poor, and received the first significant volatile delivery after it reached 60–80% of its current size. Later accretion is dominated by volatile-rich bodies (*blue*). The accretion percentage is given relative to today's mass of the Earth. *White bodies*: volatile-poor mantle fragments or undifferentiated material originally from the 1 AU region. *Blue bodies*: water-rich mantle fragments or undifferentiated material originally from (i) the primordial asteroid belt (e.g., carbonaceous chondrites for classical model; Raymond et al. 2006) or (ii) from between and beyond the giant planets (Grand Tack model; O'Brien et al. 2014). In *black*: core material. Figure is based on a sketch in Nimmo and Kleine (2015)

1% CI chondrite material (with > 10% H_2O; e.g., King et al. 2015) can already deliver ~4.5 times the mass of the present Earth's oceans. However, up to 30% of volatile-rich material may have been added before the late veneer (Schönbächler et al. 2010; Rubie et al. 2011), which implies that the water mass delivered to the Earth—during ongoing core formation—was likely orders of magnitude higher than today's water budget. This requires significant water loss from the terrestrial atmosphere during impact-driven accretion, the magma ocean state, and/or during the late veneer (Chaps. 12–14), to match the current Earth's water budget. In addition, water was also likely delivered through the late veneer, which is discussed in the next section.

5.2 Origins of the Earth's Water

As discussed above (Sects. 3 and 5), there are two first-order conclusions from the studies on the water distribution in the Earth.

(i) The total amount of water in the Earth is small (0.06 wt% to ~3.9 wt% H_2O or ~3 to ~18 ocean masses; Fig. 8), compared to that of the most primitive meteorites, carbonaceous chondrites, which can contain up to 10–20 wt% H_2O (e.g., Alexander et al. 2012; King et al. 2015; Stephant et al. 2017). Hence, moderately water-rich materials, such as CI chondrites are sufficient to supply the Earth's total water budget, including the ocean and interior water. Other materials such as comets are even more water-rich and thus less such material would be required to explain the Earth's water content.

The amount of water in other—more water-poor—materials that were potentially accreted by the Earth is not well-constrained. Although 0.1 to 1 wt% H_2O were estimated

earlier (Jarosewich 1990; Robert 2002; Alexander et al. 2012; Barnes et al. 2016), ordinary chondrites are still likely water-poor. This is based on the fact that their apatites appear generally devoid of water, except one LL chondrite that contains the driest apatite ever measured in solar system materials (Jones et al. 2014, 2016). In agreement with this observation, ordinary chondrites exhibit an overall strong depletion trend in moderately volatile elements (Schönbächler et al. 2008; Schaefer and Fegley 2010). Enstatite chondrites may have < 0.5 wt% H_2O (Robert et al. 1987; Barnes et al. 2016). Moreover, the differentiated parent bodies of angrites and eucrites contain some water (Sarafian et al. 2013, 2017; Barrett et al. 2016), but still 2–3 orders of magnitude less than CI chondrites.

(ii) Much of the initial mass of the Earth, ranging from at least 60% to up to almost 90% of present Earth mass (based on the moderately volatile elements, Sect. 5.1.), accreted from volatile-depleted precursor material (e.g., Albarède 2009; Schönbächler et al. 2010; Rubie et al. 2011). It has been suggested that only the last 1% of accreting mass, the "late veneer" (Sect. 5.1), provided the bulk of the terrestrial water. The initial material that formed the Earth (and the other terrestrial planets) may have lost some of its volatiles by vaporization on impact. However, the main reason for the volatile depletion of the precursor material is that most volatile elements were likely not present in the first place in the earlier building blocks (Albarède 2009; Schönbächler et al. 2010; Rubie et al. 2015, and references therein).

The origin of the water and the nature of its source(s), whether accreted early or late in Earth's evolution, is not entirely determined. The highly volatile elements H, C, N and the noble gases can potentially provide new constraints on the origin of Earth's volatiles. Particularly helpful are their isotopes, as the Earth and many of the reservoirs that are potential sources, show distinct isotopic signatures. In the following, we aim to briefly summarize these efforts with the main focus on *isotopic* characterization. More comprehensive models and considerations beyond the major realm of this chapter can be found in recent, dedicated reviews (e.g., Robert 2001; Drake 2005; Marty and Yokochi 2006; Alexander et al. 2012; Marty 2012; Halliday 2013; Dauphas and Morbidelli 2014; Genda 2016; Marty et al. 2016; Hallis 2017; Chaps. 5, 6, 11–14). First, we will summarize the D/H and $^{15}N/^{14}N$ ratios detected in various inner solar system bodies that then can be compared with terrestrial values. This is followed by the discussion of noble gas isotopes that provide further constraints on the origin of Earth's water.

5.2.1 Constraints from Hydrogen Isotopes

The D/H ratio might be the most diagnostic isotope ratio to assess the origin of water, due to its large observed range in solar system reservoirs (Fig. 12; e.g., Alexander et al. 2012; Bockelée-Morvan et al. 2015; Alexander 2017; Hallis 2017). We express here the D/H ratio by the delta notation, which describes the variation of the measured ratio relative to a standard in permil, i.e. the D/H ratio of terrestrial oceanic water ("SMOW"). Most reservoirs including the Earth ($\delta D \sim 0$ to $< -220‰$ in its interior, Table 1), are enriched—to different degrees—relative to the initial value of the solar nebula ($\delta D = -872 \pm 22‰$; Geiss and Gloeckler 2003). Nebular H, with the lowest D/H ratio in the solar system, is sampled essentially unmodified by the giant planets Jupiter and Saturn (e.g., Alexander et al. 2012; Bockelée-Morvan et al. 2015; Chaps. 3, 6 and 8).

Comets Cometary isotope compositions were detected by remote sensing (e.g., Bockelée-Morvan et al. 2015), in-situ study by spacecraft (Balsiger et al. 1995; Eberhardt et al. 1995; Altwegg et al. 2015) and in the laboratory—by examining returned samples (comet Wild 2 dust, McKeegan et al. 2006; Sandford et al. 2006) or bona-fide cometary interplanetary dust particles (IDPs, e.g., dust from comet Grigg-Skjellerup; Busemann et al. 2009;

Bradley et al. 2014 and references therein). Comets display the highest D/H ratios, in H_2O, and C- and N-bearing organic molecules (e.g., Altwegg et al. 2015; Bockelée-Morvan et al. 2015; Chaps. 3 and 6). These high D/H ratios are usually assumed to be inherited from D enrichments produced in the cold interstellar medium and the slightly warmer solar nebula, in low-temperature ion-derived reactions (e.g., Aikawa and Herbst 1999; Cleeves et al. 2014; Bockelée-Morvan et al. 2015). Incomplete mixing of the nebula, heliocentric temperature gradients, and migrating planets affecting the snowline, cause the H isotope variations between inner and outer solar system, and the distinct compositions of all its planetary bodies (Fig. 12; Brownlee 2014; Bockelée-Morvan et al. 2015; Chaps. 2 and 8).

Earth The Earth ocean has per definition $\delta D = 0‰$. The silicate Earth reservoirs (Table 1, Fig. 12) display lower δD values, e.g., for the convecting mantle δD of $-60 \pm 5‰$ (Clog et al. 2013), δD of -60 to $-130‰$ for the oceanic and continental mantle lithosphere (Deloule et al. 1991; Bell and Ihinger 2000), $\delta D < -126‰$ for subducting material (Shaw et al. 2012) and a bulk Earth δD of $-43 \pm 19‰$ (Lécuyer et al. 1998).

Moon The Moon is, in contrast to early assumptions, not entirely dry and may contain significant amounts of water (the bulk silicate Moon may have 133–292 ppm H_2O; Saal et al. 2008; Hauri et al. 2015). This includes water in volcanic glass, mare basalt melt inclusions and minerals such as apatite, olivine and plagioclase. From these, up to a few 100 ppm H_2O is calculated for the mantle source rocks, with a $\delta D \sim -100‰$ (Saal et al. 2013; Füri et al. 2014; Hui et al. 2017). Similarly, most lunar highland rocks show Earth-like δD values (δD between -281 and $-27‰$, Barnes et al. 2014). A much higher ratio compared to the Earth ($\delta D = 310 \pm 110‰$) was observed in highland plagioclase, which has been interpreted as being the result of degassing of the lunar magma ocean (Hui et al. 2017).

However, the bulk interior of the Moon could also contain only little water (< 10 ppm H_2O), with the D-rich water being supplied to the magma ocean late and more superficially by impact (Elkins-Tanton and Grove 2011). In any case, the range of the various Earth-like isotopic H compositions observed in the Moon is suggestive of a provenance of the volatiles similar to those in the Earth (Saal et al. 2013).

Mars In order to determine the mantle H isotopic composition for Mars, the D/H was examined in various phases from Martian meteorites (e.g., apatite, amphibole, melt inclusions and impact melts, Chap. 5). Tucker et al. (2015) measured a range between -300 to $+100‰$ in various Martian meteorites. An upper limit for the D/H in the Martian mantle has been given as $\delta D < 275‰$ (Usui et al. 2012; Hallis et al. 2012). Much higher values ($\delta D \sim$ 900–5500‰) have been detected elsewhere in Martian meteorites (e.g., Bogard et al. 2001; Hu et al. 2014; Usui et al. 2015). These ratios represent samples affected by atmospheric or surficial water components and fractionating losses.

Achondrites In addition to contributions from primitive chondrites, differentiated (achondritic) planetesimals could also have brought volatiles to Earth (Chaps. 11 and 12), because even this material, which is severely depleted in volatile elements relative to CI chondrites, may contain significant indigenous water (Chaps. 11 and 12). The D/H isotope examinations of achondrites are still rare. Recent studies of the D/H composition of the water in eucritic phosphates show similarities to that in Earth and carbonaceous chondrites ($\delta D \sim -162 \pm 127‰$, Sarafian et al. 2014; $\delta D \sim -34 \pm 67‰$, Barrett et al. 2016; $\delta D \sim -210$–$50‰$, Guan et al. 2016). Eucrites, supposed to originate from Vesta, formed early (e.g., 4561 ± 13 Ma; Hopkins et al. 2015), which implies that water similar to that in

Earth, the Moon and Vesta could have been incorporated into all inner solar system objects, from a similar source such as, e.g., carbonaceous chondrites (see below). On the other hand, phosphates in angrites, another particularly old achondrite class (4564.42 ± 0.12 Ma, Amelin 2008), appear to contain water with significant enrichments in D (δD > 500‰, > 400 ppm H_2O, Sarafian et al. 2017). The same authors also report 20–60 ppm of water in olivine, which may suggest, albeit deduced with some reservation, that the angrites' parent melt was water-rich and contained > 1 wt% water (Sarafian et al. 2017). The high D/H ratio could be the result of a D-rich, potentially cometary source or the result of strong fractionation during degassing (Sarafian et al. 2017). Similar to the work discussed in the preceding paragraph, Stephant et al. (2016) found low D/H ratios in phosphate ($\delta D = -173 \pm 72$‰), but also in pyroxene ($\delta D = -241 \pm 64$‰) of eucrites. Hydrogen in pyroxenes may better represent the parent melt composition than phosphates. The pyroxenes show lower H_2O content and D/H ratios than phosphates. The ratios are similar to an upper limit recently reported for the terrestrial deep mantle based on melt inclusions in olivine phenocrysts ($\delta D < -218$‰, Hallis et al. 2015). The similarity in low D/H ratios of the terrestrial deep mantle and of pyroxenes in eucrites was interpreted as potential evidence for the presence of a primordial, nebula-inherited (low D, see Sect. 5.2.1) component present in both Vesta and Earth.

A Carbonaceous Chondrite Origin of Earth's Water The general similarity of the Earth's D/H ratios measured in ocean water and silicate Earth reservoirs with ratios reported for the Moon, Mars, Vesta and, perhaps, the angrite parent body (Fig. 12), strongly implies a common source for the delivery of the water. This was suggested in numerous publications (e.g., Marty and Yokochi 2006; Saal et al. 2008). The most likely source are the carbonaceous chondrites, and more precisely CI chondrites (Alexander et al. 2012; Chap. 3). Bulk carbonaceous chondrites show a range of D/H ratios (δD between −230 and +766‰; Alexander et al. 2012). However, much of the D enrichments in primitive chondrites is carried by organic matter (bulk OM δD reaches up to 3500‰, whereas small organic aggregates show ratios up to 19000‰; e.g., Busemann et al. 2006; Alexander et al. 2007). The D/H ratios of chondritic water can be deduced by comparing measurements on bulk meteorite and organic matter. The calculated and extrapolated D/H ratios of the water bound in the hydrous phases of carbonaceous chondrites show a characteristic variability between the various carbonaceous chondrite groups ($\delta D \sim -587$ to +98‰; Alexander et al. 2012). This can be used, together with other isotope ratios, particularly N (see below), to further constrain the most probable chondritic provider of Earth's water. Isotopic similarities with the Earth for many elements may argue for a close link of enstatite chondrites to Earth and, hence, the origin of the terrestrial water through enstatite chondrites (Javoy et al. 2010). A recent publication supports a significant contribution to the Earth from enstatite chondrites (Dauphas 2017). However, the Si isotopic system (Fitoussi and Bourdon 2012), as well as other geochemical evidence (Wang and Becker 2013), do not support this.

In principle, the rough isotopic match of the terrestrial δD and δD in the other bodies of the inner solar system, with carbonaceous chondrite δD could be fortuitous. Mixing of low δD primordial nebula water with other sources such as cometary δD contributions could also result in chondritic δD values. The δD values of cometary water measured in 8 out of 12 comets are so far consistent with a high value of $\delta D \geq 1050$‰ (Bockelée-Morvan et al. 2015). Vice versa, the δD values in comet Hartley 2 ($\delta D = 34 \pm 154$‰, Hartogh et al. 2011) and three further comets (only upper limits given, Bockelée-Morvan et al. 2015) are consistent with the D/H of Earth's water. However, the cometary organic matter would still be more D-rich than the water ice and would deliver too much D to Earth (Alexander et al. 2012).

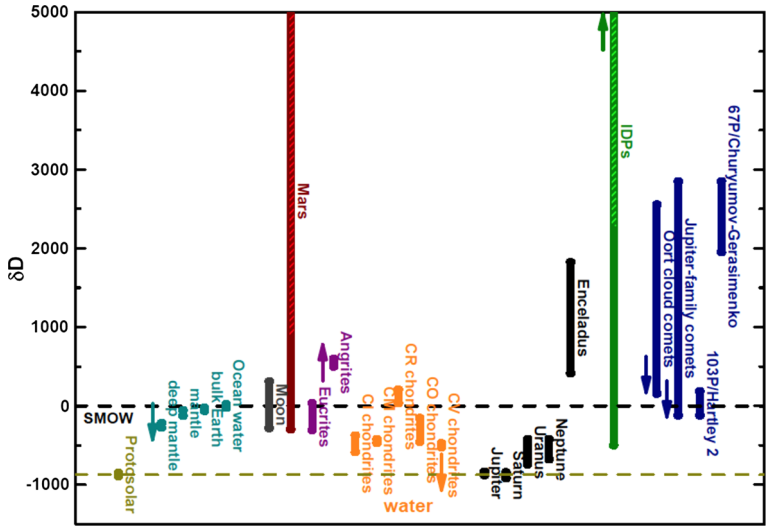

Fig. 12 Hydrogen isotope ratios, i.e. D/H ratios, in Earth and solar system reservoirs, given in delta notation (δD). The delta notation for H gives the variation of the measured ratio relative to a standard in permil. Standards are terrestrial mean ocean water for H ("SMOW"). Most data represent the D/H ratio as measured in water or hydroxyl groups in minerals. The protosolar value is observed essentially unaltered in the atmospheres of Jupiter and Saturn. Elevated ratios can be the result of D-enrichments during ion–molecule reactions in cold environments and can be found in pristine water and organic phases in comets, the outer icy planets and IDPs. The water of only a few comets including Hartley 2 may match the D/H of the Earth's water (further comets show upper limits consistent with SMOW). The high D/H in IDPs is mostly carried in organic matter in so-called "hotspots", although IDPs with "cometary" D/H, residing most likely in hydrous phases, were also observed (Mukhopadhyay and Nittler 2003). Organic matter is also responsible for most of the D enrichments in bulk carbonaceous chondrites (not shown). Here only D/H ratios of non-organic phases of carbonaceous chondrites (CI, CM, CR, CO, CV) are shown (labelled "water"). The high D/H ratios of many Martian samples and reservoirs are the result of incorporation of Martian surface material with atmospheric signatures because fractionation of H isotopes occurs during H escape from the planet's atmosphere with preferential loss of H over D (Watson et al. 1994). *Arrows* illustrate/symbolize that a precise upper and lower limits, respectively, for a given range is not known. References are given in the main text, apart from those for the giant planets and Enceladus (Feuchtgruber et al. 1999; Lellouch et al. 2001; Waite et al. 2009)

Most importantly, the N isotopic composition of comets probably excludes a significant cometary input (see below). In this context, it is also important to keep in mind that the volatile-depleted material initially accreted to the Earth (pre-late-veneer), or some of the volatile-rich (up to 30%, see above) Earth-forming material, will contain some primordial water. Another mean to compensate the heavy H isotopic composition of cometary water to achieve terrestrial ocean D/H was suggested to be IDP, which are exposed to the solar wind in space and would carry isotopically light water (Pavlov et al. 1999). Water-bearing rims in anhydrous IDPs due to space-weathering by solar wind have indeed been observed (Bradley 2015) and dust might have been an important source of volatiles during the early evolution (100 Ma) of the Earth (Marty and Yokochi 2006).

Finally, an alternative view is that indeed a substantial amount of Earth's water was accreted early from the nebula (Halliday 2013; Hallis 2017), e.g., by water adsorption (Drake 2005; Vattuone et al. 2013) and incorporation into olivine grains. This water would have been strongly isotopically fractionated during condensation in the nebula (Asaduzzaman

et al. 2015; Ganguly et al. 2016). The low D/H ratio of nebular water could have been increased by mass fractionation during atmospheric hydrogen loss (Genda and Ikoma 2008).

Indeed, the large D/H variations reported for various minerals in the eucrite and angrite achondrites, Martian meteorites and the Earth, indicate that comparing D/H ratios alone might not be conclusive, without a full understanding of melting and impact processing on the planetary/parent body that could cause D/H fractionation during partitioning, diffusion and degassing.

5.2.2 Constraints from Nitrogen and Carbon Isotopes

The discussion on H isotopes above illustrates the need for additional constraints to determine the possible origin(s) for Earth's water. The volatile element N is commonly the first choice to be added. Similar to H, the N isotopic compositions of the reservoirs in the solar system show a significant range. It is given here in the delta notation, i.e. the difference to the N isotopic ratio of the Earth atmosphere ($\delta^{15}N = 0‰$). The Sun, assumed to represent nebular N, has a strongly negative $\delta^{15}N$ value of $-389 \pm 5‰$, which is, as for H isotopes, supported by measurements of N isotope data of Jupiter ($\delta^{15}N = -396 \pm 141‰$, Fouchet et al. 2004). In contrast, comets and carbonaceous chondrites are strongly enriched: carbonaceous chondrites bulk $\delta^{15}N$ range between -20 to up to $+350‰$ (Alexander et al. 2012). Almost all N-bearing molecules detected in comets show $\delta^{15}N$ in the range 650 to 2000‰, with only two detections roughly consistent with terrestrial N (Bockelée-Morvan et al. 2015). The N isotopic compositions of terrestrial silicate reservoirs scatter around $\delta^{15}N \sim 0‰$. For example, the $\delta^{15}N$ for bulk-silicate Earth + atmosphere, MORB-source, and continental crust are 2.7‰, $-5‰$ and 7.3‰, respectively (Johnson and Goldblatt 2015). Others reported a larger range between $\delta^{15}N \sim -40‰$ and $-5‰$ for the terrestrial mantle (Cartigny and Marty 2013). An even larger range between -46 and $+27‰$ was reported for indigenous lunar N, which is challenging to determine (Füri et al. 2015), and suggests a link to N in Earth's pristine mantle and in carbonaceous chondrites. The $\delta^{15}N$ in eucrites, i.e. Vesta, is similar to the Earth, Moon and carbonaceous chondrites (Sarafian et al. 2014). In agreement with the high δD in most comets, their high $\delta^{15}N$, however, excludes them as the dominant N source for the Earth. On the other hand, similarly to the interpretation of H isotopic values, a mixture of ^{15}N-enriched cometary material and nebula N, either primordially accreted by the Earth, or trapped in cometary ices (Marty et al. 2016), could in principle provide the terrestrial N composition.

The $^{13}C/^{12}C$ ratios in all examined solar system reservoirs, the Earth, carbonaceous chondrites and comets (with large uncertainties) are within $< 10\%$ similar (e.g., Marty et al. 2013). Their values are slightly higher than the protosolar value, consistent with any of the currently proposed origins of Earth's water, and not sufficiently well constrained to distinguish subtle differences in the source reservoirs (Marty et al. 2013).

5.2.3 Constraints from the Isotopes of Noble Gases

While the study of H and N isotopes are most instructive, isotope compositions of the chemically inert noble gases He to Xe will add additional constraints to the question of the origin of Earth's water, and we will summarize here the major points. The moon-forming giant impact, as many preceding impacts on Earth, may have erased most signatures of a pre-existing primary atmosphere (Chap. 13). These impacts, combined with global magma oceans over an extended period, led to partial degassing of the Earth's mantle. Outgassing of mostly radiogenic noble gases, together with incoming volatile-rich chondritic or cometary material, replenished the terrestrial atmosphere (e.g., Pepin and Porcelli 2002; Porcelli and Ballentine 2002).

Protosolar Cloud and Planetary Atmospheres The noble gas composition of the protosolar cloud is best represented by the Sun. The exception is solar ^{3}He, which significantly increased immediately after the Sun's accretion due to solar D-burning (e.g., Geiss and Gloeckler 2003). The protosolar pre-D-burning ^{3}He/^{4}He ratio might be best represented by Jovian He or, perhaps, primitive meteorites (Mahaffy et al. 1998; Busemann et al. 2000, 2001). All other noble gas isotopic ratios of the solar nebula are best sampled by the solar wind (e.g., Heber et al. 2009; Vogel et al. 2011; Meshik et al. 2012). So-called "planetary" noble gases (the atmospheres of Earth and Mars, but also certain components in chondrites) are isotopically and elementally heavy compared to solar gases. The exception is Xe in the present terrestrial atmosphere, which is more depleted compared to Kr and the solar composition (e.g., Dauphas and Morbidelli 2014). These planetary patterns, i.e. fractionation relative to the protoplanetary cloud can be the result of processes that favour the depletion of the lighter species such as (i) incomplete or selective trapping by adsorption and dissolution, or (ii) diffusive, evaporative or gravitationally-controlled losses from reservoirs of an originally solar composition.

Earth's Mantle Helium and Ne isotopes in the mantle, measured in oceanic basalts in numerous locations, show a mixing range between atmosphere and solar end-members. The presence of solar He and Ne in the Earth's mantle (e.g., Pepin and Porcelli 2002; Yokochi and Marty 2004; Moreira and Charnoz 2016, and references therein) suggests either that (i) an early magma ocean has dissolved parts of a thick proto-atmosphere of solar nebula gas (e.g., Hayashi et al. 1979), (ii) dust precursors delivered elementally fractionated adsorbed nebula gas (e.g., Pepin and Porcelli 2002), or (iii) small dust grains incorporated solar wind by irradiation, perhaps by an early active Sun after dissipation of the nebula (Podosek et al. 2000; Trieloff et al. 2000; Moreira and Charnoz 2016). In all cases, the noble gases were likely accompanied by abundant H_2 that then formed H_2O in the Earth by oxidization (e.g., Marty and Yokochi 2006). In contrast to these hints for solar gases, chondritic (non-solar) Xe and Kr are observed in mantle gases (Holland et al. 2009; Caracausi et al. 2016). This supports the general idea that most water (see above) is of chondritic, i.e. asteroidal origin.

Most (~85%; e.g., Allègre et al. 1995) of the Earth's ^{129}I-derived ^{129}Xe was possibly lost within the first 90–110 Ma, either by transferal into a "hidden Xe" reservoir in the deep mantle (e.g., Podosek and Ozima 2000), or during continued magma ocean degassing and subsequent escape from the atmosphere into space (e.g., Marty and Yokochi 2006). In the latter case, water could have been similarly lost. However, the relatively low D/H ratio in the Earth does not support such losses, which implies that the water remained dissolved in the mantle (Marty and Yokochi 2006). Sophisticated considerations of the Ne and Xe isotopes in the Earth provide evidence for two distinct noble gas reservoirs in the mantle, isolated since ~100 Ma after the formation of the solar system (Mukhopadhyay 2012). In particular, these reservoirs show (i) distinct abundances of ^{129}Xe (produced by decay of once extant ^{129}I), (ii) the distinct presence of primordial ^{22}Ne relative to nucleogenic ^{21}Ne, and (iii) different primordial ^{20}Ne/^{22}Ne endmember compositions. These mantle reservoirs, which could also have distinct water contents, are individually sampled by OIB and MORB (Sect. 3.2.2; Caracausi et al. 2016).

The present, secondary atmosphere likely contains mostly radiogenic noble gas isotopes replenished from the interior and from the "late veneer". The elemental noble gas pattern shows the characteristic depletion in Xe relative to lighter elements (if normalized to solar composition), which was taken as evidence that the noble gases were delivered from volatile-rich comets (see above; Dauphas 2003). Comets would then have delivered abundant cometary water. However, the predominantly high D/H ratios reported for comets limit

this contribution (Sect. 5.2.1). In the following, we discuss briefly further potential source reservoirs.

Chondrites Bulk noble gas isotopes in primitive chondrites are carried in (i) presolar grains, dominating He and Ne (e.g., the "HL" and "Ne-E" components) with significant "exotic" isotopic anomalies related to stellar nucleosynthesis (e.g., Wieler et al. 2006; Ott 2014, and references therein), (ii) most likely organic matter (the component called "phase Q" dominating Ar-Xe; e.g., Busemann et al. 2000; Ott 2014, and references therein) and (iii)—not negligible but often neglected—less abundant bulk silicates (Wieler et al. 2006, and references therein). Apart from the rare but important observations of chondritic Kr and Xe signatures in the terrestrial mantle (Holland et al. 2009; Caracausi et al. 2016), other typical isotopic signatures of primitive meteorites (see above) are not observed in the atmosphere or interior. However, if substantiated, the observation of chondritic Kr and Xe in the Earth's mantle supports an origin of the Earth's water from asteroidal sources.

Achondrites and Moon *Achondrites:* Noble gas concentrations in achondrites are, as expected in view of the experienced elevated temperatures, severely depleted, by orders of magnitude compared to primitive carbonaceous chondrites (e.g., Busemann and Eugster 2002). Only Ar-Xe in the most primitive achondrites (e.g., lodranites) survived the increased temperatures during metamorphism and incipient differentiation (Busemann and Eugster 2002), likely in the most thermally-resistant phase Q component.

Moon: In contrast to hydrogen isotopes (Sect. 5.2.1), primordial "indigenous" noble gases in lunar samples that survived the harsh process of lunar formation have not been detected yet (Füri et al. 2015).

Comets and IDPs Noble gases in comets are notoriously difficult to observe and only fragmentary information could be collected so far. For the first time, cometary Ar could clearly be detected ($^{36}Ar/^{38}Ar = 5.4 \pm 1.4$) in the coma of comet 67P/Churyumov-Gerasimenko (Balsiger et al. 2015). If the volatiles did not fractionate during emission from the comet, the Ar/H_2O ratio implies that comets are less likely than carbonaceous chondrites to have contributed Ar and water to Earth, because the ratio is, as the D/H ratio (Altwegg et al. 2015), much higher than the terrestrial values. Helium and Ne in comet Wild 2 dust seem very abundant (Marty et al. 2008). The Ne is isotopically consistent with "Phase Q" (Ne found in minor amounts in meteorites), while He is rich in ^3He compared to phase Q, suggesting some exchange from inner and outer solar system material. Most likely He and Ne represent a component incorporated by strong irradiation (Marty et al. 2008).

First attempts to detect trapped Kr and Xe in IDPs show large concentrations, perhaps similar to those found in primitive meteorites (Kehm et al. 2009; Busemann et al. 2010; Spring et al. 2014). However, the Kr and Xe isotopic compositions in bona-fide cometary dust could not be analyzed sufficiently precisely yet, although they are essential to clarify the origin and character of the cometary noble gases. The light noble gases are dominated by solar wind and cosmogenic components, and the primordially trapped He and Ne isotopic compositions are hence still unknown (e.g., Nier and Schlutter 1992). Altogether, evidence from cometary noble gases is currently inconclusive regarding the origin of Earth's water. Major advances might arise from future results on the noble gas isotopic compositions in comet Churyumov-Gerasimenko. Until then, trapping experiments on noble gases in ices at various temperatures (e.g., Owen et al. 1992; Bar-Nun and Owen 1998) are the best tool for a better understanding of the crucial cometary noble gases.

5.2.4 Summary

In summary, isotopic considerations alone cannot reveal the origin of Earth's water. Generally, large contributions from chondritic asteroidal sources fit better than cometary material. However, at least for the noble gases, two distinct sources for mantle and atmosphere are probable. More sophisticated modeling involving relative abundances of many volatile elements leads to a variety of detailed conclusions: Alexander et al. (2012) suggest that Earth's water is essentially delivered with carbonaceous chondrites, in this case mainly (90%) CI chondrites. This is in agreement with considerations from platinum group elements and elemental abundances of S, Se and Te, which argue for a CM-like late veneer (Dauphas 2003; Marty and Yokochi 2006; Wang and Becker 2013). Other work pleads for an enstatite chondrite-like late veneer (Fischer-Gödde and Kleine 2017). Marty et al. (2016) suggest a significant cometary contribution (possibly as IDPs) to the noble gases at least in the terrestrial atmosphere during the late veneer or late heavy bombardment phase. However, Marty (2012) and Marty et al. (2016) limit cometary contributions to the other volatiles in the Earth to a few percent. Halliday (2013) envisions 10–30% of cometary material mixing with the CI chondritic late veneer. CI-CM chondritic contributions of ~2–4% of the Earth's mass could have delivered volatiles to the dry proto-Earth (Marty 2012; Alexander 2017). While most volatiles in the Earth may be present in chondritic relative proportions, N is depleted, possibly residing in the core (Marty 2012). Halliday (2013) also includes H, C and Xe for possible elements residing in the core. All, Marty (2012), Halliday (2013) and Dauphas and Morbidelli (2014) favour volatile-rich outer asteroid belt sources to deliver the Earth's water.

In order to finally clarify the origin of Earth's water, it will be essential to determine (i) the H and N isotopic compositions of more comets, and (ii) the noble gas elemental and isotopic compositions of cometary solids and ices, as well as of the terrestrial core and mantle.

6 Conclusion

The present consensus on the origin of Earth's water seems to converge on the following scenario (Fig. 11), although many details are still debated. The Earth initially accreted water-poor from the inner part of the solar nebula 4.56 Ga ago. After the Earth had reached ~60–90% of its current size, water-rich bodies from further away from the Sun were delivered to the Earth, while core segregation was well underway. This delivery likely already brought more water than needed to explain the Earth's water content. Evidence suggests that the late veneer, the last < 1% of accretion of material to the Earth after core formation, predominantly delivered ~~carbonaceous chondrites~~ from the asteroid belt to the Earth. The late veneer may have brought 20 to 100% of the H and C to the Earth's mantle depending on which estimates are used for the water and C contents of the bulk silicate Earth (Wang and Becker 2013). Accretion through giant impacts and radioactive decay of isotopes released sufficient heat such that deep magma oceans were generated. While these lasted for several million years (Elkins-Tanton 2008), significant degassing of the oceans occurred and resulted in water transport from the Earth's interior to the atmosphere, which in turn could be lost by interaction with the irradiation of the early active Sun. Differentiation of our planet into core, mantle and crust likely initially generated a layered distribution of water. The early Earth probably operated in a stagnant lid regime before the onset of plate tectonics and this could have resulted in the upper part of the mantle being depleted in water by crust

formation events, leaving deeper parts of the mantle comparatively water-rich. Degassing and cooling allowed the formation of water oceans early in the Earth's history, > 4 Ga ago (Wilde et al. 2001). The onset of plate tectonics ~3 Ga ago started to rehydrate the mantle by subducting water-rich lithologies of the crust back into the mantle. This resulted in a heterogeneously hydrated mantle. Despite fast H diffusion in minerals at mantle temperatures, large (> km in size) water-rich zones could not be erased on billion-year time scales. The heterogeneous mantle also implies that convection was not efficient enough to homogenize water in the mantle.

This story line has many uncertainties. The deeper the Earth, the less certain are the concentration and distribution estimates for water. In particular, estimates for H in the lower mantle and core are very uncertain, while also fluxes of water between reservoirs, including at the crucial subduction zones, have large errors. When considering these uncertainties, the total water amount in the Earth could range from the equivalent of 3 to 18 times the present mass of the oceans. This uncertainty also affects the determination of the origin and amount of water-rich material from which the Earth accreted or the material that was delivered later over the Earth history. Moreover, solar nebula condensation models have large uncertainties on condensation mechanisms and the position of the snowline, the temperature-driven boundary of water condensation. These uncertainties strongly affect the initial conditions that are used for dynamic models (e.g., Grand Tack), which describe the delivery of water-rich material to the inner solar system and the Earth. Carbonaceous chondrites are the most promising candidates to date for supplying the Earth's water, but we have not yet sampled and analyzed all potential water-rich materials of the solar system, in particular data are missing for comets and bodies from the outer solar system.

These open questions require more comprehensive future studies of terrestrial and extraterrestrial samples, with continuously improved analytical techniques, including robot or human solar-system exploration. For example, two robotic missions, OSIRIS-REx (NASA, USA) and Hayabusa 2 (JAXA, Japan) are presently travelling towards asteroids and are planned to return samples of carbonaceous chondrite composition in 2023 and 2020, respectively. These missions are vital to complement the meteorite collection and Apollo samples used to study the formation of the Earth and our solar system in general. Observation of protoplanetary disks and planetary systems around other stars will further constrain our planetary formation scenarios. For Earth, progress can also be expected from geophysical methods such as seismology and electrical conductivity, globally by increasing geographical coverage of measurements, and in the laboratory by better constraining physical properties of deep Earth phases. Increased computational power will also improve models of Earth's formation and geodynamics, as well as ab initio calculations of water incorporation in high pressure phases. Water plays such a key role in planetary differentiation, volcanism, plate-tectonics, mantle convection, and the origin of life that we expect the flowering of studies of the last 10-years on water in the Earth to be sustained by a high rate of discoveries.

Acknowledgements The authors are very grateful to Rosie Jones and an anonymous reviewer for careful detailed comments that greatly improved this manuscript. MS also thanks Hilke Schlichting for inspiring discussions that helped to improve the manuscript. Thanks to editor Michel Blanc and ISSI in Bern (Switzerland) for organizing in February 2016 the workshop on Water delivery to the Solar System from which this book originates. This work was supported by NSF grant #OCE1624310 to AHP and, in part (HB and MS), has been carried out within the frame of the National Centre for Competence in Research 'PlanetS' supported by the Swiss National Science Foundation (SNSF).

References

N. Abe, E. Ohtani, T. Okuchi, K. Righter, M.J. Drake, Water in the early Earth, in *Origin of the Earth and Moon*, ed. by R.M. Canup, K. Righter (University of Arizona Press, Tucson, 2000), pp. 413–433

G.A. Abers, P.E. van Keken, B.R. Hacker, The cold and relatively dry nature of mantle forearcs in subduction zones. Nat. Geosci. **10**, 333–337 (2017)

J. Adam, M. Turner, E.H. Hauri, S. Turner, Crystal/melt partitioning of water and other volatiles during the near-solidus melting of mantle peridotite: comparisons with non-volatile incompatible elements and implications for the generation of intraplate magmatism. Am. Mineral. **101**, 876–888 (2016)

Y. Aikawa, E. Herbst, Deuterium fractionation in protoplanetary disks. Astrophys. J. **526**, 314–326 (1999)

R.D. Aines, G.R. Rossman, The hydrous component in garnets: pyralspites. Am. Mineral. **69**, 1116–1126 (1984)

F. Albarède, Volatile accretion history of the terrestrial planets and dynamic implications. Nature **461**, 1227–1233 (2009)

F. Albarède, C. Ballhaus, J. Blichert-Toft, C.-T. Lee, B. Marty, F. Moynier, Q.-Z. Yin, Asteroidal impacts and the origin of terrestrial and lunar volatiles. Icarus **222**, 44–52 (2013)

C.M.O.D. Alexander, R. Bowden, M.L. Fogel, K.T. Howard, C.D.K. Herd, L.R. Nittler, The provenances of asteroids, and their contributions to the volatile inventories of the terrestrial planets. Science **337**, 721–723 (2012)

C.M.O.D. Alexander, M. Fogel, H. Yabuta, G.D. Cody, The origin and evolution of chondrites recorded in the elemental and isotopic compositions of their macromolecular organic matter. Geochim. Cosmochim. Acta **71**, 4380–4403 (2007)

C.M.O.D. Alexander, The origin of inner Solar System water. Philos. Trans. R. Soc. Lond. A **375**, 20150384 (2017)

C.J. Allègre, G. Manhès, C. Göpel, The age of the Earth. Geochim. Cosmochim. Acta **59**, 1445–1456 (1995)

K. Altwegg, H. Balsiger, A. Bar-Nun, J.J. Berthelier, A. Bieler, P. Bochsler, C. Briois, U. Calmonte, M. Combi, J. De Keyser, P. Eberhardt, B. Fiethe, S. Fuselier, S. Gasc, T.I. Gombosi, K.C. Hansen, M. Hässig, A. Jäckel, E. Kopp, A. Korth, L. LeRoy, U. Mall, B. Marty, O. Mousis, E. Neefs, T. Owen, H. Rème, M. Rubin, T. Sémon, C.-Y. Tzou, H. Waite, P. Wurz, 67P/Churyumov-Gerasimenko, a Jupiter family comet with a high D/H ratio. Science **347**, 1261952 (2015)

Y. Amelin, U–Pb ages of angrites. Geochim. Cosmochim. Acta **72**, 221–232 (2008)

T. Andersen, E.-R. Neumann, Fluid inclusions in mantle xenoliths. Lithos **55**, 301–320 (2001)

M. Andrut, M. Wildner, J. Ingrin, A. Beran, Mechanisms of OH defect incorporation in naturally occurring, hydrothermally formed diopside and jadeite. Phys. Chem. Miner. **34**, 543–549 (2007)

P. Ardia, M.M. Hirschmann, A.C. Withers, T.J. Tenner, H_2O storage capacity of olivine at 5–8 GPa and consequences for dehydration partial melting of the upper mantle. Earth Planet. Sci. Lett. **345–348**, 104–116 (2012)

L.S. Armstrong, M.M. Hirschmann, B.D. Stanley, E.G. Falksen, S.D. Jacobsen, Speciation and solubility of reduced C-O-H-N volatiles in mafic melt: implications for volcanism, atmospheric evolution, and deep volatile cycles in terrestrial planets. Geochim. Cosmochim. Acta **171**, 283–302 (2015)

I.M. Artemieva, W.D. Mooney, Thermal thickness and evolution of Precambrian lithosphere: a global study. J. Geophys. Res. **106**, 16387–16414 (2001)

A. Asaduzzaman, K. Muralidharan, J. Ganguly, Incorporation of water into olivine during nebular condensation: insights from density functional theory and thermodynamics, and implications for phyllosilicate formation and terrestrial water inventory. Meteorit. Planet. Sci. **50**, 578–589 (2015)

C. Aubaud, E. Hauri, M.M. Hirschmann, Hydrogen partition coefficients between nominally anhydrous minerals and basaltic melts. Geophys. Res. Lett. **31**, L20611 (2004). doi:10.1029/2004GL021341

C. Aubaud, M.M. Hirschmann, A.C. Withers, R.L. Hervig, Hydrogen partitioning between melt, clinopyroxene, and garnet at 3 GPa in a hydrous MORB with 6 wt.% H_2O. Contrib. Mineral. Petrol. **156**, 607–625 (2008)

C. Aubaud, A.C. Withers, M.M. Hirschmann, Y. Guan, L.A. Leshin, S.J. Mackwell, D.R. Bell, Intercalibration of FTIR and SIMS for hydrogen measurements in glasses and nominally anhydrous minerals. Am. Mineral. **92**, 811–828 (2007)

S. Aulbach, R.L. Rudnick, W.F. McDonough, Li-Sr-Nd isotope signatures of the plume and cratonic lithospheric mantle beneath the margin of the rifted Tanzanian craton (Labait). Contrib. Mineral. Petrol. **155**, 79–92 (2008)

K. Baba, A. Chave, R.L. Evans, G. Hirth, R.L. Mackie, Mantle dynamics beneath the East Pacific Rise at 17 S: insights from the Mantle Electromagnetic and Tomography (MELT) experiment. J. Geophys. Res. **111**, B02101 (2006)

J. Badro, A.S. Côté, J.P. Brodholt, A seismologically consistent compositional model of Earth's core. Proc. Natl. Acad. Sci. **111**, 7542–7545 (2014)

E. Bali, A. Audédat, H. Keppler, Water and hydrogen are immiscible in Earth's mantle. Nature **495**, 220–222 (2013)
E. Bali, N. Bolfan-Casanova, K.T. Koga, Pressure and temperature dependence of H solubility in forsterite: an implication to water activity in the Earth interior. Earth Planet. Sci. Lett. **268**, 354–363 (2008)
C. Ballhaus, V. Laurenz, C. Münker, R.O.C. Fonseca, F. Albarède, A. Rohrbach, M. Lagos, M.W. Schmidt, K.-P. Jochum, B. Stoll, U. Weis, H.M. Helmy, The U/Pb ratio of the Earth's mantle—a signature of late volatile addition. Earth Planet. Sci. Lett. **362**, 237–245 (2013)
H. Balsiger, K. Altwegg, J. Geiss, D/H and $^{18}O/^{16}O$ ratio in the hydronium ion and in neutral water from in situ ion measurements in comet Halley. J. Geophys. Res. **100**, 5827–5834 (1995)
H. Balsiger, K. Altwegg, A. Bar-Nun, J.-J. Berthelier, A. Bieler, P. Bochsler, C. Briois, U. Calmonte, M. Combi, J. De Keyser, P. Eberhardt, B. Fiethe, S.A. Fuselier, S. Gasc, T.I. Gombosi, K.C. Hansen, M. Hässig, A. Jäckel, E. Kopp, A. Korth, L. Le Roy, U. Mall, B. Marty, O. Mousis, T. Owen, H. Rème, M. Rubin, T. Sémon, C.-Y. Tzou, J.H. Waite, P. Wurz, Detection of argon in the coma of comet 67P/Churyumov–Gerasimenko. Sci. Adv. **1** (2015)
V. Baptiste, S. Demouchy, S. Keshav, F. Parat, N. Bolfan-Casanova, P. Condamine, P. Cordier, Decrease of hydrogen incorporation in forsterite from CO_2-H_2O-rich kimberlitic liquid. Am. Mineral. **100**, 1912–1920 (2015)
V. Baptiste, A. Tommasi, Petrophysical constraints on the seismic properties of the Kaapvaal craton mantle root. Solid Earth **5**, 1–19 (2014)
V. Baptiste, A. Tommasi, S. Demouchy, Deformation and hydration of the lithospheric mantle beneath the Kaapvaal craton, South Africa. Lithos **149**, 31–50 (2012)
A. Bar-Nun, T. Owen, Trapping of gases in water ice and consequences to comets and the atmospheres of the inner planets, in *Solar System Ices*, ed. by B. Schmitt, C. De Bergh, M. Festou (Springer, Dordrecht, 1998), pp. 353–366
J.J. Barnes, D.A. Kring, R. Tartèse, I.A. Franchi, M. Anand, S.S. Russell, An asteroidal origin for water in the Moon. Nat. Commun. **7**, 11684 (2016)
J.J. Barnes, R. Tartèse, M. Anand, F.M. McCubbin, I.A. Franchi, N.A. Starkey, S.S. Russell, The origin of water in the primitive Moon as revealed by the lunar highlands samples. Earth Planet. Sci. Lett. **390**, 244–252 (2014)
T.J. Barrett, J.J. Barnes, R. Tartèse, M. Anand, I.A. Franchi, R.C. Greenwood, B.L.A. Charlier, M.M. Grady, The abundance and isotopic composition of water in eucrites. Meteorit. Planet. Sci. **51**, 1110–1124 (2016)
G.E. Bebout, Volatile transfer and recycling at convergent margins: mass-balance and insights from high-P/T metamorphic rocks, in *Subduction Top to Bottom*, ed. by G.E. Bebout, D.W. Scholl, S.H. Kirby, J.P. Platt (American Geophysical Union, Washington, 1996), pp. 179–193
W. Behr, D. Smith, Deformation in the mantle wedge associated with Laramide flat-slab subduction. Geochem. Geophys. Geosyst. **17**, 1–18 (2016)
D.R. Bell, Water in mantle minerals. Nature **357**, 646–647 (1992)
D.R. Bell, M. Grégoire, T.L. Grove, N. Chatterjee, R.W. Carlson, P.R. Buseck, Silica and volatile-element metasomatism of Archean mantle: a xenolith-scale example from the Kaapvaal craton. Contrib. Mineral. Petrol. **150**, 251–267 (2005)
D.R. Bell, P.D. Ihinger, The isotopic composition of hydrogen in nominally anhydrous mantle minerals. Geochim. Cosmochim. Acta **64**, 2109–2118 (2000)
D.R. Bell, P.D. Ihinger, G.R. Rossman, Quantitative analysis of trace OH in garnet and pyroxenes. Am. Mineral. **80**, 465–474 (1995)
D.R. Bell, R.O. Moore, Deep chemical structure of the southern African mantle from kimberlite megacrysts. S. Afr. J. Geol. **107**, 59–80 (2004)
D.R. Bell, G.R. Rossman, The distribution of hydroxyl in garnets from the subcontinental mantle in southern Africa. Contrib. Mineral. Petrol. **111**, 161–178 (1992a)
D.R. Bell, G.R. Rossman, Water in Earth's mantle: the role of nominally anhydrous minerals. Science **255**, 1391–1397 (1992b)
D.R. Bell, G.R. Rossman, J. Maldener, D. Endisch, F. Rauch, Hydroxide in olivine: a quantitative determination of the absolute amount and calibration of the IR spectrum. J. Geophys. Res. **108**(B2), 2105 (2003a)
D.R. Bell, M.D. Schmitz, P.E. Janney, Mesozoic thermal evolution of the southern African mantle lithosphere. Lithos **71**, 273–287 (2003b)
D.R. Bell, G.R. Rossman, J. Maldener, D. Endisch, F. Rauch, Hydroxide in kyanite; a quantitative determination of the absolute amount and calibration of the IR spectrum. Am. Mineral. **89**, 998–1003 (2004a)
D.R. Bell, G.R. Rossman, R.O. Moore, Abundance and partitioning of OH in a high pressure magmatic system: megacrysts from the Monastery kimberlite, South Africa. J. Petrol. **45**, 1539–1564 (2004b)

W. Ben-Ismail, G. Barruol, D. Mainprice, The Kaapvaal craton seismic anisotropy: petrophysical analyses of upper mantle kimberlite nodules. Geophys. Res. Lett. **28**, 2497–2500 (2001)
A. Bénard, K.T. Koga, N. Shimizu, M.A. Kendrick, D.A. Ionov, O. Nebel, R.J. Arculus, Chlorine and fluorine partition coefficients and abundances in sub-arc mantle xenoliths (Kamchatka, Russia): implications for melt generation and volatile recycling processes in subduction zones. Geochim. Cosmochim. Acta **199**, 324–350 (2017)
W. Benz, W.L. Slattery, A.G.W. Cameron, The origin of the moon and the single-impact hypothesis I. Icarus **66**, 515–535 (1986)
A. Beran, Messung des Ultrarot-Pleochroismus von Mineralen. XIV. Der Pleochroismus der OH-Streckfrequenz in Diopsid. Tschermak's Mineral. Petrogr. Mitt. **23**, 79–85 (1976)
A. Beran, E. Libowitzky, Water in natural mantle minerals II: olivine, garnet and accessory minerals, in *Water in Nominally Anhydrous Minerals*, ed. by H. Keppler, J.R. Smyth (Mineralogical Society of America, Chantilly, 2006), pp. 169–191
D. Bercovici, S.-I. Karato, Whole-mantle convection and the transition-zone water filter. Nature **425**, 39–44 (2003)
M.I. Billen, M. Gurnis, A low viscosity wedge in subduction zones. Earth Planet. Sci. Lett. **193**, 227–236 (2001)
F. Birch, Elasticity and constitution of the Earth's interior. J. Geophys. Res. **57**, 227–286 (1952)
M. Bizimis, A.H. Peslier, Water in Hawaiian garnet pyroxenites: implications for water heterogeneity in the mantle. Chem. Geol. **397**, 61–75 (2015)
M. Bizimis, G. Sen, V.J.M. Salters, Hf-Nd isotope decoupling in the oceanic lithosphere: constraints from spinel peridotites from Oahu, Hawaii. Earth Planet. Sci. Lett. **217**, 43–58 (2004)
D. Bockelée-Morvan, U. Calmonte, S. Charnley, J. Duprat, C. Engrand, A. Gicquel, M. Hässig, E. Jehin, H. Kawakita, B. Marty, S. Milam, A.D. Morse, P. Rousselot, S. Sheridan, E. Wirström, Cometary isotopic measurements. Space Sci. Rev. **197**, 47–83 (2015)
J.-L. Bodinier, M. Godard, Orogenic, ophiolitic, and abyssal peridotites, in *Treatise on Geochemistry*, ed. by R. Carlson (Elsevier, Oxford, 2003), pp. 103–170
R.J. Bodnar, T. Azbej, S.P. Becker, C. Cannatelli, A. Fall, M. Severs, Whole Earth geohydrologic cycle, from the clouds to the core: the distribution of water in the dynamic Earth system. Spec. Pap., Geol. Soc. Am. **500**, 431–461 (2013)
D.D. Bogard, R.N. Clayton, K. Marti, T. Owen, G. Turner, Martian volatiles: isotopic composition, origin, and evolution. Space Sci. Rev. **96**, 425–458 (2001)
N. Bolfan-Casanova, Water in the Earth's mantle. Mineral. Mag. **69**, 229–257 (2005)
N. Bolfan-Casanova, H. Keppler, D.C. Rubie, Water partitioning between nominally anhydrous minerals in the MgO-SiO_2-H_2O system up to 24 GPa: implications for the distribution of water in the Earth's mantle. Earth Planet. Sci. Lett. **182**, 209–221 (2000)
F.R. Boyd, Compositional distinction between oceanic and cratonic lithosphere. Earth Planet. Sci. Lett. **96**, 15–26 (1989)
F.R. Boyd, J.J. Gurney, S.H. Richardson, Evidence for a 150–200 km thick Archean lithosphere from diamond inclusion thermobarometry. Nature **315**, 387–389 (1985)
F.R. Boyd, N.P. Pokhilenko, D.G. Pearson, S.A. Mertzman, N.V. Sobolev, L.W. Finger, Composition of the Siberian cratonic mantle: evidence from Udachnaya peridotite xenoliths. Contrib. Mineral. Petrol. **128**, 228–246 (1997)
J.P. Bradley, *Water and organics in interplanetary dust particles* (American Astronomical Society Assembly, Honolulu, 2015)
J.P. Bradley, H.A. Ishii, J.J. Gillis-Davis, J. Ciston, M.H. Nielsen, H.A. Bechtel, M.C. Martin, Detection of solar wind-produced water in irradiated rims on silicate minerals. Proc. Natl. Acad. Sci. **111**, 1732–1735 (2014)
A.D. Brandon, D.S. Draper, Constraints on the origin of the oxidation state of mantle overlying subduction zones: an example from Simcoe, Washington, USA. Geochim. Cosmochim. Acta **60**, 1739–1749 (1996)
A.D. Brandon, R.J. Walker, J.W. Morgan, M.D. Norman, H.M. Prichard, Coupled ^{186}Os and ^{187}Os evidence for core-mantle interaction. Science **280**, 1570–1573 (1998)
J. Braunmiller, S. van der Lee, L. Doermann, Mantle transition zone thickness in the central South-American subduction zone, in *Earth's Deep Water Cycle*, ed. by S. Jacobsen, S. Lee (AGU Geophysical Monograph, Washington D.C., 2006), pp. 215–224
G.P. Brey, T. Köhler, Geothermobarometry in four-phase lherzolites II. New thermobarometers, and practical assessment of existing thermobarometers. J. Petrol. **31**, 1353–1378 (1990)
G.P. Brey, T. Köhler, K.G. Nickel, Geothermobarometry in four-phase lherzolites I. Experimental results from 10 to 60 kb. J. Petrol. **31**, 1313–1352 (1990)
D.E. Brownlee, Comets, in *Treatise on Geochemistry*, ed. by A.S. Davis 2nd edn. (Elsevier, Amsterdam, 2014), pp. 335–363

H. Bureau, H. Keppler, Complete miscibility between silicate melts and hydrous fluids in the upper mantle: experimental evidence and geochemical implication. Earth Planet. Sci. Lett. **165**, 187–196 (1999)
S.R. Burgess, B. Harte, Tracing lithosphere evolution through the analysis of heterogeneous G9–G10 garnets in peridotite xenoliths, II: REE chemistry. J. Petrol. **43**, 609–634 (2004)
K. Burke, B. Steinberger, T.H. Torsvik, M.A. Smethurst, Plume generation zones at the margins of Large Low Shear Velocity Provinces on the core-mantle boundary. Earth Planet. Sci. Lett. **265**, 49–60 (2008)
H. Busemann, H. Baur, R. Wieler, Primordial noble gases in "phase Q" in carbonaceous and ordinary chondrites studied by closed-system stepped etching. Meteorit. Planet. Sci. **35**, 949–973 (2000)
H. Busemann, H. Baur, R. Wieler, Helium isotopic ratios in carbonaceous chondrites: significant for the early solar nebula and circumstellar diamonds? in *32nd Lunar and Planetary Science Conference*, The Woodlands, TX (2001)
H. Busemann, O. Eugster, The trapped noble gas component in achondrites. Meteorit. Planet. Sci. **37**, 1865–1891 (2002)
H. Busemann, A.N. Nguyen, G.D. Cody, P. Hoppe, A.L.D. Kilcoyne, R.M. Stroud, T.J. Zega, L.R. Nittler, Ultra-primitive interplanetary dust particles from the comet 26P/Grigg-Skjellerup dust stream collection. Earth Planet. Sci. Lett. **288**, 44–57 (2009)
H. Busemann, N. Spring, S. Crowther, J. Claydon, J. Gilmour, L. Nittler, Abundant primordial xenon in interplanetary dust particles from the comet Grigg-Skjellerup collection, in *Lunar Planet. Sci. Conf.*, The Woodlands, TX (2010), p. 1947
H. Busemann, A.F. Young, C.M.O.D. Alexander, P. Hoppe, S. Mukhopadhyay, L.R. Nittler, Interstellar chemistry recorded in organic matter from primitive meteorites. Science **312**, 727–730 (2006)
J.A. Cabato, C.J. Stefano, S.B. Mukasa, Volatile concentrations in olivine-hosted melt inclusions from the Columbia River flood basalts and associated lavas of the Oregon Plateau: implications for magma genesis. Chem. Geol. **392**, 59–73 (2015)
R.A. Cabral, M.G. Jackson, K.T. Koga, E.F. Rose-Koga, E.H. Hauri, M.J. Whitehouse, A.A. Price, J.M.D. Day, N. Shimizu, K.A. Kelley, Volatile cycling of H_2O, CO_2, F, and Cl in the HIMU mantle: a new window provided by melt inclusions from oceanic hot spot lavas at Mangaia, Cook Islands. Geochem. Geophys. Geosyst. **15**, 4445–4467 (2014). doi:10.1002/2014GC005473
R.M. Canup, Forming a Moon with an Earth-like composition via a giant impact. Science **338**, 1052–1055 (2012)
Y. Cao, H. Jung, S. Song, M. Park, S. Jung, J. Lee, Plastic deformation and seismic properties in fore-arc mantles: a petrofabric analysis of the Yushigou harzburgites, North Qilian Suture Zone, NW China. J. Petrol. **56**, 1897–1944 (2015)
R. Caracas, The influence of hydrogen on the seismic properties of solid iron. Geophys. Res. Lett. **42**, 3780–3785 (2015)
A. Caracausi, G. Avice, P.G. Burnard, E. Füri, B. Marty, Chondritic xenon in the Earth's mantle. Nature **533**, 82–85 (2016)
R.W. Carlson, M. Boyet, H. Rizo, R.J. Walker, Early differentiation and its long-term consequences for Earth evolution, in *The Early Earth: Accretion and Differentiation*, ed. by J. Badro, M.J. Walter (Wiley, New Jersey, 2015), pp. 143–172
R.W. Carlson, D.G. Pearson, F.R. Boyd, S.B. Shirey, G. Irvine, A.H. Menzies, J.J. Gurney, Re-Os systematics of lithospheric peridotites: implications for lithosphere formation and preservation, in *Proc. VIIth International Kimberlite Conference, B.J. Dawson Volume*, ed. by J.J. Gurney, J.L. Gurney, M.D. Pascoe, S.R. Richardson (1999), pp. 99–108
M.R. Carroll, J.D. Webster, Solubilities of sulfur, noble gases, nitrogen, chlorine, and fluorine in magmas, in *Volatiles in Magmas*, ed. by M.R. Carroll, J.R. Holloway (Mineralogical Society of America, Washington D.C., 1994), pp. 231–279
P. Cartigny, B. Marty, Nitrogen isotopes and mantle geodynamics: the emergence of life and the atmosphere-crust-mantle connection. Elements **9**, 359–366 (2013)
N.L. Chabot, E.A. Wollack, M. Humayun, E.M. Shank, The effect of oxygen as a light element in metallic liquids on partitioning behavior. Meteorit. Planet. Sci. **50**, 530–546 (2015)
Y.-Y. Chang, W.-P. Hsieh, E. Tan, J. Chen, Hydration-reduced lattice thermal conductivity of olivine in Earth's upper mantle. Proc. Natl. Acad. Sci. **114**, 4078–4081 (2017)
Y. Chen, A. Provost, P. Schiano, N. Cluzel, Magma ascent rate and initial water concentration inferred from diffusive water loss from olivine-hosted melt inclusions. Contrib. Mineral. Petrol. **165**, 525–541 (2013)
E.J. Chin, V. Soustelle, G. Hirth, A.E. Saal, S.C. Kruckenberg, J.M. Eiler, Microstructural and geochemical constraints on the evolution of deep arc lithosphere. Geochem. Geophys. Geosyst. **17**, 2497–2521 (2016)
C.-L. Chou, Fractionation of siderophile elements in the Earth's upper mantle, in *Proc. Lunar Planet. Sci. Conf*, vol. 9 (1978), pp. 219–230

P.L. Clay, H. Busemann, S.C. Sherlock, T.L. Barry, S.P. Kelley, D.W. McGarvie, $^{40}Ar/^{39}Ar$ ages and residual volatile contents in degassed subaerial and subglacial glassy volcanic rocks from Iceland. Chem. Geol. **403**, 99–110 (2015)
L.I. Cleeves, E.A. Bergin, C.M.O.D. Alexander, F. Du, D. Graninger, K.I. Öberg, T.J. Harries, The ancient heritage of water ice in the solar system. Science **345**, 1590–1593 (2014)
M. Clog, C. Aubaud, P. Cartigny, L. Dosso, The hydrogen isotopic composition and water content of southern Pacific MORB: a reassessment of the D/H ratio of the depleted mantle reservoir. Earth Planet. Sci. Lett. **381**, 156–165 (2013)
J.N. Connelly, M. Bizzarro, Lead isotope evidence for a young formation age of the Earth-Moon system. Earth Planet. Sci. Lett. **452**, 36–43 (2016)
A.M. Courtier, J. Revenaugh, A water-rich transition zone beneath the Eastern United States and Gulf of Mexico from multiple ScS reverberations, in *Earth's Deep Water Cycle*, ed. by S. Jacobsen, S. Lee (AGU Geophysical Monograph, Washington D.C., 2006), pp. 181–194
S. Creighton, T. Stachel, S. Matveev, H. Höfer, C.A. McCammon, R.W. Luth, Oxidation of the Kaapvaal lithospheric mantle derived by metasomatism. Contrib. Mineral. Petrol. **157**, 491–504 (2009)
L. Dai, S.-I. Karato, Electrical conductivity of orthopyroxene: implications for the water content of the asthenosphere. Proc. Jpn. Acad. Ser. B, Phys. Biol. Sci. **85**, 466–475 (2009)
L.V. Danyushevsky, Experimental and petrological studies of melt inclusions in phenocrysts from mantle-derived magmas: an overview of techniques, advantages and complications. Chem. Geol. **183**, 5–24 (2002)
L.V. Danyushevsky, T.J. Fallon, A.V. Sobolev, A.J. Crawford, M. Carroll, R.C. Price, The H_2O content of basalt glasses from southwest Pacific back-arc basins. Earth Planet. Sci. Lett. **117**, 347–362 (1993)
N. Dauphas, The dual origin of the terrestrial atmosphere. Icarus **165**, 326–339 (2003)
N. Dauphas, A. Morbidelli, Geochemical and planetary dynamical views on the origin of Earth's atmosphere and oceans, in *Treatise on Geochemistry*, ed. by A.S. Davis 2nd edn. (Elsevier, Amsterdam, 2014), pp. 1–35
N. Dauphas, The isotopic nature of the Earth's accreting material through time. Nature **541**, 521–524 (2017)
J.B. Dawson, J.V. Smith, The MARID (mica-amphibole-rutile-ilmenite-diopside) suite of xenoliths in kimberlite. Geochim. Cosmochim. Acta **41**, 309–323 (1977)
J.C.M. De Hoog, C.J. Lissenberg, R.A. Brooker, R. Hinton, D. Trail, E. Hellebrand, Hydrogen incorporation and charge balance in natural zircon. Geochim. Cosmochim. Acta **141**, 472–486 (2014)
V. Debaille, C. O'Neill, A.D. Brandon, P. Haenecour, Q.-Z. Yin, N. Mattielli, A.H. Treiman, Stagnant-lid tectonics in early Earth revealed by ^{142}Nd variations in late Archean rocks. Earth Planet. Sci. Lett. **373**, 83–92 (2013)
B. Debret, N. Bolfan-Casanova, J.A. Padrón-Navarta, F. Martin-Hernandez, M. Andreani, C.J. Garrido, V. López Sánchez-Vizcaíno, M.T. Gómez-Pugnaire, M. Muñoz, N. Trcera, Redox state of iron during high-pressure serpentinite dehydration. Contrib. Mineral. Petrol. **169**, 1–18 (2015)
H. Delavault, C. Chauvel, E. Thomassot, C. Devey, B. Dazas, *Relicts of Archean Sediment in the Present Earth Mantle* (Goldschmidt, Yokohama, 2016), p. 633
E. Deloule, F. Albarède, S.M.F. Sheppard, Hydrogen isotope heterogeneities in the mantle from ion probe analysis of amphibole from ultramafic rocks. Earth Planet. Sci. Lett. **105**, 543–553 (1991)
S. Demouchy, N. Bolfan-Casanova, Distribution and transport of hydrogen in the lithospheric mantle: a review. Lithos **240–243**, 402–425 (2016)
S. Demouchy, E. Deloule, D.J. Frost, H. Keppler, Pressure and temperature dependence of water solubility in Fe-free wadsleyite. Am. Mineral. **90**, 1084–1091 (2005)
S. Demouchy, A. Ishikawa, A. Tommasi, O. Alard, S. Keshav, Characterization of hydration in the mantle lithosphere: peridotite xenoliths from the Ontong Java Plateau as an example. Lithos **212–215**, 189–201 (2015)
S. Demouchy, S.D. Jacobsen, F. Gaillard, C.R. Stern, Rapid magma ascent recorded by water diffusion profiles in olivine from Earth's mantle. Geology **34**, 429–432 (2006)
S. Demouchy, S. Mackwell, Mechanisms of hydrogen incorporation and diffusion in iron-bearing olivine. Phys. Chem. Miner. **33**, 347 (2006)
S. Demouchy, A. Tommasi, F. Barou, D. Mainprice, P. Cordier, Deformation of olivine in torsion under hydrous conditions. Phys. Earth Planet. Inter. **202–203**, 56–70 (2012)
C.M.M. Denis, O. Alard, S. Demouchy, Water content and hydrogen behaviour during metasomatism in the uppermost mantle beneath Ray Pic volcano (Massif Central France). Lithos **236–237**, 256–274 (2015)
C.M.M. Denis, S. Demouchy, C.S.J. Shaw, Evidence of dehydration in peridotites from Eifel volcanic field and estimates of the rate of magma ascent. J. Volcanol. Geotherm. Res. **258**, 85–99 (2013)
J.E. Dixon, Degassing of alkalic basalts. Am. Mineral. **82**, 368–378 (1997)
J.E. Dixon, D.A. Clague, Volatiles in basaltic glasses from Loihi seamount, Hawaii: evidence for a relatively dry plume component. J. Petrol. **42**, 627–634 (2001)

J.E. Dixon, D.A. Clague, B. Cousens, M.L. Monsalve, J. Uhl, Carbonatite and silicate melt metasomatism of the mantle surrounding the Hawaiian plume: evidence from volatiles, trace elements, and radiogenic isotopes in rejuvenated-stage lavas from Niihau, Hawaii. Geochem. Geophys. Geosyst. **9**, 1–34 (2008)
J.E. Dixon, D.A. Clague, E.M. Stolper, Degassing history of water, sulfur, and carbon in submarine lavas from Kilauea volcano, Hawaii. J. Geol. **99**, 371–394 (1991)
J.E. Dixon, T.H. Dixon, D.R. Bell, R. Malservisi, Lateral variation in upper mantle viscosity: role of water. Earth Planet. Sci. Lett. **222**, 451–467 (2004)
J.E. Dixon, L. Leist, C. Langmuir, J.-G. Schilling, Recycled dehydrated lithosphere observed in plume-influenced mid-ocean-ridge basalt. Nature **420**, 385–389 (2002)
J.E. Dixon, E. Stolper, J.R. Delaney, Infrared spectroscopic measurements of CO_2 and H_2O in Juan de Fuca basaltic glasses. Earth Planet. Sci. Lett. **90**, 87–104 (1988)
J.E. Dixon, E.M. Stolper, An experimental study of water and carbon dioxide solubilities in mid-ocean ridge basaltic liquids. Part II: application to degassing. J. Petrol. **36**, 1633–1646 (1995)
L.S. Doucet, D.A. Ionov, A.V. Golovin, The origin of coarse garnet peridotites in cratonic lithosphere: new data on xenoliths from the Udachnaya kimberlite, central Siberia. Contrib. Mineral. Petrol. **165**, 1225–1242 (2013)
L.S. Doucet, D.A. Ionov, A.V. Golovin, Paleoproterozoic formation age for the Siberian cratonic mantle: Hf and Nd isotope data on refractory peridotite xenoliths from the Udachnaya kimberlite. Chem. Geol. **391**, 42–55 (2015)
L.S. Doucet, A.H. Peslier, D.A. Ionov, A.D. Brandon, A.V. Golovin, A.G. Goncharov, I.V. Ashchepkov, High water contents in the Siberian cratonic mantle linked to metasomatism: an FTIR study of Udachnaya peridotite xenoliths. Geochim. Cosmochim. Acta **137**, 159–187 (2014)
M.J. Drake, Origin of water in the terrestrial planets. Meteorit. Planet. Sci. **40**, 519–527 (2005). doi:10.1111/j.1945-5100.2005.tb00960.x
A.M. Dziewonski, D.L. Anderson, Preliminary reference Earth model. Phys. Earth Planet. Inter. **25**, 297–356 (1981)
D.W. Eaton, F. Darbyshire, R.L. Evans, H. Grütter, A.G. Jones, X. Yuan, The elusive lithosphere-asthenosphere boundary (LAB) beneath cratons. Lithos **109**, 1–22 (2008)
P. Eberhardt, M. Reber, D. Krankowsky, R.R. Hodges, The D/H and $^{18}O/^{16}O$ ratios in water from comet P/Halley. Astron. Astrophys. **302**, 301–316 (1995)
M. Edmonds, S.C. Kohn, E.H. Hauri, M.C.S. Humphreys, M. Cassidy, Extensive, water-rich magma reservoir beneath southern Montserrat. Lithos **252–253**, 216–233 (2016)
R.A. Eggleton, J.N. Boland, A.E. Ringwood, High pressure synthesis of a new aluminium silicate: $Al_5Si_5O_{17}(OH)$. Geochem. J. **12**, 191–194 (1978)
L.T. Elkins-Tanton, Linked magma ocean solidification and atmospheric growth for Earth and Mars. Earth Planet. Sci. Lett. **271**, 181–191 (2008)
L.T. Elkins-Tanton, T.L. Grove, Water (hydrogen) in the lunar mantle: results from petrology and magma ocean modeling. Earth Planet. Sci. Lett. **307**, 173–179 (2011)
R.L. Evans, G. Hirth, K. Baba, D.W. Forsyth, A. Chave, R. Mackie, Geophysical evidence from the MELT area for compositional controls on oceanic plates. Nature **437**, 249–252 (2005)
M. Faccenda, Water in the slab: a trilogy. Tectonophysics **614**, 1–30 (2014)
M. Faccenda, T.V. Gerya, N.S. Mancktelow, L. Moresi, Fluid flow during slab unbending and dehydration: implications for intermediate-depth seismicity, slab weakening and deep water recycling. Geochem. Geophys. Geosyst. **13**, 1–23 (2012)
J. Farquhar, B. Wing, K.D. McKeegan, J.W. Harris, P. Cartigny, M.H. Thiemens, Mass-independent sulfur of inclusions in diamond and sulfur recycling on early Earth. Science **298**, 2369–2372 (2002)
J.R. Farver, Oxygen and hydrogen diffusion in minerals, in *Diffusion in Minerals and Melts*, ed. by Y. Zhang, D.J. Cherniak (Mineralogical Society of America, Geochemical Society, Chantilly, 2010), pp. 447–507
U.H. Faul, C.J. Cline Ii, E.C. David, A.J. Berry, I. Jackson, Titanium-hydroxyl defect-controlled rheology of the Earth's upper mantle. Earth Planet. Sci. Lett. **452**, 227–237 (2016)
A. Férot, N. Bolfan-Casanova, Water storage capacity in olivine and pyroxene to 14 GPa: implications for the water content of the Earth's upper mantle and nature of seismic discontinuities. Earth Planet. Sci. Lett. **349–350**, 218–230 (2012)
E. Ferriss, T. Plank, D. Walker, Site-specific hydrogen diffusion rates during clinopyroxene dehydration. Contrib. Mineral. Petrol. **171**, 1–24 (2016)
H. Feuchtgruber, E. Lellouch, B. Bézard, T. Encrenaz, T. de Graauw, G. Davis, Detection of HD in the atmospheres of Uranus and Neptune: a new determination of the D/H ratio. Astron. Astrophys. **341**, L17–L21 (1999)
J. Filip, M. Novák, A. Beran, R. Zbořil, Crystal chemistry and OH defect concentrations in spodumene from different granitic pegmatites. Phys. Chem. Miner. **32**, 733–746 (2006)
G. Fiquet, F. Guyot, J. Badro, The Earth's lower mantle and core. Elements **4**, 177–182 (2008)

M. Fischer-Gödde, T. Kleine, Ruthenium isotopic evidence for an inner Solar System origin of the late veneer. Nature **541**, 525–527 (2017)
K.M. Fisher, H.A. Ford, D.L. Abt, C.A. Rychert, The lithosphere-asthenosphere boundary. Annu. Rev. Earth Planet. Sci. **38**, 551–575 (2010)
C. Fitoussi, B. Bourdon, Silicon isotope evidence against an enstatite chondrite Earth. Science **335**, 1477–1480 (2012)
K. Fleming, Z. Martinec, D. Wolf, Glacial-isostatic adjustment and the viscosity structure underlying the Vatnajökull ice cap, Iceland. Pure Appl. Geophys. **164**, 751–768 (2007)
S.F. Foley, S. Buhre, D.E. Jacob, Evolution of the Archaean crust by delamination and shallow subduction. Nature **421**, 249–252 (2003)
T. Fouchet, P.G.J. Irwin, P. Parrish, S.B. Calcutt, F.W. Taylor, C.A. Nixon, T. Owen, Search for spatial variation in the jovian $^{15}N/^{14}N$ ratio from Cassini/CIRS observations. Icarus **172**, 50–58 (2004)
M.L. Frezzotti, S. Ferrando, The chemical behavior of fluids released during deep subduction based on fluid inclusions. Am. Mineral. **100**, 352–377 (2015)
M.L. Frezzotti, S. Ferrando, F. Tecce, D. Castelli, Water content and nature of solutes in shallow-mantle fluids from fluid inclusions. Earth Planet. Sci. Lett. **351–352**, 70–83 (2012)
I. Friedman, R.L. Smith, W.D. Long, Hydration of natural glass and formation of perlite. Geol. Soc. Am. Bull. **77**, 323–328 (1966)
D.J. Frost, The stability of hydrous mantle phases, in *Water in Nominally Anhydrous Minerals*, ed. by H. Keppler, J.R. Smyth (Mineralogical Society of America, Chantilly, 2006), pp. 243–271
D.J. Frost, The upper mantle and transition zone. Elements **4**, 171–176 (2008)
D.J. Frost, D. Dolejš, Experimental determination of the effect of H_2O on the 410-km seismic discontinuity. Earth Planet. Sci. Lett. **256**, 182–195 (2007)
D.J. Frost, C.A. McCammon, The redox state of the Earth's mantle. Annu. Rev. Earth Planet. Sci. **36**, 389–420 (2008)
Y. Fukai, The iron-water reaction and the evolution of the Earth. Nature **308**, 174–175 (1984)
Y. Fukao, M. Obayashi, T. Nakakuki, Stagnat slab: a review. Annu. Rev. Earth Planet. Sci. **37**, 19–46 (2009)
E. Füri, E. Deloule, A.A. Gurenko, B. Marty, New evidence for chondritic lunar water from combined D/H and noble gas analyses of single Apollo 17 volcanic glasses. Icarus **229**, 109–120 (2014)
E. Füri, P.H. Barry, L.A. Taylor, B. Marty, Indigenous nitrogen in the Moon: constraints from coupled nitrogen–noble gas analyses of mare basalts. Earth Planet. Sci. Lett. **431**, 195–205 (2015)
G.A. Gaetani, J.A. O'Leary, K.T. Koga, E.H. Hauri, E.F. Rose-Koga, B.D. Monteleone, Hydration of mantle olivine under variable water and oxygen fugacity conditions. Contrib. Mineral. Petrol. **167**, 965–979 (2014)
J. Ganguly, A. Asaduzzaman, K. Muralidharan, Origin of water in Earth with high D/H ratio relative to protosolar nebula, and an explanation of its similarity with the isotopic ratios of carbonaceous chondrites and asteroid Vesta, in *79th Meteoritical Society Meeting*, Berlin, Germany (2016), p. 6055
E. Gardés, F. Gaillard, P. Tarits, Toward a unified hydrous olivine electrical conductivity law. Geochem. Geophys. Geosyst. **15**, 4984–5000 (2014)
E.J. Garnero, A.K. McNamara, Structure and dynamics of Earth's lower mantle. Science **320**, 626–628 (2008)
E.J. Garnero, A.K. McNamara, S.-H. Shim, Continent-sized anomalous zones with low seismic velocity at the base of Earth's mantle. Nat. Geosci. **9**, 481–489 (2016)
T. Garth, A. Rietbrock, Order of magnitude increase in subducted H_2O due to hydrated normal faults within the Wadati-Benioff zone. Geology **42**, 207–210 (2014)
P. Gavrilenko, T. Boffa Ballaran, H. Keppler, The effect of Al and water on the compressibility of diopside. Am. Mineral. **95**, 608–616 (2010)
J. Geiss, G. Gloeckler, Isotopic composition of H, He and Ne in the protosolar cloud, in *Solar System History from Isotopic Signatures of Volatile Elements*, ed. by R. Kallenbach, T. Encrenaz, J. Geiss, K. Mauersberger, T.C. Owen, F. Robert (Springer, Dordrecht, 2003), pp. 3–18
H. Genda, Origin of Earth's oceans: an assessment of the total amount, history and supply of water. Geochem. J. **50**, 27–42 (2016)
H. Genda, M. Ikoma, Origin of the ocean on the Earth: early evolution of water D/H in a hydrogen-rich atmosphere. Icarus **194**, 42–52 (2008)
S. Ghosh, M.W. Schmidt, Melting of Phase D in the lower mantle and implications for recycling and storage of H_2O in the deep mantle. Geochim. Cosmochim. Acta **145**, 72–88 (2014)
J. Girard, J. Chen, P.C. Raterron, C.W. Holyoke, Hydrolytic weakening of olivine at mantle pressure: evidence of [1 0 0](0 1 0) slip system softening from single-crystal deformation experiments. Phys. Earth Planet. Inter. **216**, 12–20 (2013)
A. Giuliani, D. Phillips, V.S. Kamenetsky, M.L. Fiorentini, J. Farquhar, M.A. Kendrick, Stable isotope (C, O, S) compositions of volatile-rich minerals in kimberlites: a review. Chem. Geol. **374–375**, 61–83 (2014)

J. Gose, E. Schmädicke, A. Beran, Water in enstatite from Mid-Atlantic Ridge peridotite: evidence for water content of suboceanic mantle? Geology **37**, 543–546 (2009)
J. Gose, E. Schmädicke, R. Stalder, Water in mantle orthopyroxene—no visible change in defect water during serpentinization. Eur. J. Mineral. **23**, 529–536 (2011)
K. Grant, J. Ingrin, J.P. Lorand, P. Dumas, Water partitioning between mantle minerals from peridotite xenoliths. Contrib. Mineral. Petrol. **154**, 15–34 (2007a)
K.J. Grant, S.C. Kohn, R.A. Brooker, The partitioning of water between olivine, orthopyroxene and melt synthesised in the system albite-forsterite-H_2O. Earth Planet. Sci. Lett. **260**, 227–241 (2007b)
D.H. Green, Experimental melting studies on a model upper mantle composition at high pressure under H_2O-saturated and H_2O undersaturated conditions. Earth Planet. Sci. Lett. **19**, 37–45 (1973)
M. Grégoire, D.R. Bell, A.P. Le Roex, Trace element geochemistry of phlogopite-rich mafic mantle xenoliths: their classification and relationship to phlogopite-bearing peridotites and to kimberlites revisited. Contrib. Mineral. Petrol. **142**, 603–625 (2002)
M. Grégoire, D.R. Bell, A.P. Le Roex, Garnet lherzolites from the Kaapvaal craton (South Africa): trace element evidence for a metasomatic history. J. Petrol. **44**, 629–657 (2003)
W.L. Griffin, S. Graham, S.Y. O'Reilly, N.J. Pearson, Lithosphere evolution beneath the Kaapvaal craton: Re-Os systematics of sulfides in mantle-derived peridotites. Chem. Geol. **208**, 89–118 (2004)
W.L. Griffin, S.Y. O'Reilly, J.C. Afonso, G.C. Begg, The composition and evolution of lithospheric mantle: a re-evaluation and its tectonic implications. J. Petrol. **50**, 1185–1204 (2009)
W.L. Griffin, S.R. Shee, C.G. Ryan, T.T. Win, B.A. Wyatt, Harzburgite to lherzolite and back again: metasomatic processes in ultramafic xenoliths from the Wesselton kimberlite, Kimberley, South Africa. Contrib. Mineral. Petrol. **134**, 232–250 (1999)
T.L. Grove, C.B. Till, M.J. Krawczynski, The role of H_2O in subduction zone magmatism. Annu. Rev. Earth Planet. Sci. **40**, 413–439 (2012)
Y. Guan, Y. Wang, W. Hsu, J.M. Eiler, Analysis of OH and D/H of Apatites from Eucrites, in *79th Meteoritical Society Meeting*, Berlin, Germany (2016)
Y. Gung, M. Panning, B. Romanowicz, Global anisotropy and the thickness of continents. Nature **422**, 707–711 (2003)
A.A. Gurenko, V.S. Kamenetsky, A.C. Kerr, Oxygen isotopes and volatile contents of the Gorgona komatiites, Colombia: a confirmation of the deep mantle origin of H_2O. Earth Planet. Sci. Lett. **454**, 154–165 (2016)
B.R. Hacker, H_2O subduction beyond arcs. Geochem. Geophys. Geosyst. **9**, 1–24 (2008)
A.N. Halliday, Mixing, volatile loss and compositional change during impact-driven accretion of the Earth. Nature **427**, 505–509 (2004)
A.N. Halliday, The origins of volatiles in the terrestrial planets. Geochim. Cosmochim. Acta **105**, 146–171 (2013)
A.N. Halliday, D. Porcelli, In search of lost planets—the paleocosmochemistry of the inner solar system. Earth Planet. Sci. Lett. **192**, 545–559 (2001)
L.J. Hallis, G.R. Huss, K. Nagashima, G.J. Taylor, S.A. Halldórsson, D.R. Hilton, M.J. Motti, K.J. Meech, Evidence for primordial water in Earth's deep mantle. Science **350**, 795–797 (2015)
L.J. Hallis, G.J. Taylor, K. Nagashima, G.R. Huss, Magmatic water in the martian meteorite Nakhla. Earth Planet. Sci. Lett. **359–360**, 84–92 (2012)
L.J. Hallis, D/H ratios of the inner Solar System. Philos. Trans. R. Soc. Lond. A **375**, 20150390 (2017)
M. Hamada, T. Kawamoto, E. Takahashi, T. Fujii, Polybaric degassing of island arc low-K tholeiitic basalt magma recorded by OH concentrations in Ca-rich plagioclase. Earth Planet. Sci. Lett. **308**, 259–266 (2011)
M. Hamada, M. Ushioda, T. Fujii, E. Takahashi, Hydrogen concentration in plagioclase as a hygrometer of arc basaltic melts: approaches from melt inclusion analyses and hydrous melting experiments. Earth Planet. Sci. Lett. **365**, 253–262 (2013)
U. Hans, T. Kleine, B. Bourdon, Rb–Sr chronology of volatile depletion in differentiated protoplanets: BABI, ADOR and ALL revisited. Earth Planet. Sci. Lett. **374**, 204–214 (2013)
Y. Hao, Q.-K. Xia, Q. Li, H. Chen, M. Feng, Partial melting control of water contents in the Cenozoic lithospheric mantle of the Cathaysia block of South China. Chem. Geol. **380**, 7–19 (2014)
Y.-T. Hao, Q.-K. Xia, Z.-B. Jia, Q.-C. Zhao, P. Li, M. Feng, S.-C. Liu, Regional heterogeneity in the water content of the Cenozoic lithospheric mantle of Eastern China. J. Geophys. Res. **121**, 517–537 (2016)
S.H. Hart, E.H. Hauri, L.A. Oschmann, J.A. Whitehead, Mantle plumes and entrainment: isotopic evidence. Science **256**, 517–519 (1992)
B. Harte, Mantle peridotites and processes—the kimberlite sample, in *Continental Basalts and Mantle Xenoliths*, ed. by C.J. Hawkesworth, M.J. Norry (Shiva Publishing Limited, Cambridge, 1983), p. 272
M.E. Hartley, D.A. Neave, J. MacLennan, M. Edmonds, Diffusive over-hydration of olivine-hosted melt inclusions. Earth Planet. Sci. Lett. **425**, 168–178 (2015)

P. Hartogh, D.C. Lis, D. Bockelee-Morvan, M. de Val-Borro, N. Biver, M. Kuppers, M. Emprechtinger, E.A. Bergin, J. Crovisier, M. Rengel, R. Moreno, S. Szutowicz, G.A. Blake, Ocean-like water in the Jupiter-family comet 103P/Hartley 2. Nature **478**, 218–220 (2011)
E. Hauri, SIMS analysis of volatiles in silicate glasses, 2: isotopes and abundances in Hawaiian melt inclusions. Chem. Geol. **183**, 115–141 (2002)
E. Hauri, J. Wang, J.E. Dixon, P.L. King, C. Mandeville, S. Newman, SIMS analysis of volatiles in silicate glasses 1. Calibration, matrix effects and comparison with FTIR. Chem. Geol. **183**, 99–114 (2002)
E.H. Hauri, G.A. Gaetani, T.H. Green, Partitioning of water during melting of the Earth's upper mantle at H_2O-undersaturated conditions. Earth Planet. Sci. Lett. **248**, 715–734 (2006)
E.H. Hauri, A.E. Saal, M.C. Rutherford, J.A. Van Orman, Water in the Moon's interior: truth and consequences. Earth Planet. Sci. Lett. **409**, 252–264 (2015)
E.H. Hauri, T. Weinreich, A.E. Saal, M.C. Rutherford, J.A. Van Orman, High pre-eruptive water contents preserved in lunar melt inclusions. Science **333**, 213–215 (2011)
C. Hayashi, Structure of the solar nebula, growth and decay of magnetic fields and effects of magnetic and turbulent viscosities on the nebula. Prog. Theor. Phys. Suppl. **70**, 35–53 (1981)
C. Hayashi, K. Nakazawa, H. Mizuno, Earth's melting due to the blanketing effect of the primordial dense atmosphere. Earth Planet. Sci. Lett. **43**, 22–28 (1979)
V.S. Heber, R. Wieler, H. Baur, C. Olinger, T.A. Friedmann, D.S. Burnett, Noble gas composition of the solar wind as collected by the Genesis mission. Geochim. Cosmochim. Acta **73**, 7414–7432 (2009)
C.D.K. Herd, R.C. Peterson, G.R. Rossman, Violet-colored diopside from southern Baffin island, Nunavut, Canada. Can. Mineral. **38**, 1193–1199 (2000)
D.R. Hilton, T.P. Fischer, B. Marty, Noble gases and volatile recycling at subduction zones. Rev. Mineral. Geochem. **47**, 319–370 (2002)
K. Hirose, T. Kawamoto, Hydrous partial melting of lherzolite at 1 GPa: the effect of H_2O on the genesis of basaltic magmas. Earth Planet. Sci. Lett. **133**, 463–473 (1995)
M.M. Hirschmann, Water, melting, and the deep Earth H_2O cycle. Annu. Rev. Earth Planet. Sci. **34**, 629–653 (2006)
M.M. Hirschmann, Constraints on the early delivery and fractionation of Earth's major volatiles from C/H, C/N, and C/S ratios. Am. Mineral. **101**, 540–553 (2016)
M.M. Hirschmann, C. Aubaud, A.C. Withers, Storage capacity of H_2O in nominally anhydrous minerals in the upper mantle. Earth Planet. Sci. Lett. **236**, 167–181 (2005)
M.M. Hirschmann, T.J. Tenner, C. Aubaud, A.C. Withers, Dehydration melting of nominally anhydrous mantle: the primacy of partitioning. Phys. Chem. Earth **176**, 54–68 (2009)
M.M. Hirschmann, A.C. Withers, P. Ardia, N.T. Foley, Solubility of molecular hydrogen in silicate melts and consequences for volatile evolution of terrestrial planets. Earth Planet. Sci. Lett. **345–348**, 38–48 (2012)
G. Hirth, R.L. Evans, A.D. Chave, Comparison of continental and oceanic mantle electrical conductivity: is the Archean lithosphere dry? Geochem. Geophys. Geosyst. **1**, 1030 (2000)
G. Hirth, D.L. Kohlstedt, Water in the oceanic upper mantle; implications for rheology, melt extraction and the evolution of the lithosphere. Earth Planet. Sci. Lett. **144**, 93–108 (1996)
G. Hirth, D.L. Kohlstedt, Rheology of the upper mantle and the mantle wedge: a view from the experimentalists, in *Inside the Subduction Factory*, ed. by J. Eiler (American Geophysical Union, Washington, 2004), pp. 83–106
A.W. Hofmann, Lead isotopes and the age of the Earth—a geochemical accident. Geol. Soc. (Lond.) Spec. Publ. **190**, 223–236 (2001)
A.W. Hofmann, Sampling mantle heterogeneity through oceanic basalts: isotopes and trace elements, in *The Mantle and Core*, ed. by H.D. Holland, K.K. Turekian (Elsevier, Oxford, 2003), pp. 1–44
G. Holland, M. Cassidy, C.J. Ballentine, Meteorite Kr in Earth's mantle suggests a late accretionary source for the atmosphere. Science **326**, 1522–1525 (2009)
D. Holloway, J.G. Blank, Application of experimental results to C-O-H species in natural melts, in *Volatiles in Magmas*, ed. by M.R. Carroll, J.R. Holloway (Mineralogical Society of America, Washington D.C., 1994), pp. 187–230
M.D. Hopkins, S.J. Mojzsis, W.F. Bottke, O. Abramov, Micrometer-scale U–Pb age domains in eucrite zircons, impact re-setting, and the thermal history of the HED parent body. Icarus **245**, 367–378 (2015)
C. Houser, Global seismic data reveal little water in the mantle transition zone. Earth Planet. Sci. Lett. **448**, 94–101 (2016)
Q. Hu, D.Y. Kim, J. Liu, Y. Meng, L. Yang, D. Zhang, W.L. Mao, H-k. Mao, Dehydrogenation of goethite in Earth's deep lower mantle. Proc. Natl. Acad. Sci. **114**, 1498–1501 (2017)
Q. Hu, D.Y. Kim, W. Yang, L. Yang, Y. Meng, L. Zhang, H.-K. Mao, FeO_2 and FeOOH under deep lower-mantle conditions and Earth's oxygen–hydrogen cycles. Nature **534**, 241–244 (2016)

S. Hu, Y. Lin, J. Zhang, J. Hao, L. Feng, L. Xu, W. Yang, J. Yang, NanoSIMS analyses of apatite and melt inclusions in the GRV 020090 Martian meteorite: hydrogen isotope evidence for recent past underground hydrothermal activity on Mars. Geochim. Cosmochim. Acta **140**, 321–333 (2014)

J.-X. Huang, P. Li, W.L. Griffin, Q.-K. Xia, Y. Gréau, N.J. Pearson, S.Y. O'Reilly, Water contents of Roberts Victor xenolithic eclogites: primary and metasomatic controls. Contrib. Mineral. Petrol. **168**, 1–13 (2014)

X. Huang, Y. Xu, S.-I. Karato, Water content in the transition zone from electrical conductivity of wadsleyite and ringwoodite. Nature **434**, 746–749 (2005)

H. Hui, Y. Guan, Y. Chen, A.H. Peslier, Y. Zhang, Y. Liu, R.L. Flemming, G.R. Rossman, J.M. Eiler, C.R. Neal, G.R. Osinsky, A heterogeneous lunar interior for hydrogen isotopes as revealed by the lunar highlands samples. Earth Planet. Sci. Lett. **473**, 14–23 (2017). doi:10.1016/j.epsl.2017.05.029

H. Hui, A.H. Peslier, R.L. Rudnick, A. Simonetti, C.R. Neal, Plume-cratonic lithosphere interaction recorded by water and other trace elements in peridotite xenoliths from the Labait volcano, Tanzania. Geochem. Geophys. Geosyst. **16**, 1–24 (2015)

M. Ichiki, K. Baba, H. Toh, K. Fuji-ta, An overview of electrical conductivity structures of the crust and upper mantle beneath the northwestern Pacific, the Japanese Islands, and continental East Asia. Gondwana Res. **16**, 545–562 (2009)

R. Iizuka-Oku, T. Yagi, H. Gotou, T. Okuchi, T. Hattori, A. Sano-Furukawa, Hydrogenation of iron in the early stage of Earth's evolution. Nat. Commun. **8**, 14096 (2017)

N.K. Inamdar, H.E. Schlichting, The formation of super-Earths and mini-Neptunes with giant impacts. Mon. Not. R. Astron. Soc. **448**, 1751–1760 (2015)

J. Ingrin, M. Blanchard, Diffusion of hydrogen in minerals, in *Water in Nominally Anhydrous Minerals*, ed. by H. Keppler, J.R. Smyth (Mineralogical Society of America, Chantilly, 2006), pp. 291–320

T. Inoue, H. Yurimoto, Y. Kudoh, Hydrous modified spinel, $Mg_{1.75}SiH_{0.5}O_4$: a new water reservoir in the mantle transition region. J. Geophys. Res. **22**, 117–120 (1995)

D.A. Ionov, L.S. Doucet, I.V. Ashchepkov, Composition of the lithospheric mantle in the Siberian craton: new constraints from fresh peridotites in the Udachnaya-East kimberlite. J. Petrol. **51**, 2177–2210 (2010)

Y. Ito, S. Nakashima, Water distribution in low-grade siliceous metamorphic rocks by micro-FTIR and its relation to grain size: a case from the Kanto Mountain region, Japan. Chem. Geol. **189**, 1–18 (2002)

M.G. Jackson, S.R. Hart, J.G. Konter, M.D. Kurz, J. Blusztajn, K.A. Farley, Helium and lead isotopes reveal the geochemical geometry of the Samoan plume. Nature **514**, 355–358 (2014)

M.G. Jackson, S.R. Hart, A.A.P. Koppers, H. Staudigel, J. Konter, J. Blusztajn, M.D. Kurz, J.A. Russell, The return of subducted continental crust in Samoan lavas. Nature **448**, 684–687 (2007)

M.G. Jackson, K.T. Koga, A. Price, J.G. Konter, A.A.P. Koppers, V.A. Finlayson, K. Konrad, E.H. Hauri, A. Kylander-Clark, K.A. Kelley, M.A. Kendrick, Deeply dredged submarine HIMU glasses from the Tuvalu Islands, Polynesia: implications for volatile budgets of recycled oceanic crust. Geochem. Geophys. Geosyst. **16**, 3210–3234 (2015)

D.E. Jacob, Nature and origin of eclogite xenoliths from kimberlites. Lithos **77**, 295–316 (2004)

S.D. Jacobsen, Effect of water on the equation of state of nominally anhydrous minerals, in *Water in Nominally Anhydrous Minerals*, ed. by H. Keppler, J.R. Smyth (Mineralogical Society of America, Chantilly, 2006), pp. 321–342

A. Jambon, J.L. Zimmermann, Major volatiles from a North Atlantic MORB glass and calibration to He: a size fraction analysis. Chem. Geol. **62**, 177–189 (1987)

B. Jamtveit, R. Brooker, K. Brooks, L.M. Larsen, T. Pedersen, The water content of olivines from the North Atlantic volcanic province. Earth Planet. Sci. Lett. **186**, 401–415 (2001)

E. Jarosewich, Chemical analyses of meteorites: a compilation of stony and iron meteorite analyses. Meteoritics **25**, 323–337 (1990)

R.D. Jarrard, Subduction fluxes of water, carbon dioxide, chlorine, and potassium. Geochem. Geophys. Geosyst. **4**, 1–50 (2003)

C. Jaupart, J.C. Mareschal, The thermal structure and thickness of continental roots. Lithos **48**, 93–114 (1999)

M. Javoy, E. Kaminski, F. Guyot, D. Andrault, C. Sanloup, M. Moreira, S. Labrosse, A. Jambon, P. Agrinier, A. Davaille, C. Jaupart, The chemical composition of the Earth: enstatite chondrite models. Earth Planet. Sci. Lett. **293**, 259–268 (2010)

M.M. Jean, L.A. Taylor, G.H. Howarth, A.H. Peslier, L. Fedele, R.J. Bodnar, Y. Guan, L.S. Doucet, D.A. Ionov, A.M. Logvinova, A.V. Golovin, N.V. Sobolev, Contrasting water and trace elements in olivines from Siberian diamonds versus mantle xenoliths. Lithos **265**, 31–41 (2016). doi:10.1016/j.lithos.2016.07.023

B. Johnson, C. Goldblatt, The nitrogen budget of Earth. Earth-Sci. Rev. **148**, 150–173 (2015)

E.A. Johnson, G.R. Rossman, The concentration and speciation of hydrogen in feldspars using FTIR and ^{1}H MAS NMR spectroscopy. Am. Mineral. **88**, 901–911 (2003)

E.A. Johnson, G.R. Rossman, A survey of hydrous species and concentrations in igneous feldspars. Am. Mineral. **89**, 586–600 (2004)
E.A. Johnson, G.R. Rossman, The diffusion behavior of hydrogen in plagioclase feldspar at 800–1000 °C: implications for re-equilibration of hydroxyl in volcanic phenocrysts. Am. Mineral. **98**, 1779–1787 (2013)
A.G. Jones, J. Ledo, I.J. Ferguson, J.A. Craven, M.J. Unsworth, M. Chouteau, J.E. Spratt, The electrical resistivity of Canada's lithosphere and correlation with other parameters: contributions from LITHOPROBE and other programmes. Can. J. Earth Sci. **51**, 573–617 (2013a)
A.G. Jones, M.R. Muller, S. Fishwick, R.L. Evans, J. Fullea, Velocity-conductivity relations for cratonic lithosphere and their application: example of southern Africa. Geochem. Geophys. Geosyst. **14**, 806–827 (2013b)
R.H. Jones, F.M. McCubbin, L. Dreeland, Y. Guan, P.V. Burger, C.K. Shearer, Phosphate minerals in LL chondrites: a record of the action of fluids during metamorphism on ordinary chondrite parent bodies. Geochim. Cosmochim. Acta **132**, 120–140 (2014)
R.H. Jones, F.M. McCubbin, Y. Guan, Phosphate minerals in the H group of ordinary chondrites, and fluid activity recorded by apatite heterogeneity in the Zag H3-6 regolith breccia. Am. Mineral. **101**, 2452–2467 (2016)
T.H. Jordan, Composition and development of the continental tectosphere. Nature **274**, 544–548 (1978)
H. Jung, S. Karato, Effects of water on dynamically recrystallized grain-size of olivine. J. Struct. Geol. **23**, 1337–1344 (2001a)
H. Jung, S. Karato, Water-induced fabric transitions in olivine. Science **293**, 1460–1463 (2001b)
V.S. Kamenetsky, A.V. Golovin, R. Maas, A. Giuliani, M.B. Kamenetsky, Y. Weiss, Towards a new model for kimberlite petrogenesis: evidence from unaltered kimberlites and mantle minerals. Earth-Sci. Rev. **139**, 145–167 (2014)
F. Kaminsky, O. Zakharchenko, R. Davies, W. Griffin, G. Khachatryan-Blinova, A. Shiryaev, Superdeep diamonds from the Juina area, Mato Grosso State, Brazil. Contrib. Mineral. Petrol. **140**, 734–753 (2001)
S. Karato, Does partial melting reduce the creep strength of the upper mantle? Nature **319**, 309–310 (1986)
S. Karato, The role of hydrogen in the electrical conductivity of the upper mantle. Nature **347**, 272–273 (1990)
S. Karato, Rheology of the upper mantle: a synthesis. Science **260**, 771–778 (1993)
S. Karato, Influence of hydrogen-related defects on the electrical conductivity and plastic deformation of mantle minerals: a critical review, in *Earth's Deep Water Cycle*, ed. by S.D. Jacobsen, S. van der Lee (American Geophysical Union, Washington, 2006a), pp. 113–130
S. Karato, Remote sensing of hydrogen in Earth's mantle, in *Water in Nominally Anhydrous Minerals*, ed. by H. Keppler, J.R. Smyth (Mineralogical Society of America, Chantilly, 2006b), pp. 343–375
S. Karato, Rheology of the deep upper mantle and its implications for the preservation of the continental roots: a review. Tectonophysics **481**, 82–98 (2010)
S. Karato, Water distribution across the mantle transition zone and its implications for global material circulation. Earth Planet. Sci. Lett. **301**, 413–423 (2011)
S. Karato, M.R. Riedel, D.A. Yuen, Rheological structure and deformation of subducted slabs in the mantle transition zone: implications for mantle circulation and deep earthquakes. Phys. Earth Planet. Inter. **127**, 83–108 (2001)
S.-I. Karato, Microscopic models for the effects of hydrogen on physical and chemical properties of Earth materials, in *Superplumes: Beyond Plate Tectonics*, ed. by D.A. Yuen, S. Maruyama, S.-I. Karato, B.F. Windley (Springer, Dordrecht, 2007), pp. 321–356
S.-I. Karato, Water in the evolution of Earth and other terrestrial planets, in *Treatise on Geophysics*, ed. by G. Schubert (Elsevier, Amsterdam, 2015), pp. 105–144
S.-I. Karato, Physical basis of trace element partitioning: a review. Am. Mineral. **101**, 2577–2593 (2016)
S.-I. Karato, H. Jung, I. Katayama, P. Skemer, Geodynamic significance of seismic anisotropy of the upper mantle: new insights from laboratory studies. Annu. Rev. Earth Planet. Sci. **36**, 59–95 (2008)
S.-I. Karato, D. Wang, Electrical conductivity of minerals and rocks, in *Physics and Chemistry of the Deep Earth*, ed. by S.-I. Karato (Wiley, New York, 2013), pp. 145–182
I. Katayama, K. Hirose, H. Yurimoto, S. Nakashima, Water solubility in majoritic garnet in subducting oceanic crust. Geophys. Res. Lett. **30**, 2155 (2003)
I. Katayama, S. Nakashima, Hydroxyl in clinopyroxene from the deep subducted crust: evidence for H_2O transport into the mantle. Am. Mineral. **88**, 229–234 (2003)
I. Katayama, S. Nakashima, H. Yurimoto, Water content in natural eclogite and implication for water transport into the deep upper mantle. Lithos **86**, 245–259 (2006)
H. Kawakatsu, S. Watada, Seismic evidence for deep-water transportation in the mantle. Science **316**, 1468–1471 (2007)

T. Kawamoto, Hydrous phases and water transport in the subducting slab, in *Water in Nominally Anhydrous Minerals*, ed. by H. Keppler, J.R. Smyth (Mineralogical Society of America, Chantilly, 2006), pp. 273–289

K. Kehm, S. Crowther, J.D. Gilmour, R.K. Mohapatra, C.M. Hohenberg, Upper limit concentrations of trapped xenon in individual interplanetary dust particles from the stratosphere. Meteorit. Planet. Sci. **44**, 249–259 (2009)

P.B. Kelemen, S.R. Hart, S. Bernstein, Silica enrichment in the continental upper mantle via melt/rock reaction. Earth Planet. Sci. Lett. **164**, 387–406 (1998)

M.A. Kendrick, M. Jackson, E.H. Hauri, D. Phillips, The halogen (F, Cl, Br, I) and H_2O systematics of Samoan lavas: assimilated-seawater, EM2 and high-$^3He/^4He$ components. Earth Planet. Sci. Lett. **410**, 197–2069 (2015)

M.A. Kendrick, M.G. Jackson, A.J.R. Kent, E.H. Hauri, P.J. Wallace, J. Woodhead, Contrasting behaviours of CO_2, S, H_2O and halogens (F, Cl, Br and I) in enriched-mantle melts from Pitcairn and Society seamounts. Chem. Geol. **370**, 69–81 (2014)

G.C. Kennedy, G.J. Wasserburg, H.C. Heard, R.C. Newton, The upper-three phase region in the system SiO_2-H_2O. Am. J. Sci. **260**, 501–521 (1962)

A.J.R. Kent, Melt inclusions in basaltic and related volcanic rocks, in *Minerals, Inclusions and Volcanic Processes*, ed. by K.D. Purtika, F.J. Tepley III. (Mineralogical Society of America, Chantilly, 2008), pp. 273–331

H. Keppler, Fluids and trace element transport in subduction zones. Am. Mineral. **102**, 5–20 (2017)

S.E. Kesson, A.E. Ringwood, Slab-mantle interactions: 2. The formation of diamonds. Chem. Geol. **78**, 97–118 (1989)

A. Khan, On Earth's mantle constitution and structure from joint analysis of geophysical and laboratory-based data: an example. Surv. Geophys. **37**, 149–189 (2016)

A. Khan, A. Kushinov, A. Semenov, On the heterogeneous electrical conductivity structure of the Earth's mantle with implications for transition zone water content. J. Geophys. Res. **116**, B01103 (2011)

A. Khan, T.J. Shankland, A geophysical perspective on mantle water content and melting: inverting electromagnetic sounding data using laboratory-based electrical conductivity profiles. Earth Planet. Sci. Lett. **317–318**, 27–43 (2012)

A.J. King, J.R. Solomon, P.F. Schofield, S.S. Russell, Characterising the CI and CI-like carbonaceous chondrites using thermogravimetric analysis and infrared spectroscopy. Earth Planets Space **67**, 198 (2015)

P.L. King, P.F. McMillan, G.M. Moore, Infrared spectroscopy of silicate glasses with application to natural systems, in *Infrared Spectroscopy in Geochemistry, Exploration Geochemistry, and Remote Sensing*, ed. by P.L. King, M.S. Ramsey, G.A. Swayze (Mineralogical Association of Canada, London, 2004), pp. 92–133

E.S. Kiseeva, B.J. Wood, A simple model for chalcophile element partitioning between sulphide and silicate liquids with geochemical applications. Earth Planet. Sci. Lett. **383**, 68–81 (2013)

M. Koch-Müller, I. Abs-Wurmbach, D. Rhede, V. Kahlenberg, S. Matsyuk, Dehydration experiments on natural omphacites: qualitative and quantitative characterization by various spectroscopic methods. Phys. Chem. Miner. **34**, 663–678 (2007)

M. Koch-Müller, S.S. Matsyuk, R. Wirth, Hydroxyl in omphacite and omphacitic clinopyroxenes of upper mantle to lower crustal origin beneath the Siberian platform. Am. Mineral. **89**, 921–931 (2004)

M. Koch-Müller, D. Rhede, IR absorption coefficients for water in nominally anhydrous high-pressure minerals. Am. Mineral. **95**, 770–775 (2010)

K.T. Koga, E. Hauri, M.M. Hirschmann, D. Bell, Hydrogen concentration analyses using SIMS and FTIR: comparison and calibration for nominally anhydrous minerals. Geochem. Geophys. Geosyst. **4**, 1019 (2003). doi:10.1029/2002GC000378

D.L. Kohlstedt, H. Keppler, D.C. Rubie, Solubility of water in the α, β and γ phases of $(Mg, Fe)_2SiO_4$. Contrib. Mineral. Petrol. **123**, 345–357 (1996)

D.L. Kohlstedt, S.J. Mackwell, Diffusion of hydrogen and intrinsic point defects in olivine. Z. Phys. Chem. **207**, 147–162 (1998)

S.C. Kohn, The dissolution mechanism of water in silicate melts; a synthesis of recent data. Mineral. Mag. **64**, 389–408 (2000)

M.V. Kolesnichenko, D.A. Zedgenizov, K.D. Litasov, I.Y. Safonova, A.L. Ragozin, Heterogeneous distribution of water in the mantle beneath the central Siberian Craton: implications from the Udachnaya Kimberlite Pipe. Gondwana Res. **47**, 249–266 (2016)

T. Komabayashi, Phase relations of hydrous peridotite: implications for water circulation in the Earth's mantle, in *Earth's Deep Water Cycle*, ed. by S. Jacobsen, S. Lee (AGU Geophysical Monograph, Washington D.C., 2006), pp. 29–43

J. Konzett, R.A. Armstrong, R.J. Sweeney, W. Compston, The timing of MARID metasomatism in the Kaapvaal mantle: an ion probe study of zircons from MARID xenoliths. Earth Planet. Sci. Lett. **160**, 133–145 (1998)

J. Konzett, K. Krenn, D. Rubatto, C. Hauzenberger, R. Stalder, The formation of saline mantle fluids by open-system crystallization of hydrous silicate-rich vein assemblages—evidence from fluid inclusions and their host phases in MARID xenoliths from the central Kaapvaal Craton, South Africa. Geochim. Cosmochim. Acta **147**, 1–25 (2014)

T. Koyama, H. Shimizu, H. Utada, M. Ichiki, E. Ohtani, R. Hae, Water content in the mantle transition zone beneath the North Pacific derived from the electrical conductivity anomaly, in *Earth's Deep Water Cycle* (American Geophysical Union, Washington, 2013), pp. 171–179

A.K. Kronenberg, R.A. Yund, G.R. Rossman, Stationary and mobile hydrogen defects in potassium feldspar. Geochim. Cosmochim. Acta **60**, 4075–4094 (1996)

K. Kuramoto, T. Matsui, Partitioning of H and C between the mantle and core during the core formation in the Earth: its implications for the atmospheric evolution and redox state of early mantle. J. Geophys. Res. **101**, 14909–14932 (1996)

M. Kurosawa, H. Yurimoto, S. Sueno, Patterns in the hydrogen and trace element compositions of mantle olivines. Phys. Chem. Miner. **24**, 385–395 (1997)

S. Labrosse, J.W. Hernlund, N. Coltice, A crystallizing dense magma ocean at the base of the Earth's mantle. Nature **450**, 866–869 (2007)

C.F. Larsen, R.J. Motyka, J.T. Freymueller, K.A. Echelmeyer, E.R. Ivins, Rapid viscoelastic uplift in southeast Alaska caused by post-Little Ice Age glacial retreat. Earth Planet. Sci. Lett. **237**, 548–560 (2005)

J.F. Lawrence, M.E. Wysession, Seismic evidence for subduction-transported water in the lower mantle, in *Earth's Deep Water Cycle*, ed. by S. Jacobsen, S. Lee (AGU Geophysical Monograph, Washington D.C., 2006), pp. 251–262

M. Le Voyer, P.D. Asimow, J.L. Mosenfelder, Y. Guan, P.J. Wallace, P. Schiano, E.M. Stolper, J.M. Eiler, Zonation of H_2O and F concentrations around melt inclusions in olivines. J. Petrol. **55**, 685–707 (2014)

C. Lécuyer, P. Gillet, F. Robert, The hydrogen isotope composition of seawater and the global water cycle. Chem. Geol. **145**, 249–261 (1998)

C.-T. Lee, P. Luffi, E.J. Chin, Building and destroying continental mantle. Annu. Rev. Earth Planet. Sci. **39**, 59–90 (2010)

C.-T. Lee, R.L. Rudnick, Compositionally stratified cratonic lithosphere: petrology and geochemistry of peridotite xenoliths from the Labait Volcano, Tanzania, in *Proc. VIIth International Kimberlite Conference, B.J. Dawson volume*, ed. by J.J. Gurney, J.L. Gurney, M.D. Pascoe, S.R. Richardson (1999), pp. 503–521

E. Lellouch, B. Bézard, T. Fouchet, H. Feuchtgruber, T. Encrenaz, T. de Graauw, The deuterium abundance in Jupiter and Saturn from ISO-SWS observations. Astron. Astrophys. **370**, 610–622 (2001)

Y. Li, Immiscible C-H-O fluids formed at subduction zone conditions. Geochem. Perspect. Lett. **3**, 12–21 (2017)

Z.-X.A. Li, C.-T. Lee, A.H. Peslier, A. Lenardic, S.J. Mackwell, Water contents in mantle xenoliths from the Colorado Plateau and vicinity: implications for the mantle rheology and hydration-induced thinning of continental lithosphere. J. Geophys. Res. **113**, 1–22 (2008)

E. Libowitzky, A. Beran, IR spectroscopic characterization of hydrous species in minerals, in *Spectroscopic Methods in Mineralogy. European Mineralogical Union*, ed. by A. Beran, E. Libowitzky (2004), pp. 227–279

J. Liu, Q.-K. Xia, E. Deloule, J. Ingrin, H. Chen, M. Feng, Water content and oxygen isotopic composition of alkali basalts from the Taihang Mountains, China: recycled oceanic components in the mantle source. J. Petrol. **56**, 681–702 (2015)

A.S. Lloyd, T. Plank, P. Ruprecht, E.H. Hauri, W. Rose, Volatile loss from melt inclusions in pyroclasts of differing sizes. Contrib. Mineral. Petrol. **165**, 129–153 (2013)

A.S. Lloyd, P. Ruprecht, E.H. Hauri, W. Rose, H.M. Gonnerman, T. Plank, NanoSIMS results from olivine-hosted melt embayments: magma ascent rate during explosive basaltic eruptions. J. Volcanol. Geotherm. Res. **283**, 1–18 (2014)

K. Lodders, Solar system abundances and condensation temperatures of the elements. Astrophys. J. **591**, 1220–1247 (2003)

F. Lucassen, M. Koch-Müller, M. Taran, G. Franz, Coupled H and Nb, Cr, and V trace element behavior in synthetic rutile at 600 °C, 400 MPa and possible geological application. Am. Mineral. **98**, 7–18 (2013)

R.W. Luth, Mantle volatiles—distribution and consequences, in *Treatise on Geochemistry*, ed. by R.W. Carlson (Elsevier, Amsterdam, 2003), pp. 319–361

I.D. MacGregor, W.I. Manton, Roberts Victor eclogites: ancient oceanic crust. J. Geophys. Res. **91**, 14063–14079 (1986)

S.J. Mackwell, D.L. Kohlstedt, M.S. Paterson, The role of water in the deformation of olivine single crystals. J. Geophys. Res. **90**, 11319–11333 (1985)

V. Magni, P. Bouilhol, J. van Hunen, Deep water recycling through time. Geochem. Geophys. Geosyst. **15**, 4203–4216 (2014)

P.R. Mahaffy, T.M. Donahue, S.K. Atreya, T.C. Owen, H.B. Niemann, Galileo probe measurements of D/H and ^{3}He/^{4}He in Jupiter's atmosphere. Space Sci. Rev. **84**, 251–263 (1998)
D. Mainprice, P.G. Silver, Interpretation of SKS-waves using samples from the subcontinental lithosphere. Phys. Earth Planet. Inter. **78**, 257–280 (1993)
B. Marty, The origins and concentrations of water, carbon, nitrogen and noble gases on Earth. Earth Planet. Sci. Lett. **313–314**, 56–66 (2012)
B. Marty, C.M.O.D. Alexander, S.N. Raymond, Primordial Origins of Earth's Carbon. Rev. Mineral. Geochem. **75**, 149–181 (2013)
B. Marty, G. Avice, Y. Sano, K. Altwegg, H. Balsiger, M. Hässig, A. Morbidelli, O. Mousis, M. Rubie, Origins of volatile elements (H, C, N, noble gases) on Earth and Mars in light of recent results from the ROSETTA cometary mission. Earth Planet. Sci. Lett. **441**, 91–102 (2016)
B. Marty, R.L. Palma, R.O. Pepin, L. Zimmermann, D.J. Schlutter, P.G. Burnard, A.J. Westphal, C.J. Snead, S. Bajt, R.H. Becker, J.E. Simones, Helium and neon abundances and compositions in cometary matter. Science **319**, 75–78 (2008)
B. Marty, R. Yokochi, Water in the early Earth. Rev. Mineral. Geochem. **62**, 421–450 (2006)
S. Masuti, S.D. Barbot, S.-I. Karato, L. Feng, P. Banerjee, Upper-mantle water stratification inferred from observations of the 2012 Indian Ocean earthquake. Nature **538**, 373–377 (2016)
S.S. Matsyuk, K. Langer, Hydroxyl in olivines from mantle xenoliths in kimberlites of the Siberian platform. Contrib. Mineral. Petrol. **147**, 413–437 (2004)
S.S. Matsyuk, K. Langer, A. Hösch, Hydroxyl defects in garnets from mantle xenoliths in kimberlites of the Siberian platform. Contrib. Mineral. Petrol. **132**, 163–179 (1998)
S. Matveev, C. Ballhaus, K. Fricke, J. Truckenbrodt, D. Ziegenbein, Volatiles in the Earth's mantle: synthesis of CHO fluids at 1273 K and 2.4 GPa. Geochim. Cosmochim. Acta **61**, 3081–3088 (1997)
C.A. McCammon, M.G. Kopylova, A redox profile of the Slave mantle and oxygen fugacity control in the cratonic mantle. Contrib. Mineral. Petrol. **148**, 55–68 (2004)
W.F. McDonough, Compositional model for the Earth's core, in *Treatise on Geochemistry; The Mantle and Core*, ed. by R.W. Carlson (Elsevier, Amsterdam, 2005), pp. 547–568
R.S. McGary, R.L. Evans, P.E. Wannamaker, J. Elsenbeck, S. Rondenay, Pathway from subducting slab to surface for melt and fluids beneath Mount Rainier. Nature **511**, 338–340 (2014)
B.I.A. McInnes, M. Gregoire, R.A. Binns, P.M. Herzig, M.D. Hannington, Hydrous metasomatism of oceanic sub-arc mantle, Lihir, Papua New Guinea: petrology and geochemistry of fluid-metasomatised mantle wedge xenoliths. Earth Planet. Sci. Lett. **188**, 169–183 (2001)
K.D. McKeegan, J. Aléon, J.P. Bradley, D.E. Brownlee, H. Busemann, A. Butterworth, M. Chaussidon, S. Fallon, C. Floss, J. Gilmour, M. Gounelle, G. Graham, Y.N. Guan, P.R. Heck, P. Hoppe, I.D. Hutcheon, J. Huth, H.A. Ishii, M. Ito, S.B. Jacobsen, A. Kearsley, L.A. Leshin, M.-C. Liu, I.C. Lyon, K. Marhas, B. Marty, G. Matrajt, A. Meibom, S.M. Messenger, S. Mostefaoui, S. Mukhopadhyay, K. Nakamura-Messenger, L.R. Nittler, R.L. Palma, R.O. Pepin, D.A. Papanastassiou, F. Robert, D.J. Schlutter, C.J. Snead, F.J. Stadermann, R.M. Stroud, P. Tsou, A. Westphal, E.D. Young, K. Ziegler, L. Zimmermann, E. Zinner, Isotopic compositions of cometary matter returned by Stardust. Science **314**, 1724–1728 (2006)
D. McKenzie, The extraction of magma from the crust and mantle. Earth Planet. Sci. Lett. **74**, 81–91 (1985)
E. Médard, T.L. Grove, The effect of H_2O on the olivine liquidus of basaltic melts: experiments and thermodynamic models. Contrib. Mineral. Petrol. **155**, 417–432 (2008)
M.A. Menzies, C.J. Hawkesworth (eds.), *Mantle Metasomatism* (Academic Press Inc., London, 1987). 472 pp.
A. Meshik, C.M. Hohenberg, D.S. Burnett, O. Pravdivtseva, Measuring the isotopic composition of solar wind noble gases, in *Exploring the Solar Wind*, ed. by M. Lazar (INTECH Open Access Publisher, Winchester, 2012), pp. 93–120
K. Mibe, M. Kanzaki, T. Kawamoto, K.N. Matsukage, Y. Fei, S. Ono, Second critical endpoint in the peridotite-H_2O system. J. Geophys. Res. **112**, 1–8 (2007)
P. Michael, Regionally distinctive sources of depleted MORB: evidence from trace elements and H_2O. Earth Planet. Sci. Lett. **131**, 301–320 (1995)
P.J. Michael, The concentration, behavior and storage of H_2O in the suboceanic upper mantle: implications for mantle metasomatism. Geochim. Cosmochim. Acta **52**, 555–566 (1988)
C. Michaut, C. Jaupart, J.-C. Mareshal, Thermal evolution of cratonic roots. Lithos **109**, 47–60 (2009)
K. Mierdel, H. Keppler, J.R. Smyth, F. Langenhorst, Water solubility in aluminous orthopyroxene and the origin of Earth's asthenosphere. Science **315**, 364–368 (2007)
R.H. Mitchell, *Kimberlites. Mineralogy, Geochemistry, and Petrology* (Springer, New York, 1986)
M. Mookherjee, L. Stixrude, B. Karki, Hydrous silicate melt at high pressure. Nature **452**, 983–986 (2008)
J.G. Moore, Water content of basalt erupted on the ocean floor. Contrib. Mineral. Petrol. **28**, 272–279 (1970)
J.G. Moore, J.-G. Schilling, Vesicles, water, and sulfur in Reykjanes Ridge basalts. Contrib. Mineral. Petrol. **41**, 105–118 (1973)

M. Moreira, S. Charnoz, The origin of the neon isotopes in chondrites and on Earth. Earth Planet. Sci. Lett. **433**, 249–256 (2016)
J.L. Mosenfelder, M. Le Voyer, G.R. Rossman, Y. Guan, D.R. Bell, P.D. Asimow, J.M. Eiler, Analysis of hydrogen in olivine by SIMS: evaluation of standards and protocol. Am. Mineral. **96**, 1725–1741 (2011)
J.L. Mosenfelder, G.R. Rossman, E.A. Johnson, Hydrous species in feldspars: a reassessment based on FTIR and SIMS. Am. Mineral. **100**, 1209–1221 (2015)
S. Mukhopadhyay, Early differentiation and volatile accretion recorded in deep-mantle neon and xenon. Nature **486**, 101–104 (2012)
S. Mukhopadhyay, L. Nittler, D-rich water in interplanetary dust particles, in *Lunar Planet. Sci. Conf.*, League City, TX (2003), p. 1941
A. Müller, M. Koch-Müller, Hydrogen speciation and trace element contents of igneous, hydrothermal and metamorphic quartz from Norway. Mineral. Mag. **73**, 569–583 (2009)
A. Mundl, M. Touboul, M.G. Jackson, J.M.D. Day, M.D. Kurz, V. Lekic, R.T. Helz, R.J. Walker, Tungsten-182 heterogeneity in modern ocean island basalts. Science **356**, 66–69 (2017)
B.O. Mysen, M.L. Fogel, P.L. Morril, G.D. Cody, Solution behavior of reduced C-O-H volatiles in silicate melts at high pressure and temperature. Geochim. Cosmochim. Acta **73**, 1696–1710 (2009)
S. Naif, K. Key, S. Constable, R.L. Evans, Melt-rich channel observed at the lithosphere-asthenosphere boundary. Nature **495**, 356–359 (2013)
S. Nakashima, H. Matayoshi, T. Yuko, K. Michibayashi, T. Masuda, N. Kuroki, H. Yamagishi, Y. Ito, A. Nakamura, Infrared microspectroscopy analysis of water distribution in deformed and metamorphosed rocks. Tectonophysics **245**, 263–276 (1995)
S. Nazzareni, H. Skogby, P.F. Zanazzi, Hydrogen content in clinopyroxene phenocrysts from Salina mafic lavas (Aeolian arc, Italy). Contrib. Mineral. Petrol. **162**, 275–288 (2011)
O. Nebel, K. Mezger, W. van Westrenen, Rubidium isotopes in primitive chondrites: constraints on Earth's volatile element depletion and lead isotope evolution. Earth Planet. Sci. Lett. **305**, 309–316 (2011)
F. Nestola, P. Nimis, L. Ziberna, M. Longo, A. Marzoli, J.W. Harris, M.H. Manghnani, Y. Fedortchouk, First crystal-structure determination of olivine in diamond: composition and implications for provenance in the Earth's mantle. Earth Planet. Sci. Lett. **305**, 249–255 (2011)
F. Nestola, J.R. Smyth, Diamonds and water in the deep Earth: a new scenario. Int. Geol. Rev. **58**, 1–14 (2015). doi:10.1080/00206814.2015.1056758
A.O. Nier, D.J. Schlutter, Extraction of helium from individual interplanetary dust particles by step-heating. Meteoritics **27**, 166–173 (1992)
F. Nimmo, T. Kleine, Early differentiation and core formation: processes and timescales, in *The Early Earth: Accretion and Differentiation*, ed. by J. Badro, A.M. Walker (Wiley, New York, 2015), pp. 83–102
Y. Nishihara, K.N. Matsukage, Iron-titanium oxyhydroxides as water carriers in the Earth's deep mantle. Am. Mineral. **101**, 919–927 (2016)
R. Nomura, K. Hirose, K. Uesugi, Y. Ohishi, A. Tsuchiyama, A. Miyake, Y. Ueno, Low core-mantle boundary temperature inferred from the solidus of pyrolite. Science **343**, 522–525 (2014)
D. Novella, N. Bolfan-Casanova, F. Nestola, J.W. Harris, H_2O in olivine and garnet inclusions still trapped in diamonds from the Siberian craton: implications for the water content of cratonic lithosphere peridotites. Lithos **230**, 180–183 (2015)
D. Novella, D.J. Frost, E.H. Hauri, H. Bureau, C. Raepsaet, M. Roberge, The distribution of H_2O between silicate melt and nominally anhydrous peridotite and the onset of hydrous melting in the deep upper mantle. Earth Planet. Sci. Lett. **400**, 1–13 (2014)
D.P. O'Brien, A. Morbidelli, H.F. Levison, Terrestrial planet formation with strong dynamical friction. Icarus **184**, 39–58 (2006)
D.P. O'Brien, K.J. Walsh, A. Morbidelli, S.N. Raymond, A.V. Mandell, Water delivery and giant impacts in the 'Grand Tack' scenario. Icarus **239**, 74–84 (2014)
J.A. O'Leary, G.A. Gaetani, E.H. Hauri, The effect of tetrahedral Al^{3+} on the partitioning of water between clinopyroxene and silicate melt. Earth Planet. Sci. Lett. **297**, 111–120 (2010)
C.J. O'Neill, A. Lenardic, W.L. Griffin, S.Y. O'Reilly, Dynamics of cratons in an evolving mantle. Lithos **102**, 12–24 (2008)
H.S.C. O'Neill, H. Palme, Composition of the silicate Earth: implications for accretion and core formation, in *The Earth's Mantle: Composition, Structure, and Evolution*, ed. by I. Jackson (Cambridge University Press, Cambridge, 1998), pp. 3–126
I. Ohira, E. Ohtani, T. Sakai, M. Miyahara, N. Hirao, Y. Ohishi, M. Nishijima, Stability of a hydrous δ-phase, AlOOH–$MgSiO_2(OH)_2$, and a mechanism for water transport into the base of lower mantle. Earth Planet. Sci. Lett. **401**, 12–17 (2014)
E. Ohtani, Hydrous minerals and the storage of water in the deep mantle. Chem. Geol. **418**, 6–15 (2015)
E. Ohtani, N. Hirao, T. Kondo, M. Ito, T. Kikegawa, Iron-water reaction at high pressure and temperature, and hydrogen transport into the core. Phys. Chem. Miner. **32**, 77–82 (2005)

T. Ohuchi, T. Irifune, Development of A-type olivine fabric in water-rich deep upper mantle. Earth Planet. Sci. Lett. **362**, 20–30 (2013)
T. Ohuchi, S.-I. Karato, K. Fujino, Strength of single-crystal orthopyroxene under lithospheric conditions. Contrib. Mineral. Petrol. **161**, 961–975 (2010)
T. Ohuchi, T. Kawazoe, Y. Nishihara, N. Nishiyama, T. Irifune, High pressure and temperature fabric transitions in olivine and variations in upper mantle seismic anisotropy. Earth Planet. Sci. Lett. **304**, 55–63 (2011)
T. Okuchi, Hydrogen partitioning into molten iron at high pressure: implications for Earth's core. Science **278**, 1781–1784 (1997)
T. Okuchi, E. Takahashi, Hydrogen in molten iron at high pressure: the first measurement, in *Properties of Earth and Planetary Materials at High Pressure and Temperature* (American Geophysical Union, Washington, 1998), pp. 249–260
U. Ott, Planetary and pre-solar noble gases in meteorites. Chem. Erde **74**, 519–544 (2014)
T. Owen, A. Bar-Nun, I. Kleinfeld, Possible cometary origin of heavy noble gases in the atmospheres of Venus, Earth and Mars. Nature **358**, 43–46 (1992)
J.A. Padrón-Navarta, J. Hermann, H.S.C. O'Neill, Site-specific hydrogen diffusion rates in forsterite. Earth Planet. Sci. Lett. **392**, 100–112 (2014)
H. Palme, H.S.C. O'Neill, Cosmochemical estimates of mantle composition, in *The Mantle and Core*, ed. by A.M. Davis (Elsevier, Amsterdam, 2014a), pp. 1–39
H. Palme, H.S.C. O'Neill, Solar system abundances of the elements, in *The Mantle and Core*, ed. by A.M. Davis (Elsevier, Amsterdam, 2014b), pp. 15–36
M. Palot, S.D. Jacobsen, J.P. Townsend, F. Nestola, K. Marquardt, J.W. Harris, T. Stachel, C.A. McCammon, D.G. Pearson, Evidence for H_2O-bearing fluids in the lower mantle from diamond inclusion. Lithos **265**, 237–243 (2016). doi:10.1016/j.lithos.2016.06.023
W.R. Panero, L.R. Benedetti, R. Jeanloz, Transport of water into the lower mantle: role of stishovite. J. Geophys. Res. **108**, 2039 (2003)
W.R. Panero, J.S. Pigott, D.M. Reaman, J.E. Kabbes, Z. Liu Dry, (Mg, Fe)SiO_3 perovskite in the Earth's lower mantle. J. Geophys. Res. **120**, 894–908 (2015)
W.R. Panero, J.R. Smyth, J.S. Pigott, Z. Liu, D.J. Frost, Hydrous ringwoodite to 5 K and 35 GPa: multiple hydrogen bonding sites resolved with FTIR spectroscopy. Am. Mineral. **98**, 637–642 (2013)
R. Parai, S. Mukhopadhyay, How large is the subducted water flux? New constraints on mantle regassing rates. Earth Planet. Sci. Lett. **317–318**, 396–406 (2012)
J.D. Pasteris, Fluid inclusions in mantle xenoliths, in *Mantle Xenoliths*, ed. by P.H. Nixon (Wiley, New York, 1987), pp. 691–707
A.A. Pavlov, A.K. Pavlov, J.F. Kasting, Irradiated interplanetary dust particles as a possible solution for the deuterium/hydrogen paradox of Earth's oceans. J. Geophys. Res. **104**, 30725–30728 (1999)
S.M. Peacock, Fluid processes in subduction zones. Science **248**, 329–337 (1990)
D.G. Pearson, F.E. Brenker, F. Nestola, J. McNeill, L. Nasdala, M.T. Hutchison, S. Matveev, K. Mather, G. Silversmit, S. Schmitz, B. Vekemans, L. Vincze, Hydrous mantle transition zone indicated by ringwoodite included within diamond. Nature **507**, 221–224 (2014)
D.G. Pearson, R.W. Carlson, S.B. Shirey, F.R. Boyd, P.H. Nixon, Stabilization of Archean lithospheric mantle: a Re-Os isotope study of peridotite xenoliths from the Kaapvaal craton. Earth Planet. Sci. Lett. **134**, 341–357 (1995a)
D.G. Pearson, S.B. Shirey, R.W. Carlson, F.R. Boyd, N.P. Pokhilenko, N. Shimizu, Re-Os, Sm-Nd, and Rb-Sr isotope evidence for thick Archaean lithospheric mantle beneath the Siberian craton modified by multistage metasomatism. Geochim. Cosmochim. Acta **59**, 959–977 (1995b)
R.O. Pepin, D. Porcelli, Origin of noble gases in the terrestrial planets. Annu. Rev. Earth Planet. Sci. **47**, 191–246 (2002)
A.H. Peslier, A review of water contents of nominally anhydrous natural minerals in the mantles of Earth, Mars and the Moon. J. Volcanol. Geotherm. Res. **197**, 239–258 (2010)
A.H. Peslier, M. Bizimis, Water in Hawaiian peridotite minerals: a case for a dry metasomatized oceanic mantle lithosphere. Geochem. Geophys. Geosyst. **16**, 1–22 (2015)
A.H. Peslier, M. Bizimis, M. Matney, Water disequilibrium in olivines from Hawaiian peridotites: recent metasomatism, H diffusion and magma ascent rates. Geochim. Cosmochim. Acta **154**, 98–117 (2015)
A.H. Peslier, J.F. Luhr, Hydrogen loss from olivines in mantle xenoliths from Simcoe (USA) and Mexico: mafic alkalic magma ascent rates and water budget of the sub-continental lithosphere. Earth Planet. Sci. Lett. **242**, 302–319 (2006)
A.H. Peslier, J.F. Luhr, J. Post, Low water contents in pyroxenes from spinel-peridotites of the oxidized, sub-arc mantle wedge. Earth Planet. Sci. Lett. **201**, 69–86 (2002)
A.H. Peslier, A.B. Woodland, D.R. Bell, M. Lazarov, Olivine water contents in the continental lithosphere and the longevity of cratons. Nature **467**, 78–81 (2010)

A.H. Peslier, A.B. Woodland, D.R. Bell, M. Lazarov, T.J. Lapen, Metasomatic control of water contents in the Kaapvaal cratonic mantle. Geochim. Cosmochim. Acta **97**, 213–246 (2012)
A.H. Peslier, A.B. Woodland, J.A. Wolff, Fast kimberlite ascent rates estimated from hydrogen diffusion profiles in xenolithic olivines from Southern Africa. Geochim. Cosmochim. Acta **72**, 2711–2722 (2008)
J.S. Pigott, K. Wright, J.D. Gale, W.R. Panero, Calculation of the energetics of water incorporation in majorite garnet. Am. Mineral. **100**, 1065–1075 (2015)
T. Plank, L.B. Cooper, C.E. Manning, Emerging geothermometers for estimating slab surface temperatures. Nat. Geosci. **614**, 611–615 (2009)
T. Plank, K.A. Kelley, M.M. Zimmer, E.H. Hauri, P.J. Wallace, Why do mafic magmas contain ~4 wt% water on average? Earth Planet. Sci. Lett. **364**, 168–179 (2013)
T. Plank, C.H. Langmuir, The chemical composition of subducted sediment and its consequences for the crust and mantle. Chem. Geol. **145**, 325–394 (1998)
F.A. Podosek, M. Ozima, The xenon age of the Earth, in *Origin of the Earth and Moon*, ed. by R.M. Canup, K. Righter (University of Arizona Press, Tucson, 2000), pp. 63–72
F.A. Podosek, D.S. Woolum, P. Cassen, R.H.J. Nichols, Solar gases in the Earth by solar wind irradiation, in *Goldschmidt Conf.*, Oxford, UK (2000), p. 804
J.-P. Poirier, Light elements in the Earth's outer core: a critical review. Phys. Earth Planet. Inter. **85**, 319–337 (1994)
H.N. Pollack, Cratonization and thermal evolution of the mantle. Earth Planet. Sci. Lett. **80**, 175–182 (1986)
F.F. Pollitz, R. Bürgmann, B. Romanowicz, Viscosity of oceanic asthenosphere inferred from remote triggering of earthquakes. Science **280**, 1245–1249 (1998)
A. Pommier, Interpretation of magnetotelluric results using laboratory measurements. Surv. Geophys. **35**, 41–84 (2014)
D. Porcelli, C.J. Ballentine, Models for distribution of terrestrial noble gases and evolution of the atmosphere. Rev. Mineral. Geochem. **47**, 411–480 (2002)
K. Priestley, E. Debayle, Seismic evidence for a moderately thick lithosphere beneath the Siberian platform. Geophys. Res. Lett. **30**, 1118 (2003)
K. Priestley, D. McKenzie, The thermal structure of the lithosphere from shear wave velocities. Earth Planet. Sci. Lett. **244**, 285–301 (2006)
L. Qin, C.M.O.D. Alexander, R.W. Carlson, M.F. Horan, T. Yokoyama, Contributors to chromium isotope variation of meteorites. Geochim. Cosmochim. Acta **74**, 1122–1145 (2010)
S.N. Raymond, T. Quinn, J.I. Lunine, High-resolution simulations of the final assembly of Earth-like planets I. Terrestrial accretion and dynamics. Icarus **183**, 265–282 (2006)
J. Revenaugh, R. Meyer, Seismic evidence of partial melt within a possibly ubiquitous low-velocity layer at the base of the mantle. Science **277**, 670–673 (1997)
J. Revenaugh, S.A. Sipkin, Seismic evidence for silicate melt atop the 410-km mantle discontinuity. Nature **369**, 474–476 (1994)
G.G. Richards, D. Bercovici, Water-induced convection in the Earth's mantle transition zone. J. Geophys. Res. **114**, B01205 (2009)
F. Robert, The origin of water on Earth. Science **293**, 1056–1058 (2001)
F. Robert, The D/H ratio in chondrites, in *Solar System History from Isotopic Signatures of Volatile Elements: Volume Resulting from an ISSI Workshop*, 14–18 January, 2003, Bern, Switzerland, ed. by R. Kallenbach, T. Encrenaz, J. Geiss, K. Mauersberger, T.C. Owen, F. Robert (Springer, Dordrecht, 2002), pp. 87–101.
F. Robert, M. Javoy, J. Halbout, B. Dimon, L. Merlivat, Hydrogen isotope abundances in the solar system. Part II: meteorites with terrestrial-like DH ratio. Geochim. Cosmochim. Acta **51**, 1807–1822 (1987)
E. Roedder, Liquid CO_2 inclusions in olivine-bearing nodules and phenocrysts from basalts. Am. Mineral. **10**, 1746–1773 (1965)
E. Roedder, *Fluid Inclusions* (Mineralogical Society of America, Chantilly, 1984). 644 pp.
S. Rondenay, G.A. Abers, P.E. van Keken, Seismic imaging of subduction zone metamorphism. Geology **36**, 275–278 (2008)
A. Rosenthal, E.H. Hauri, M.M. Hirschmann, Experimental determination of C, F, and H partitioning between mantle minerals and carbonated basalt, CO_2/Ba and CO_2/Nb systematics of partial melting, and the CO_2 contents of basaltic source regions. Earth Planet. Sci. Lett. **412**, 77–87 (2015)
G.R. Rossman, Studies of OH in nominally anhydrous minerals. Phys. Chem. Miner. **23**, 299–304 (1996)
G.R. Rossman, Analytical methods for measuring water in nominally anhydrous minerals, in *Water in Nominally Anhydrous Minerals*, ed. by H. Keppler, J.R. Smyth (Mineralogical Society of America, Chantilly, 2006), pp. 1–28
G.R. Rossman, J.R. Smyth, Hydroxyl contents of accessory minerals in mantle eclogites and related rocks. Am. Mineral. **75**, 775–780 (1990)

D.C. Rubie, D.J. Frost, U. Mann, Y. Asahara, F. Nimmo, K. Tsuno, P. Kegler, A.H. Holzheid, H. Palme, Heterogeneous accretion, composition and core–mantle differentiation of the Earth. Earth Planet. Sci. Lett. **301**, 31–42 (2011)
D.C. Rubie, S.A. Jacobson, A. Morbidelli, D.P. O'Brien, E.D. Young, J. de Vries, F. Nimmo, H. Palme, D.J. Frost, Accretion and differentiation of the terrestrial planets with implications for the compositions of early-formed Solar System bodies and accretion of water. Icarus **248**, 89–108 (2015)
R.L. Rudnick, Making continental crust. Nature **378**, 571–578 (1995)
R.L. Rudnick, D.M. Fountain, Nature and composition of the continental crust: a lower crustal perspective. Rev. Geophys. **33**, 267–309 (1995)
L. Rüpke, J.P. Morgan, J.E. Dixon, Implications of subduction rehydration for Earth's deep water cycle, in *Earth's Deep Water Cycle*, ed. by S.D. Jacobsen, S. van der Lee (American Geophysical Union, Washington, 2006), pp. 263–276
L.H. Rüpke, J.P. Morgan, M. Hort, J.A.D. Connolly, Serpentine and the subduction zone water cycle. Earth Planet. Sci. Lett. **223**, 17–34 (2004)
D.M. Ruscitto, P.J. Wallace, L.B. Cooper, T. Plank, Global variations in H_2O/Ce: 2. Relationships to arc magma geochemistry and volatile fluxes. Geochem. Geophys. Geosyst. **13**, 1–27 (2012)
J.K. Russell, L.A. Porritt, Y. Lavallée, D.B. Dingwell, Kimberlite ascent by assimilation-fuelled buoyancy. Nature **481**, 352–356 (2012)
C.A. Rychert, P.M. Shearer, A global view of the lithosphere-asthenosphere boundary. Science **324**, 495–498 (2009)
A.E. Saal, E.H. Hauri, C.H. Langmuir, M.R. Perfit, Vapour undersaturation in primitive mid-ocean-ridge basalt and the volatile content of Earth's upper mantle. Nature **419**, 451–455 (2002)
A.E. Saal, E.H. Hauri, M. Lo Cascio, J.A. Van Orman, M.C. Rutherford, R.F. Cooper, Volatile content of lunar volcanic glasses and the presence of water in the Moon's interior. Nature **454**, 192–196 (2008)
A.E. Saal, E.H. Hauri, J.A. Van Orman, M.C. Rutherford, Hydrogen isotopes in lunar volcanic glasses and melt inclusions reveal a carbonaceous chondrite heritage. Science **340**, 1317–1320 (2013)
T. Sakamaki, A. Suzuki, E. Ohtani, Stability of hydrous melt at the base of the Earth's upper mantle. Nature **439**, 192–194 (2006)
S.A. Sandford, J. Aléon, C.M.O.D. Alexander, T. Araki, S. Bajt, G.A. Baratta, J. Borg, J.P. Bradley, D.E. Brownlee, J.R. Brucato, M.J. Burchell, H. Busemann, A. Butterworth, S.J. Clemett, G.D. Cody, L. Colangeli, G. Cooper, L. D'Hendecourt, Z. Djouadi, J.P. Dworkin, G. Ferrini, H. Fleckenstein, G.J. Flynn, I.A. Franchi, M. Fries, M.K. Gilles, D.P. Glavin, M. Gounelle, F. Grossemy, C. Jacobsen, L.P. Keller, A.L.D. Kilcoyne, J. Leitner, G. Matrajt, A. Meibom, V. Mennella, S. Mostefaoui, L.R. Nittler, M.E. Palumbo, D.A. Papanastassiou, F. Robert, A. Rotundi, C.J. Snead, M.K. Spencer, F.J. Stadermann, A. Steele, T. Stephan, P. Tsou, T. Tyliszczak, A.J. Westphal, S. Wirick, B. Wopenka, H. Yabuta, R.N. Zare, M.E. Zolensky, Organics captured from comet 81P/Wild 2 by the Stardust Spacecraft. Science **314**, 1720–1724 (2006)
A. Sano, E. Ohtani, T. Kondo, N. Hirao, T. Sakai, N. Sata, Y. Ohishi, T. Kikegawa, Aluminous hydrous mineral δ-AlOOH as a carrier of hydrogen into the core-mantle boundary. Geophys. Res. Lett. **35**, L03303 (2008)
A.R. Sarafian, S.G. Nielsen, H.R. Marschall, F.M. McCubbin, B.D. Monteleone, Early accretion of water in the inner solar system from a carbonaceous chondrite-like source. Science **346**, 623–626 (2014)
A.R. Sarafian, M.F. Roden, A.E. Patiño-Douce, The volatile content of Vesta: clues from apatite in eucrites. Meteorit. Planet. Sci. **48**, 2135–2154 (2013)
A.R. Sarafian, E.H. Hauri, F.M. McCubbin, T.J. Lapen, E.L. Berger, S.G. Nielsen, H.R. Marschall, G.A. Gaetani, K. Righter, E. Sarafian, Early accretion of water and volatile elements to the inner Solar System: evidence from angrites. Philos. Trans. R. Soc. Lond. A **375**, 1–27 (2017)
E. Sarafian, R.L. Evans, J.A. Collins, J. Elsenbeck, G.A. Gaetani, J.B. Gaherty, G. Hirth, D. Lizarralde, The electrical structure of the central Pacific upper mantle constrained by the NoMelt experiment. Geochem. Geophys. Geosyst. **16**, 1115–1132 (2015)
L. Schaffer, A.H. Peslier, A.D. Brandon, M. Bizimis, M. Matney, *Why Are Mantle Melting Residues Still Hydrous?* (Goldschmidt, Yokohama, 2016)
L. Schaefer, B. Fegley Jr., Volatile element chemistry during metamorphism of ordinary chondritic material and some of its implications for the composition of asteroids. Icarus **205**, 483–496 (2010)
P. Schiano, R. Clocchiatti, N. Shimizu, R.C. Maury, K.P. Jochum, A.W. Hofmann, Hydrous, silica-rich melts in the sub-arc mantle and their relationship with erupted arc lavas. Nature **377**, 595–600 (1995)
E. Schmädicke, J. Gose, J. Reinhardt, T.M. Will, R. Stalder, Garnet in cratonic and non-cratonic mantle and lower crustal xenoliths from southern Africa: composition, water incorporation and geodynamic constraints. Precambrian Res. **270**, 285–299 (2015)
E. Schmädicke, J. Göse, T.M. Will, Heterogeneous mantle underneath the North Atlantic: evidence from water in orthopyroxene, mineral composition and equilibrium conditions of spinel peridotite from different locations at the Mid-Atlantic ridge. Lithos **125**, 308–320 (2011)

B. Schmandt, S.D. Jacobsen, T.W. Becker, Z. Liu, K. Ducker, Dehydration melting at the top of the lower mantle. Science **344**, 1265–1268 (2014)
M.W. Schmidt, S. Poli, Experimentally based water budgets for dehydrating slabs and consequences for arc magma generation. Earth Planet. Sci. Lett. **163**, 361–379 (1998)
M. Schönbächler, R.W. Carlson, M.F. Horan, T.D. Mock, E.H. Hauri, Silver isotope variations in chondrites: volatile depletion and the initial 107Pd abundance of the solar system. Geochim. Cosmochim. Acta **72**, 5330–5341 (2008)
M. Schönbächler, R.W. Carlson, M.F. Horan, T.D. Mock, E.H. Hauri, Heterogeneous accretion and the moderately volatile element budget of Earth. Science **328**, 884–887 (2010)
M. Schönbächler, F. Nimmo, Heterogeneous accretion of the Earth and the timing of volatile element depletion, in *AGU Fall Meeting*, San Francisco (2011)
J.E.C. Scully, C.T. Russell, A. Yin, R. Jaumann, E. Carey, J. Castillo-Rogez, H.Y. McSween, C.A. Raymond, V. Reddy, L. Le Corre, Geomorphological evidence for transient water flow on Vesta. Earth Planet. Sci. Lett. **411**, 151–163 (2015)
S.J. Seaman, M.L. Williams, M.J. Jercinovic, G.C. Koteas, L.B. Brown, Water in nominally anhydrous minerals: implications for partial melting and strain localization in the lower crust. Geology **41**, 1051–1054 (2013)
A.N. Seligman, I.N. Bindeman, J.M. Watkins, A.M. Ross, Water in volcanic glass: from volcanic degassing to secondary hydration. Geochim. Cosmochim. Acta **191**, 216–238 (2016)
K. Selway, J. Yi, S.-I. Karato, Water content of the Tanzanian lithosphere from magnetotelluric data: implications for cratonic growth and stability. Earth Planet. Sci. Lett. **388**, 175–186 (2014)
S.S. Shapiro, B.H. Hager, T.H. Jordan, Stability and dynamics of the continental tectosphere. Lithos **48**, 135–152 (1999)
Z.D. Sharp, F.M. McCubbin, C.K. Shearer, A hydrogen-based oxidation mechanism relevant to planetary formation. Earth Planet. Sci. Lett. **380**, 88–97 (2013)
A.M. Shaw, E.H. Hauri, M.D. Behn, D.R. Hilton, C.G. McPherson, J.M. Sinton, Long-term preservation of slab signatures in the mantle inferred from hydrogen isotopes. Nat. Geosci. **5**, 224–228 (2012)
A. Shen, H. Keppler, Infrared spectroscopy of hydrous silicate melts to 1000 °C and 10 kbars: direct observation of H_2O speciation in a diamond-anvil cell. Am. Mineral. **80**, 1335–1338 (1995)
Y. Shibazaki, E. Ohtani, H. Fukui, T. Sakai, S. Kamada, D. Ishikawa, S. Tsutsui, A.Q.R. Baron, N. Nishitani, N. Hirao, K. Takemura, Sound velocity measurements in dhcp-FeH up to 70 GPa with inelastic X-ray scattering: implications for the composition of the Earth's core. Earth Planet. Sci. Lett. **313–314**, 79–85 (2012)
Y. Shibazaki, E. Ohtani, H. Terasaki, A. Suzuki, K-i. Funakoshi, Hydrogen partitioning between iron and ringwoodite: implications for water transport into the Martian core. Earth Planet. Sci. Lett. **287**, 463–470 (2009)
S. Shirey, S.H. Richardson, Start of the Wilson cycle at 3 Ga shown by diamonds from subcontinental Mantle. Science **333**, 434–436 (2011)
J. Siebert, J. Badro, D. Antonangeli, F.J. Ryerson, Terrestrial accretion under oxidizing conditions. Science **339**, 1194–1197 (2013)
T.W. Sisson, S. Bronto, Evidence for pressure-release melting beneath magmatic arcs from basalt at Galunggung, Indonesia. Nature **391**, 883–886 (1998)
T.W. Sisson, G.D. Layne, H_2O in basalt and basaltic andesite glass inclusions from four subduction-related volcanoes. Earth Planet. Sci. Lett. **117**, 619–635 (1993)
L.E. Sjöberg, M. Pan, E. Asenjo, S. Erlingsson, Glacial rebound near Vatnajökull, Iceland, studied by GPS campaigns in 1992 and 1996. J. Geodyn. **29**, 63–70 (2000)
P. Skemer, J.M. Warren, L. Hansen, G. Hirth, P.B. Kelemen, The influence of water and LPO on the initiation and evolution of mantle shear zones. Earth Planet. Sci. Lett. **375**, 222–233 (2013)
N.H. Sleep, Survival of Archean cratonal lithosphere. J. Geophys. Res. **108**, 2302 (2003). doi:10.1029/2001JB000169
N.H. Sleep, Evolution of the continental lithosphere. Annu. Rev. Earth Planet. Sci. **33**, 369–393 (2005)
J.R. Smyth, A crystallographic model for hydrous wadsleyite (β-Mg_2SiO_4): an ocean in the Earth's interior? Am. Mineral. **79**, 1021–1024 (1994)
J.R. Smyth, Hydrogen in high pressure silicate and oxide mineral structures, in *Water in Nominally Anhydrous Minerals*, ed. by H. Keppler, J.R. Smyth (Mineralogical Society of America, Chantilly, 2006), pp. 85–115
J.R. Smyth, D.R. Bell, G.R. Rossman, Incorporation of hydroxyl in upper-mantle clinopyroxenes. Nature **351**, 732–735 (1991)
J.R. Smyth, F.A. Caporuscio, T.C. McCormick, Mantle eclogite: evidence of igneous fractionation in the mantle. Earth Planet. Sci. Lett. **93**, 133–141 (1989)

J.R. Smyth, D.J. Frost, The effect of water on the 410-km discontinuity: an experimental study. Geophys. Res. Lett. **29**, 123-121–123-124 (2002)
J.R. Smyth, C.M. Holl, D.J. Frost, S.D. Jacobsen, High pressure crystal chemistry of hydrous ringwoodite and water in the Earth's interior. Phys. Earth Planet. Inter. **143–144**, 271–278 (2004)
J.R. Smyth, S.D. Jacobsen, Nominally anhydrous minerals and Earth's deep water cycle, in *Earth's Deep Water Cycle*, ed. by S. Jacobsen, S. Lee (AGU Geophysical Monograph, Washington D.C., 2006), pp. 1–11
A.V. Sobolev, E.V. Asafov, A.A. Gurenko, N.T. Arndt, V.G. Batanova, M. Portnyagin, D. Garbe-Schönberg, S.P. Krashenninnikov, Komatiites reveal a hydrous Archaean deep-mantle reservoir. Nature **531**, 628–632 (2016)
A.V. Sobolev, M. Chaussidon, H_2O concentrations in primary melts from supra-subduction zones and mid-ocean ridges: implications for H_2O storage and recycling in the mantle. Earth Planet. Sci. Lett. **137**, 45–55 (1996)
S. Song, L. Su, Y. Niu, Y. Lai, L. Zhang, CH_4 inclusions in orogenic harzburgite: evidence for reduced slab fluids and implications for redox melting in mantle wedge. Geochim. Cosmochim. Acta **73**, 1737–1754 (2009)
T.-R.A. Song, D.V. Helmberger, S.P. Grand, Low-velocity zone atop the 410-km seismic discontinuity in the northwestern United States. Nature **427**, 530–533 (2004)
V. Soustelle, A. Tommasi, S. Demouchy, L. Franz, Melt-rock interactions, deformation, hydration and seismic properties in the sub-arc lithospheric mantle inferred from xenoliths from seamounts near Lihir, Papua New Guinea. Tectonophysics **608**, 330–345 (2013)
V. Soustelle, A. Tommasi, S. Demouchy, D.A. Ionov, Deformation and fluid-rock interaction in the supra-subduction mantle: microstructures and water contents in peridotite xenoliths from the Avacha volcano, Kamchatka. J. Petrol. **51**, 363–394 (2010)
W. Soyer, M. Unsworth, Deep electrical structure of the northern Cascadia (British Columbia, Canada) subduction zone: implications for the distribution of fluids. Geology **34**, 53–56 (2006)
R.S.J. Sparks, Kimberlite volcanism. Annu. Rev. Earth Planet. Sci. **41**, 497–528 (2013)
R.S.J. Sparks, J. Barclay, C. Jaupart, H.M. Mader, J.C. Phillips, Physical aspects of magmatic degassing I. Experimental and theoretical constraints on vesiculation, in *Volatiles in Magmas*, ed. by M.R. Carroll, J.R. Holloway (Mineralogical Society of America, Washington D.C., 1994), pp. 413–446
N.H. Spring, H. Busemann, S.A. Crowther, J.D. Gilmour, C. Engrand, L.R. Nittler, Xenon in Antarctic micrometeorites (AMMs) and interplanetary dust particles (IDPs), in *45th Lunar and Planetary Science Conference*, The Woodland, TX (2014), p. 2923
T. Stachel, W.J. Harris, P.G. Brey, W. Joswig, Kankan diamonds (Guinea) II: lower mantle inclusion parageneses. Contrib. Mineral. Petrol. **140**, 16–27 (2000)
R. Stalder, Influence of Fe, Cr and Al on hydrogen incorporation in orthopyroxene. Eur. J. Mineral. **16**, 703–711 (2004)
R. Stalder, A. Karimova, J. Konzett, OH-defects in multiple-doped orthoenstatite at 4–8 GPa: filling the gap between pure and natural systems. Contrib. Mineral. Petrol. **169**, 38 (2015)
R. Stalder, J. Konzett, OH defects in quartz in the system quartz–albite–water and granite–water between 5 and 25 kbar. Phys. Chem. Miner. **39**, 817–827 (2012)
R. Stalder, H. Skogby, Hydrogen incorporation in enstatite. Eur. J. Mineral. **14**, 1139–1144 (2002)
A. Stephant, R.L. Hervig, M. Bose, M. Wadhwa, D/H ratios and water contents in eucrite minerals: implications for the source and abundance of water on Vesta, in *79th Meteoritical Society Meeting* (2016), p. 6212
A. Stephant, L. Remusat, F. Robert, Water in type I chondrules of Paris CM chondrite. Geochim. Cosmochim. Acta **199**, 75–90 (2017)
E. Stolper, The speciation of water in silicate melts. Geochim. Cosmochim. Acta **46**, 2609–2620 (1982)
E. Stolper, S. Newman, The role of water in the petrogenesis of Mariana trough magmas. Earth Planet. Sci. Lett. **293**(325), 293–325 (1994)
A. Stracke, A.W. Hofmann, S.R. Hart, FOZO, HIMU, and the rest of the mantle zoo. Geochem. Geophys. Geosyst. **6**, 1–20 (2005)
D. Suetsugu, T. Inoue, A. Yamada, D. Zhao, M. Obayashi, Towards mapping the three-dimentional distribution of water in the transition zone from P-velocity tomography and 660-km discontinuity depths, in *Earth's Deep Water Cycle*, ed. by S. Jacobsen, S. Lee (AGU Geophysical Monograph, Washington D.C., 2006), pp. 237–250
S.-S. Sun, Chemical composition and origin of the Earth's primitive mantle. Geochim. Cosmochim. Acta **46**, 179–192 (1982)
S.S. Sun, W.F. McDonough, Chemical and isotopic systematics of oceanic basalts: implications for mantle composition and processes, in *Magmatism in Ocean Basins*, ed. by A.D. Saunders, M.J. Norry (Geol. Soc. London Spec. Publ., London, 1989), pp. 313–345

W. Sun, T. Yoshino, N. Sakamoto, H. Yurimoto, Hydrogen self-diffusivity in single crystal ringwoodite: implications for water content and distribution in the mantle transition zone. Geophys. Res. Lett. **42**, 6582–6589 (2015)
R. Sundvall, R. Stalder, Water in upper mantle pyroxene megacrysts and xenocrysts: a survey study. Am. Mineral. **96**, 1215–1227 (2011)
R.J. Sweeney, A.B. Thompson, P. Ulmer, Phase relations of a natural MARID composition and implications for MARID genesis, lithospheric melting and mantle metasomatism. Contrib. Mineral. Petrol. **115**, 225–241 (1993)
N. Tada, P. Tarits, K. Baba, H. Utada, T. Kasaya, D. Suetsugu, Electromagnetic evidence for volatile-rich upwelling beneath the society hotspot, French Polynesia. Geophys. Res. Lett. **43**, 12021–12026 (2016)
R. Tappert, J. Foden, T. Stachel, K. Muehlenbachs, M. Tappert, K. Wills, Deep mantle diamonds from South Australia: a record of Pacific subduction at the Gondwanan margin. Geology **37**, 43–46 (2008)
L.A. Taylor, A.M. Logvinova, G.H. Howarth, Y. Liu, A.H. Peslier, G.R. Rossman, Y. Chen, N.V. Sobolev, Low water in diamond mineral inclusions: proto-genetic origin in a dry cratonic lithosphere. Earth Planet. Sci. Lett. **433**, 125–132 (2016)
S.R. Taylor, S.M. McLennan, *The Continental Crust: Its Composition and Evolution* (Blackwell, Oxford, 1985)
T.J. Tenner, M.M. Hirschmann, A.C. Withers, P. Ardia, H_2O storage capacity of olivine and low-Ca pyroxene from 10 to 13 GPa: consequences for dehydration melting above the transition zone. Contrib. Mineral. Petrol. **163**, 297–316 (2012)
T.J. Tenner, M.M. Hirschmann, A.C. Withers, R.L. Hervig, Hydrogen partitioning between nominally anhydrous upper mantle minerals and melt between 3 and 5 GPa and applications to hydrous peridotite partial melting. Chem. Geol. **262**, 42–56 (2009)
H. Terasaki, E. Ohtani, T. Sakai, S. Kamada, H. Asanuma, Y. Shibazaki, N. Hirao, N. Sata, Y. Ohishi, T. Sakamaki, A. Suzuki, K.-I. Funakoshi, Stability of Fe–Ni hydride after the reaction between Fe–Ni alloy and hydrous phase (δ-AlOOH) up to 1.2 Mbar: possibility of H contribution to the core density deficit. Phys. Earth Planet. Inter. **194–195**, 18–24 (2012)
S.-M. Thomas, S.D. Jacobsen, C.R. Bina, P. Reichart, M. Moser, E.H. Hauri, M. Koch-Müller, J.R. Smyth, G. Dollinger, Quantification of water in hydrous ringwoodite. Front. Earth Sci. **2**, 1–19 (2014)
S.-M. Thomas, K. Wilson, M. Koch-Müller, E.H. Hauri, C.A. McCammon, S.D. Jacobsen, J. Lazarz, D. Rhede, M. Ren, N. Blair, S. Lenz, Quantification of water in majoritic garnet. Am. Mineral. **100**, 1084–1092 (2015)
C. Thoraval, S. Demouchy, Numerical models of ionic diffusion in one and three dimensions: application to dehydration of mantle olivine. Phys. Chem. Miner. **41**, 709–723 (2014)
Z.Z. Tian, J. Liu, Q.-K. Xia, J. Ingrin, Y.T. Hao, D. Christophe, Water concentration profiles in natural mantle orthopyroxenes: a geochronometer for long annealing of xenoliths within magma. Geology **45**, 87–90 (2017)
J.A. Tielke, M.E. Zimmerman, D.L. Kohlstedt, Hydrolytic weakening in olivine single crystals. J. Geophys. Res. **122**, 3465–3479 (2017)
P.M.E. Tollan, H.S.C. O'Neill, J. Hermann, A. Benedictus, R.J. Arculus, Frozen melt-rock reaction in a peridotite xenolith from the sub-arc mantle recorded by diffusion of trace elements and water in olivine. Earth Planet. Sci. Lett. **422**, 169–181 (2015)
J.P. Townsend, J. Tsuchiya, C.R. Bina, S.D. Jacobsen, Water partitioning between bridgmanite and postperovskite in the lowermost mantle. Earth Planet. Sci. Lett. **454**, 20–27 (2016)
M. Trieloff, J. Kunz, D.A. Clague, D. Harrison, C.J. Allègre, The nature of pristine noble gases in mantle plumes. Science **288**, 1036–1038 (2000)
A. Trinquier, J.L. Birck, C.J. Allègre, C. Göpel, D. Ulfbeck, ^{53}Mn–^{53}Cr systematics of the early Solar System revisited. Geochim. Cosmochim. Acta **72**, 5146–5163 (2008)
K. Tucker, R.L. Hervig, M. Wadhwa, Hydrogen isotope systematics of nominally anhydrous phases in martian meteorites, in *46th Lunar and Planetary Science Conference*, The Woodlands, TX (2015)
K. Umemoto, K. Hirose, Liquid iron-hydrogen alloys at outer core conditions by first-principles calculations. Geophys. Res. Lett. **42**, 7513–7520 (2015)
T. Usui, C.M.O.D. Alexander, J. Wang, J.I. Simon, J.H. Jones, Origin of water and mantle-crust interactions on Mars inferred from hydrogen isotopes and volatile element abundances of olivine-hosted melt inclusions of primitive shergottites. Earth Planet. Sci. Lett. **357–358**, 119–129 (2012)
T. Usui, C.M.O.D. Alexander, J. Wang, J.I. Simon, J.H. Jones, Meteoritic evidence for a previously unrecognized hydrogen reservoir on Mars. Earth Planet. Sci. Lett. **410**, 140–151 (2015)
T. Usui, E. Nakamura, K. Kobayashi, S. Maruyama, H. Helmstaedt, Fate of the subducted Farallon plate inferred from eclogite xenoliths in the Colorado Plateau. Geology **31**, 589–592 (2003)
R. van der Hilst, E.R. Engdahl, W. Spakman, G. Nolet, Tomographic imaging of subducted lithosphere below northwest Pacific island arcs. Nature **353**, 37–43 (1991)

M. van der Meijde, F. Marone, D. Giardini, S. van der Lee, Seismic evidence for water deep in Earth's upper mantle. Science **300**, 1556–1558 (2003)
P.E. van Keken, B.R. Hacker, E.M. Syracuse, G.A. Abers, Subduction factory: 4. Depth-dependent flux of H_2O from subducting slabs worldwide. J. Geophys. Res. **116**, B01401 (2011)
W.L. van Mierlo, F. Langenhorst, D.J. Frost, D.C. Rubie, Stagnation of subducting slabs in the transition zone due to slow diffusion in majoritic garnet. Nat. Geosci. **6**, 400–403 (2013)
L. Vattuone, M. Smerieri, L. Savio, A.M. Asaduzzaman, K. Muralidharan, M.l.J. Drake, M. Rocca, Accretion disc origin of the Earth's water. Philos. Trans. R. Soc. Lond. A **371**, 20110585 (2013)
L.P. Vinnik, R.W.E. Green, L.O. Nicolaysen, Seismic constraints on dynamics of the mantle of the Kaapvaal craton. Phys. Earth Planet. Inter. **95**, 139–151 (1996)
D. Vlassopoulos, G.R. Rossman, S.E. Haggerty, Coupled substitution of H and minor elements in rutile and the implications of high OH contents in Nb- and Cr-rich rutile from the upper mantle. Am. Mineral. **78**, 1181–1191 (1993)
N. Vogel, V.S. Heber, H. Baur, D.S. Burnett, R. Wieler, Argon, krypton, and xenon in the bulk solar wind as collected by the Genesis mission. Geochim. Cosmochim. Acta **75**, 3057–3071 (2011)
J.A. Wade, T. Plank, E.H. Hauri, K.A. Kelley, K. Roggensack, M. Zimmer, Prediction of magmatic water contents measurements of H_2O in clinopyroxene phenocrysts. Geology **36**, 799–802 (2008)
J.H. Waite Jr., W.S. Lewis, B.A. Magee, J.I. Lunine, W.B. McKinnon, C.R. Glein, O. Mousis, D.T. Young, T. Brockwell, J. Westlake, M.J. Nguyen, B.D. Teolis, H.B. Niemann, R.L. McNutt Jr., M. Perry, W.H. Ip, Liquid water on Enceladus from observations of ammonia and ^{40}Ar in the plume. Nature **460**, 487–490 (2009)
R.J. Walker, Highly siderophile elements in the Earth, Moon and Mars: update and implications for planetary accretion and differentiation. Chem. Erde **69**, 101–125 (2009)
R.J. Walker, R.W. Carlson, S.B. Shirey, F.R. Boyd, Os, Sr, Nd, and Pb isotope systematics of southern African peridotite xenoliths: implications for the chemical evolution of subcontinental mantle. Geochim. Cosmochim. Acta **53**, 1583–1595 (1989)
P.J. Wallace, Volatiles in submarine basaltic glasses from the Northern Kerguelen Plateau (Site 1140): implications for source region compositions, magmatic processes, and plateau subsidence. J. Petrol. **43**, 1311–1326 (2002)
P.J. Wallace, Volatiles in subduction zone magmas: concentrations and fluxes based on melt inclusion and volcanic gas data. J. Volcanol. Geotherm. Res. **140**, 217–240 (2005)
K. Wallmann, The geological water cycle and the evolution of marine δ^{18}O values. Geochim. Cosmochim. Acta **65**, 2469–2485 (2001)
M.J. Walter, S.C. Kohn, D. Araujo, G.P. Bulanova, C.B. Smith, E. Gaillou, J. Wang, A. Steele, S.B. Shirey, Deep mantle cycling of oceanic crust: evidence from diamonds and their mineral inclusions. Science **334**, 54–57 (2011)
M.J. Walter, A.R. Thompson, W. Wang, O.T. Lord, J.L. Ross, S.C. McMahon, M.A. Baron, E. Melekhova, A.K. Kleppe, S.C. Kohn, The stability of hydrous silicates in Earth's lower mantle: experimental constraints from the systems MgO–SiO_2–H_2O and MgO–Al_2O_3–SiO_2–H_2O. Chem. Geol. **418**, 16–29 (2015)
H. Wang, J. van Hunen, D.G. Pearson, M.B. Allen, Craton stability and longevity: the roles of composition-dependent rheology and buoyancy. Earth Planet. Sci. Lett. **391**, 224–233 (2014)
J. Wang, K.H. Hattori, R. Kilian, C.R. Stern, Metasomatism of sub-arc mantle peridotites below southernmost South America: reduction of fO_2 by slab-melt. Contrib. Mineral. Petrol. **153**, 607–624 (2007)
Q. Wang, A review of water contents and ductile deformation mechanisms of olivine: implications for the lithosphere-asthenosphere boundary of continents. Lithos **120**, 30–41 (2010)
Y. Wang, H. Ren, Z. Jin, Water and fabric in an ophiolitic peridotite from a supra-subduction zone. Contrib. Mineral. Petrol. **171**, 1–17 (2016)
Z. Wang, H. Becker, Ratios of S, Se and Te in the silicate Earth require a volatile-rich late veneer. Nature **499**, 328–331 (2013)
J.M. Warren, E.H. Hauri, Pyroxenes as tracers of mantle water variations. J. Geophys. Res. **119**, 1851–1881 (2014)
L.L. Watson, I.D. Hutcheon, S. Epstein, E.M. Stolper, Water on Mars: clues from deuterium/hydrogen and water contents of hydrous phases in SNC meteorites. Science **265**, 86–90 (1994)
J.D. Webster, P.M. Piccoli, Magmatic apatite: a powerful, yet deceptive, mineral. Elements **11**, 177–182 (2015)
F.A. Weis, H. Skogby, V.R. Troll, F.M. Deegan, B. Dahren, Magmatic water contents determined through clinopyroxene: examples from the Western Canary Islands, Spain. Geochem. Geophys. Geosyst. **16**, 2127–2146 (2015)
R. Wieler, H. Busemann, I.A. Franchi, Trapping and modification processes of noble gases and nitrogen in meteorites and their parent bodies, in *Meteorites and the Early Solar System II*, ed. by D.S. Lauretta, H.Y. McSween Jr. (University of Arizona Press, Tucson, 2006), pp. 499–521

S.A. Wilde, J.W. Valley, W.H. Peck, C.M. Graham, Evidence from detrital zircons for the existence of continental crust and oceans on the Earth 4.4 Gyr ago. Nature **409**, 175–178 (2001)
M. Willbold, T. Elliott, S. Moorbath, The tungsten isotopic composition of the Earth's mantle before the terminal bombardment. Nature **477**, 195–198 (2011)
R. Wirth, C. Vollmer, F. Brenker, S.S. Matsyuk, F. Kaminsky, Inclusions of nanocrystalline hydrous aluminium silicate "Phase Egg" in superdeep diamonds from Juina (Mato Grosso State, Brazil). Earth Planet. Sci. Lett. **259**, 384–399 (2007)
A.C. Withers, H. Bureau, C. Raepsaet, M.M. Hirschmann, Calibration of infrared spectroscopy by elastic recoil detection analysis of H in synthetic olivine. Chem. Geol. **334**, 92–98 (2012)
B.J. Wood, L.T. Bryndzia, K.E. Johnson, Mantle oxidation state and its relationship to tectonic environment and fluid speciation. Science **248**, 337–345 (1990)
B.J. Wood, A.N. Halliday, The lead isotopic age of the Earth can be explained by core formation alone. Nature **465**, 767–770 (2010)
B.J. Wood, A.N. Halliday, M. Rehkamper, Volatile accretion history of the Earth. Nature **467**, E6–E7 (2010)
B.J. Wood, J.-Y. Li, A. Shahar, Carbon in the core: its influence on the properties of core and mantle. Rev. Mineral. Geochem. **75**, 231–250 (2013)
B.J. Wood, J.A. Wade, M.R. Kilburn, Core formation and the oxidation state of the Earth: additional constraints from Nb, V and Cr partitioning. Geochim. Cosmochim. Acta **72**, 1415–1426 (2008)
A.B. Woodland, M. Koch, Variation in oxygen fugacity with depth in the upper mantle beneath the Kaapvaal craton, Southern Africa. Earth Planet. Sci. Lett. **214**, 295–310 (2003)
R.K. Workman, S.H. Hart, Major and trace element composition of the depleted MORB mantle (DMM). Earth Planet. Sci. Lett. **231**, 53–72 (2005)
R.K. Workman, E. Hauri, S.R. Hart, J. Wang, J. Blusztajn, Volatile and trace elements in basaltic glasses from Samoa: implication for water distribution in the mantle. Earth Planet. Sci. Lett. **241**, 932–951 (2006)
K. Wright, Atomistic models of OH defects in nominally anhydrous minerals, in *Water in Nominally Anhydrous Minerals*, ed. by H. Keppler, J.R. Smyth (Mineralogical Society of America, Chantilly, 2006), pp. 67–83
Q.-K. Xia, Y. Hao, P. Li, E. Deloule, M. Coltorti, L. Dallai, X. Yang, M. Feng, Low water content of the Cenozoic lithospheric mantle beneath the eastern part of the North China Craton. J. Geophys. Res. **115**, B07207 (2010)
Q.-K. Xia, Y.-T. Hao, S.C. Liu, X.-Y. Gu, M. Feng, Water contents of the Cenozoic lithospheric mantle beneath the western part of the North China Craton: peridotite xenolith constraints. Gondwana Res. **23**, 108–118 (2013a)
Q.-K. Xia, J. Liu, S.-C. Liu, I. Kovács, M. Feng, L. Dang, High water content in Mesozoic primitive basalts of the North China Craton and implications on the destruction of cratonic mantle lithosphere. Earth Planet. Sci. Lett. **361**, 85–97 (2013b)
Q.-K. Xia, X.-Z. Yang, E. Deloule, Y.-M. Sheng, Y.-T. Hao, Water in the lower crustal granulite xenoliths from Nushan, eastern China. J. Geophys. Res. **111**, B11202 (2006)
X. Yang, OH solubility in olivine in the peridotite-COH system under reducing conditions and implications for water storage and hydrous melting in the reducing upper mantle. Earth Planet. Sci. Lett. **432**, 199–209 (2015)
X. Yang, Effect of oxygen fugacity on OH dissolution in olivine under peridotite-saturated conditions: an experimental study at 1.5–7 GPa and 1100–1300 °C. Geochim. Cosmochim. Acta **173**, 319–336 (2016)
X. Yang, H. Keppler, Y. Li, Molecular hydrogen in mantle minerals. Geochem. Perspect. Lett. **2**, 160–168 (2016)
X. Yang, D. Liu, Q.-K. Xia, CO_2-induced small water solubility in olivine and implications for properties of the shallow mantle. Earth Planet. Sci. Lett. **403**, 37–47 (2014)
X.-Z. Yang, E. Deloule, Q.-K. Xia, Q.-C. Fan, M. Feng, Water contrast between Precambrian and Phanerozoic continental lower crust in eastern China. J. Geophys. Res. **113**, B08207 (2008a)
X.-Z. Yang, Q.-K. Xia, E. Deloule, L. Dallai, Q.C. Fan, M. Feng, Water in minerals of the continental lithospheric mantle and overlying lower crust: a comparative study of peridotite and granulite xenoliths from the North China craton. Chem. Geol. **256**, 33–45 (2008b)
R. Yokochi, B. Marty, A determination of the neon isotopic composition of the deep mantle. Earth Planet. Sci. Lett. **225**, 77–88 (2004)
T. Yoshino, T. Matsuzaki, S. Yamashita, T. Katsura, Hydrous olivine unable to account for conductivity anomaly at the top of the asthenosphere. Nature **443**, 973–976 (2006)
H. Yuan, B. Romanowicz, Lithospheric layering in the North American craton. Nature **466**, 1063–1068 (2010)
C. Zhang, Z. Duan, A model for C-O-H fluid in the Earth's mantle. Geochim. Cosmochim. Acta **73**, 2089–2102 (2009)

Y. Zhang, H_2O in rhyolitic glasses and melts: measurement, speciation, solubility, and diffusion. Rev. Geophys. **37**, 493–516 (1999)
Y. Zhang, H. Ni, Diffusion of H, C, and O components in silicate melts, in *Diffusion in Minerals and Melts*, ed. by Y. Zhang, D.J. Cherniak (Mineralogical Society of America, Geochemical Society, Chantilly, 2010), pp. 171–225
A. Zindler, S. Hart, Chemical geodynamics. Annu. Rev. Earth Planet. Sci. **14**, 493–571 (1986)